PRELIMINARY INDIAN OCEAN BIGEYE TUNA STOCK ASSESSMENT 1950-2018 (STOCK SYNTHESIS)

PREPARED BY: DAN FU[1],

02 OCTOBER 2019

[1] IOTC Secretariat, Dan.Fu@fao.org;

Contents

SUMMARY

This report presents a preliminary stock assessment for Indian Ocean bigeye tuna (*Thunnus albacares*) using *Stock Synthesis 3* (SS3). The assessment uses a spatially structured, age-based model that integrates multiple data sources. The assessment model covers the period 1975–2018 and represents an update and revision of the 2016 assessment model with the inclusion of revised composite longline CPUE indices, the adoption of a new regional weighting scheme, and a refined procedure to process the tag data that is more consistent with recent practice. A range of exploratory models are also presented to explore the impact of key data sets and model assumptions.

The rapid declining longline CPUE for 2011–2018 is likely to drive the recent stock trend estimated in the stock assessment model. Analyses performed indicated that a non-linear relationship between recent CPUE and abundance is also possible. The final assessment models correspond to a combination of model configurations, including CPUE catchability assumptions (2 options), tag likelihood lambda (0.1 or 1) and steepness values (0.7, 0.8, and 0.9). The final model ensemble consists of 12 models which aim to capture (to some extent) uncertainties related to the interpretation of the recent longline CPUE indices, (tag) data weighting, and the stock-recruitment assumptions. These models encompass a wide range of stock trajectories. Estimates of stock status were combined across from the 12 models and incorporated uncertainty estimates from both within and across the model ensemble.

The overall stock status estimates do not differ substantially from the previous assessment. Considering the quantified uncertainty, spawning stock biomass in 2018 was estimated to be 33% of the unfished levels and 130% of the level that can support MSY (SSB_{2018}/SSB_{MSY} = 1.30). With high likelihood, current fishing mortality was estimated to be higher than F_{MSY} (F_{2018}/F_{MSY} = 1.55), primarily a result of the significant increase of the catches from purse seine FAD fishery in 2018 (over 100% increase). Current (2018) catches are higher than the estimated MSY and are likely to drive the stock to be below SSB_{MSY} in the long term. The dominance of the PSLS catches (which caught almost exclusively juvenile fish) in catch compositions had profound implications in the prediction of future stock status. The retrospective analysis provided some confidence on the robustness of the model with respect to recent data, yet the uncertainly on levels of most recent recruitment may undermine the predictive capabilities of the model.

1. INTRODUCTION

This paper presents a preliminary stock assessment of bigeye tuna (*Thunnus albacares*) in the Indian Ocean (IO) including fishery data up to 2018. The assessment implements an age- and spatially-structured population model using the Stock Synthesis software (Methot 2013, Methot & Wetzel 2013).

Previous assessments of the Indian Ocean bigeye tuna stock have been conducted using Stock Synthesis (Shono et al 2009, Kolody et al 2010, Langley et al 2013a, b, 2016) and ASPM (Nishida & Rademeyer 2011). Langley et al (2013a, b) conducted a thorough examination of the key model assumptions. The SS model results provided the basis for the management advice for bigeye tuna formulated by WPTT15. However, the spatial dynamics of these models were not considered to adequately represent the dynamics of the IO bigeye tuna stock, specifically the regional distribution of biomass and the movement dynamics. The model results were sensitive to the spatial structure of the model (1 or 3 regions), the tag mixing period (4 quarters vs 8 quarters) and the relative weighting of the length frequency data. The final assessment models did not incorporate the available IO bigeye tag release/recovery data

In 2016, the stock assessment of the IO bigeye tuna stock included a review of the spatial stratification and parameterization of the assessment model to enable the integration of the tagging data into the

assessment model (Langley 2016, IOTC 2016). The 2016 assessment model utilized the new composite longline CPUE indices derived from main distant water longline fleets, replacing the Japanese longline CPUE indices used in the previous assessment. A range of model sensitivities were conducted, specifically related to natural mortality, selectivity and SRR steepness. The modelling identified considerable conflict among the main input data sets, especially between the tag recoveries and the longline CPUE indices, and between the tag recoveries and the length composition data from the purse seine FAD fishery. The magnitude of overall stock abundance was particularly sensitive to the treatment of the tagging data set. Uncertainty in the assessment captured the uncertainty on stock recruitment relationship and the influence of tagging information. Spawning stock biomass in 2015 was estimated be above SSB_{MSY}, and fishing mortality was below F_{MSY}.

This report documents the next iteration of the stock assessment of the IO bigeye tuna stock for consideration at 21th WPTT meeting. This stock assessment is based on the 2016 modelling framework and has incorporated revised and updated data up to 2018. The assessment implements an age-structured and spatially-explicit population model and is fitted to catch rate indices, length-composition data, and tagging data. The assessment is implemented using Stock Synthesis (version V3.24z).

1.1 Biology and stock structure

Bigeye are distributed throughout the tropical and sub-tropical waters of the Indian Ocean. Qualitatively, the tagging data suggest that BET migrate reasonably quickly, and indicate at least some basin-scale movements. Unfortunately, the limited distribution of tag releases, and small number of returns (and absence of tag reporting rate estimates) outside of the European/Seychelles purse seine fleets, mainly operating in the western equatorial Indian Ocean, makes it difficult to quantify large-scale movements. While there may be some relatively discreet sub-populations, or slow mixing rates among sub-regions, there is no evidence that this is the case in the core area where most of the catch is taken, and presumably where the bulk of the population is located.

The differences in fish growth between oceans support the hypothesis of separate bigeye stocks in the Indian and Pacific Oceans (Farley et al. 2004). But genetic differentiation was minimal within the Indian Ocean (Appleyard et al. 2002). The current assessment assumes the Indian Ocean ocean bigeye tuan consists of a single stock. However, the assessment model partitions the population by regions to account for differences in exploitation level and fishery operations (
Figure **1**).

1.2 Fishery overview

The distant-water longline fishery commenced operation in the Indian Ocean during the early 1950s (Figure 2). Bigeye tuna represented a significant component of the total catch from the longline fishery and catches increased steadily over the subsequent decades, reaching a peak in the late 1990s–early 2000s (IOTC 2018). The purse-seine fisheries and fresh-chilled longline fisheries developed from the mid-1980s and total bigeye tuna catches peaked at about 150,000 mt in the late 1990s (Figure 2). During the mid-2000s, the total annual bigeye catch declined considerably, primarily due to a decline in the longline catch in the western equatorial region in response to the threat of piracy off the Somali coast. The total annual catch declined to 85,368 mt in 2010 but recovered somewhat over the following years, reaching 124,759 mt in 2012. The total annual catch has declined since then and was 86,860 in 2015 but increased slightly in 2017 and 2018 (IOTC 2019).

All the small bigeye taken by purse seiners are caught in equatorial warm surface waters. In contrast, a wide majority of adult bigeye catches taken by longliners in each ocean are caught in association with warm surface waters, close to the equatorial zones (Fonteneau 2004) Most of the bigeye tuna catch from the Indian Ocean is caught within the latitudinal range 35° S to 10° N (Figure 3). This area of the Indian Ocean was used as the spatial domain of the assessment model. The small amount of bigeye catch from higher latitudes was reassigned to fisheries of the appropriate method within the model domain.

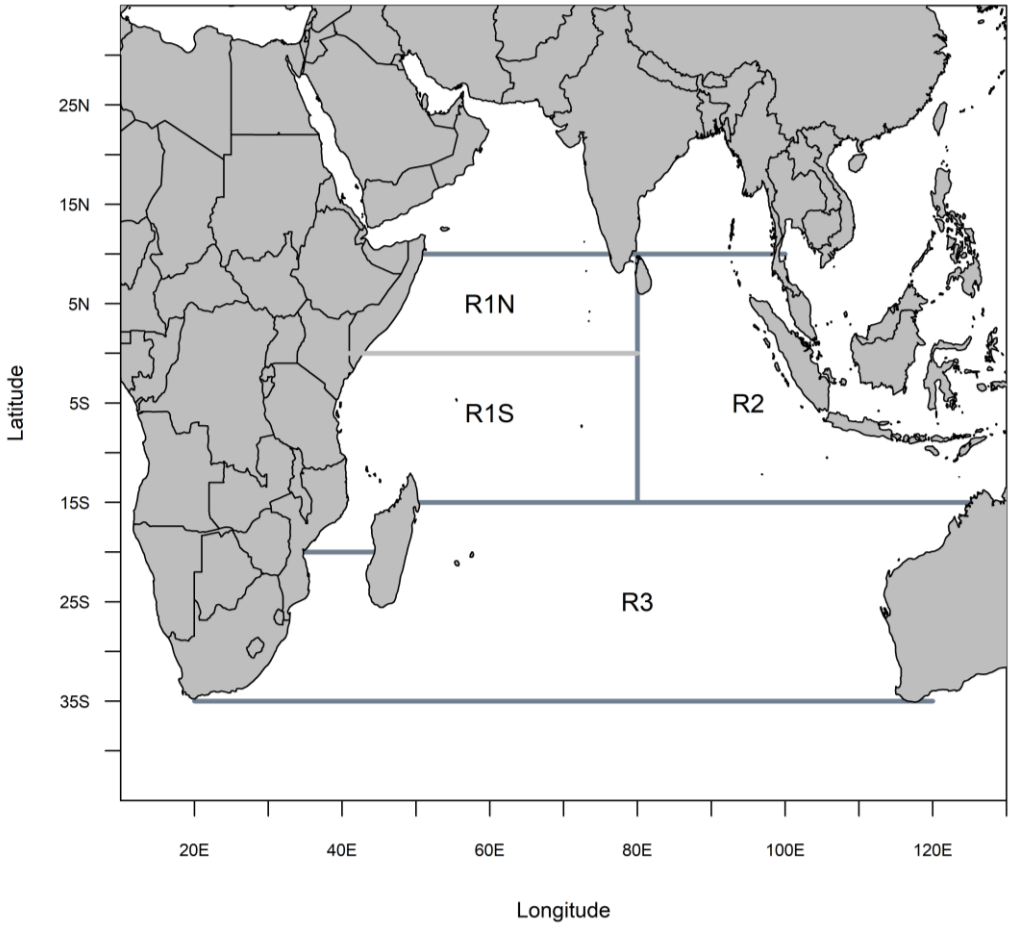

Figure 1: Spatial stratification of the Indian Ocean for the four-region assessment model.

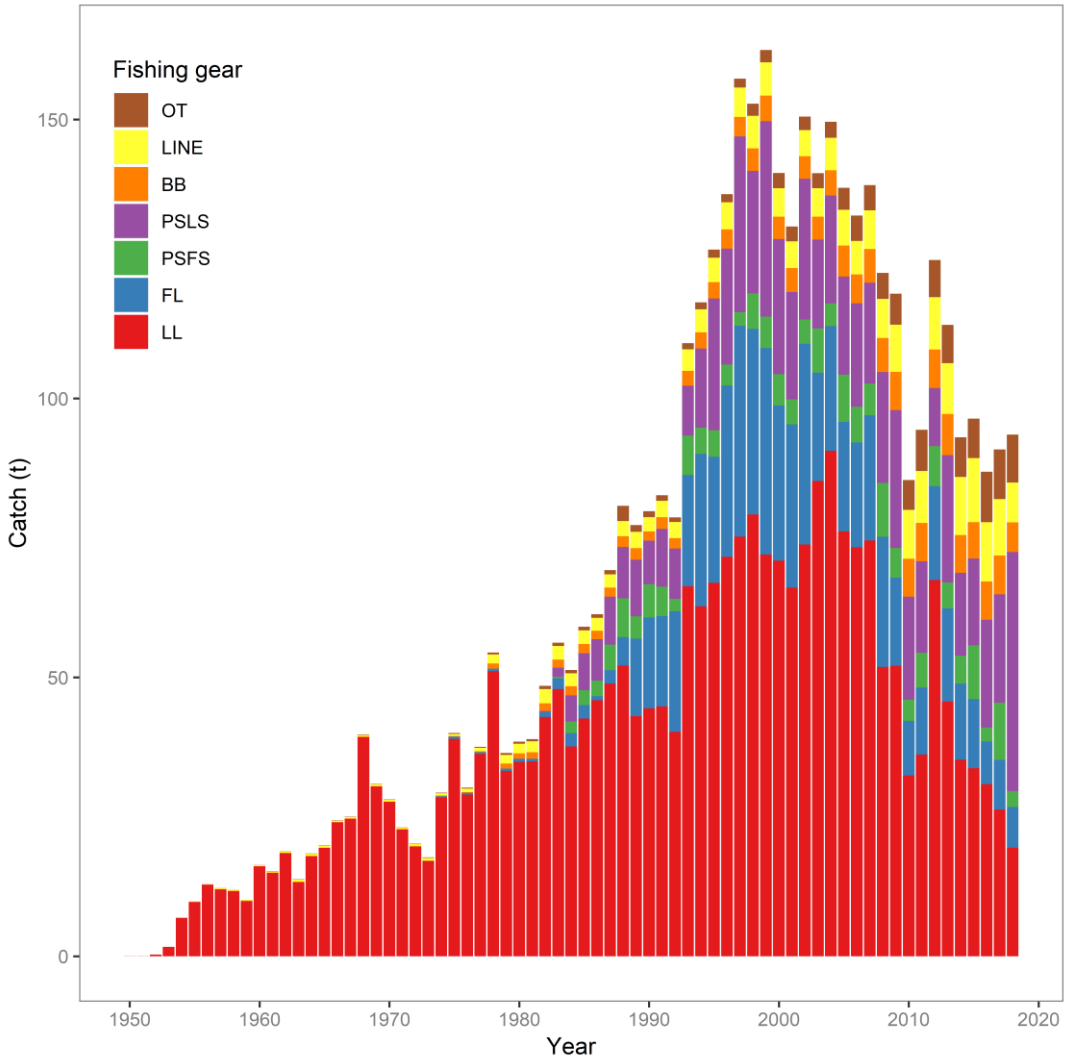

Figure 2: Total annual catch (1000s t) of bigeye tuna by fishing gear from 1950 to 2018. Gear codes are described in Table 1.

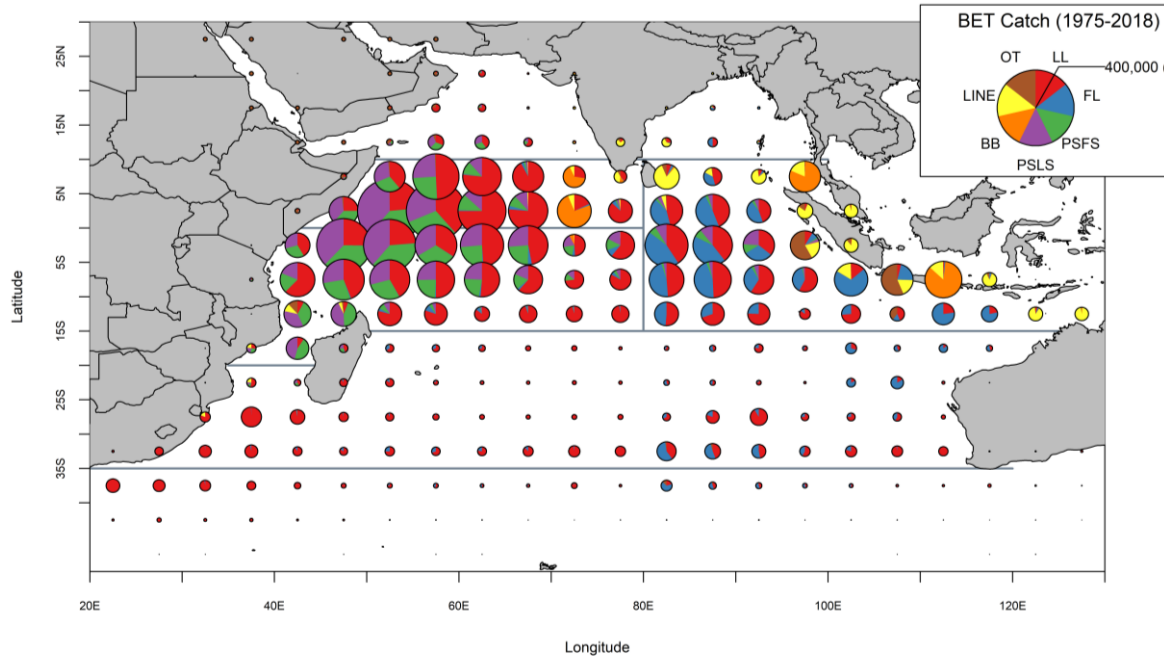

Figure 3: Spatial distribution of Indian Ocean bigeye catches by main gear types aggregated for1980-2018.

2. OBSERVATIONS AND MODEL INPUTS

The data used in the bigeye tuna assessment consist of catch and length composition data for the fisheries defined in the analysis, longline CPUE indices and tag release-recapture data. The details of the configuration of the fishery specific data sets are described below.

2.1 Spatial stratification

Stock assessment models often adopted region structures to account for differences in biological characteristics of the species, regional exploitation pattern, or the level of mixing amongst subpopulations (Vincent, et al. 2018). In the 2013 bigeye assessment (Langley *et al* 2013a), the spatial domain of the bigeye assessment model was stratified into three regions: western equatorial region (region 1), eastern equatorial region (region 2) and southern region (region 3). Most of the longline catch is taken within the two equatorial regions (15° S to 10° N), while the purse seine catch is predominantly taken within the western equatorial region. A seasonal longline fishery operates in the southern region. The longitudinal partitioning of the equatorial area subdivides the distribution of tagged fish recoveries from releases that occurred in the western area of region 1. There are also some differences in the temporal trends in the longline CPUE indices from the three regions. This regional restructure was further refined in the 2016 assessment where the western equatorial region (region 1) was subdivided to account for differences in the distribution of tags within this region (Section 2.5 of Langley 2015). The region was partitioned at the equator: the area south of the equator and the area north of the equator, denoted as Region 1S and Region 1N, respectively (Figure 1). The four-region structure was adopted in the current assessment. Alternative regional structures (e.g. 3-region and 1-region) were investigated to explore the plausibility of a simplified model structure.

2.2 Temporal stratification

The model commenced in 1975 and assumed an exploited, equilibrium initial state. The earlier CPUE indices were excluded from the assessment due to the disjunct in the series between the mid-1970s and early 1980s and the exceptionally high CPUE indices in the late 1970s. The overall change in the magnitude of the CPUE indices appears to be related to changes in the operation or reporting of the longline fishery which were not adequately accounted for in the CPUE standardisation (Hoyle et al. 2017b).

Within this model period, the annual data were compiled into quarters (Jan–Mar, Apr–Jun, Jul–Sep, Oct–Dec) (representing a total of 176-time steps), and model is iterated a quarterly time step which as treated as a model year the SS3. The time steps were used to define model "years" (of 3-month duration) enabling recruitment to be estimated for each quarter to approximate the continuous recruitment of bigeye.

An alternative model option commenced in 1952 and included the entire catch history from the history estimated a decline in stock biomass during 1952–1975 that was very similar to the level of initial depletion estimated by the 2016 reference model (Langley 2016). Another model option that partitioned the longline CPUE indices into two time periods (1953-1975 and 1979-2015) estimated a regime shift which was more likely to be caused by a model miss-specification (IOTC–WPTT18).

2.3 Definition of fisheries

The assessment adopted the equivalent fisheries definitions used in the previous SS3 stock assessment. These "fisheries" represent relatively homogeneous fishing units, with similar selectivity and catchability characteristics that do not vary greatly over time. Fifteen fisheries were defined based on

the fishing gear type and the regional stratification (Table 1). The longline fishery was split into two main components based on vessel types. The Purse seine fishery was also partitioned by the fishing mode (set type).

Freezing longline fisheries, or all those using drifting longlines for which one or more of the following three conditions apply: (i) the vessel hull is made up of steel; (ii) vessel length overall of 30 m or greater; (iii) most of the catches of target species are preserved frozen or deep-frozen. A composite longline fishery was defined in each region (LL 1N, 1S, 2,3) aggregating the longline catch from all freezing longline fleets.

Fresh-tuna longline fisheries, or all those using drifting longlines and made of vessels (i) having fibreglass, FRP, or wooden hull; (ii) having length overall less than 30 m; (iii) preserving the catches of target species fresh or in refrigerated seawater. A composite longline fishery was defined aggregating the longline catch from all fresh-tuna longline fleets (principally Indonesia and Taiwan) in region 2 (LF 2), which is where most of the fresh-tuna longlines have traditionally operated.

The purse-seine catch and effort data were apportioned into two separate method fisheries: catches from sets on associated schools of tuna (log and drifting FAD sets; PSLS) and from sets on unassociated schools (free schools; PS FS). Purse-seine fisheries operate within regions 1N, 1S, and 2 and separate purse-seine fisheries were defined in regions 1N, 1S, and 2.

A single baitboat fishery was defined within region 1N. The fishery included the pole-and-line (essentially the Maldives fishery) and small seine fisheries (catching small fish). A small proportion of the total baitboat catch and effort occurs on the periphery of region 1N, within regions 1S and 2. The additional catch was assigned to the region 1N fishery.

A Line fishery was defined within region 2, representing a mixture of gears using handlines, and small longlines (including the gillnet and longline combination fishery of Sri Lanka). Moderate handline catches are also taken in regions 1, the catch and effort from these components of the fishery were reassigned to the fishery within region 2.

For regions 1N and 2, a miscellaneous (“Other”) fishery was defined comprising catches from artisanal fisheries other than those specified above (e.g. gillnet, trolling and a range of small gears.)

Table 1: Definition of fisheries for the four-region assessment model for yellowfin tuna

Code	Method	Region	Flag	Notes
FL2	Longline, fresh tuna fleets	2	All	
LL1N	Longline, distant water	1N	All	
LL1S	Longline, distant water	1S	All	
LL2	Longline, distant water	2	All	
LL3	Longline, distant water	3	All	
PSFS1N	Purse seine, free school	1N	All	
PSFS1S	Purse seine, free school	1S	All	
PSFS2	Purse seine, free school	2	All	
PSLS1N	Purse seine, associated sets	1N	All	
PSLS1S	Purse seine, associated sets	1S	All	
PSLS2	Purse seine, associated sets	2	All	
BB1	Baitboat and small-scale encircling gears (PSS, RN)	1N	All	Primarily catch from the Maldives baitboat fishery.
LINE2	Mixed gears (hand-line, gillnet/longline combination)	2	All	Gears grouped on the basis that primarily catch large bigeye.
OT1	Other (trolling, gillnet, unclassified)	1N	All	
OT2	Other (trolling, gillnet, unclassified)	2	All	

2.4 Catch history

Catch data were compiled based on the fisheries definitions. An update of quarterly catches by fishery was provided by the IOTC Secretariat, including catches from 2016–2018 (2019-WPTT21-DATA14-BET). The time series of catches were very similar to the catch series included in the 2016 assessment except for some minor differences for a few fisheries (Figure 4). There was a small error in the previous assessment where the catches for LL 1N was off by one quarter throughout the time series (Figure 4). Total annual catches for 2016, 2017 and 2018 included in the updated catch history are 86861, 90863, 93515 mt respectively (Table 2). The total catch in 2018 is similar to the 2014 catch level.

Longline, distant-water (LL 1N, LL1S, LL2, LL3). The longline fishery operates throughout the Indian Ocean although catches are concentrated in the equatorial region (Figure 3). Catches are primarily from the Japanese, Korean and Taiwanese distant-water longline fleets. Most (62%) of the distant-water longline catch has been taken from the western equatorial region and annual catches from the LL1 fishery (LL1S and LL 1N) steadily increased from the early 1950s to reach a peak of 64,000 mt in 2003–2004. Catches of about 55,000 mt were maintained during 2005–07, declined rapidly to about 15,000 mt in 2010–2011, recovered to about 50,000 mt in 2012 and then declined to about 20000 mt in 2017–2018 (Figure 4). The catch in 2018 has been the lowest since 1975.

Annual catches from the LL2 fishery fluctuated between about 10,000–15,000 mt during 1975–2011. In the subsequent years, annual catches declined sharply to about 3,000 mt in 2018 (Figure 4).

Annual longline catches from the southern area were comparatively low, averaging about 3,000 mt, from 1960 to 1990 (Figure 4). Catches then increased to a peak of 22,000 mt in 1995, declined steadily to about 5,000 mt in 2007 and remained at that level over subsequent years.

Longline, fresh tuna fleet (FL2). The fishery developed in the late 1980s and annual catches rapidly increased to reach a peak of about 30–35,000 mt in the late 1990s–early 2000s, due to increased activity of small longliners fishing tuna to be marketed fresh. Catches declined sharply in 2003 and then again in 2010, as some vessels have moved south to target albacore. Annual catches were about 12,000–15,000 mt during 2011–2015 but decline to about 7,000–9,000 mt during 2016–2018 (Figure 4).

Purse seine (PSFS1N, PSFS1S, PSFS2, PSLS1N, PSLS1S, PSLS2). Almost all of the industrial purse-seine catch is taken within the western equatorial region (Figure 3) and catches are dominated by the fishery on associated schools (PSLS1N and PSLS1S) (Figure 4). Annual catches from the PSLS1 (N and S) fisheries reached a peak of about 30,000 mt in the late 1990s and have fluctuated at 15–25,000 mt over the last decade, with the exception of a lower catch in 2012. Since the late 1990s, annual catches from the purse-seine free-school fishery (PSFS1N and PSFS1S) have fluctuated between 5,000–10,000 mt. While the activities of purse seiners have also been affected by piracy in the Indian Ocean, the decline in catches have not been as marked as for longline fleets (IOTC 2018). Catches on the associated schools increased by more than 100% in 2018 (from 19,500 t in 2017 to about 42,900 t). Thus, the PSLS fishery has exceeded the longline fishery (19,500 mt in 2018) to become the dominant fishing mode for the bigeye tuna.

Relatively minor catches were taken intermittently by the purse-seine fisheries in the eastern equatorial region. However, there was a significant increase of catch by the PSLS in 2018 (Figure 4).

Baitboat (BB1N). Bigeye catches from the Maldives baitboat fishery are estimated to have increased steadily from a minimal level in the late 1970s to about 6–7,000 mt in recent years (Figure 4). The catch decreased significantly in 2018 (Table 2).

Line (LINE2). The LINE2 fishery includes small scale fisheries using handlines, small longlines and the gillnet/longline combination fishery of Sri Lanka. Annual catches are estimated to have increased

steadily from a minimal level in the 1970s to about 8,000 mt in recent years (Figure 4). The catch decreased significantly in 2018 (Table 2).

Other (OT1N and OT2). The "Other" fisheries include gillnet, trolling and other minor artisanal gears. The fisheries are aggregated by region for the two equatorial areas. Within the western region the OT1 fishery is primarily comprised of the Iranian driftnet fishery operating in the high seas. Total catches were negligible prior to 2005 but subsequently increased to about 2,500 mt per annum (Figure 4). The increase in catches was mainly attributed to major changes to some fleets, including increases in boat size, developments in fishing techniques and fishing grounds (IOTC 2018).

For the Other 2 (OT2) fishery, recent catches were primarily taken by the Indonesian troll and gillnet fleets. Annual catches increased steadily from the early 1990s to reach a peak of about 5,000 t in 2011–2013 (Figure 4).

Table 2: Recent bigeye tuna catches (mt) by fishery included in the stock assessment model. The annual catches are presented for 2013- 2018.

Fishery	Time period				
	2014	2015	2016	2017	2018
FL2	13 650	12 401	7 658	8 892	7 292
LL1N	7 852	7 357	4 927	3 183	2 852
LL1S	15 628	15 833	16 601	14 397	10 282
LL2	7 638	5 699	5 760	4 393	3 018
LL3	4 102	4 824	3 553	4 325	3 300
PSFS1N	907	2 227	496	4 375	1 822
PSFS1S	4 093	7 392	1 990	5 803	1 038
PSFS2	0	13	2	65	0
PSLS1N	6 896	6 839	9 201	9 308	19 461
PSLS1S	7 813	8 524	9 937	9 509	18 064
PSLS2	159	185	192	639	5 356
BB1	6 773	6 517	6 865	6 961	5 295
LINE2	10 413	11 516	10 655	10 121	7 156
OT1	2 434	2 484	3 884	4 497	5 034
OT2	4 696	4 587	5 140	4 395	3 545
Total	93 055	96 396	86 861	90 863	93 515

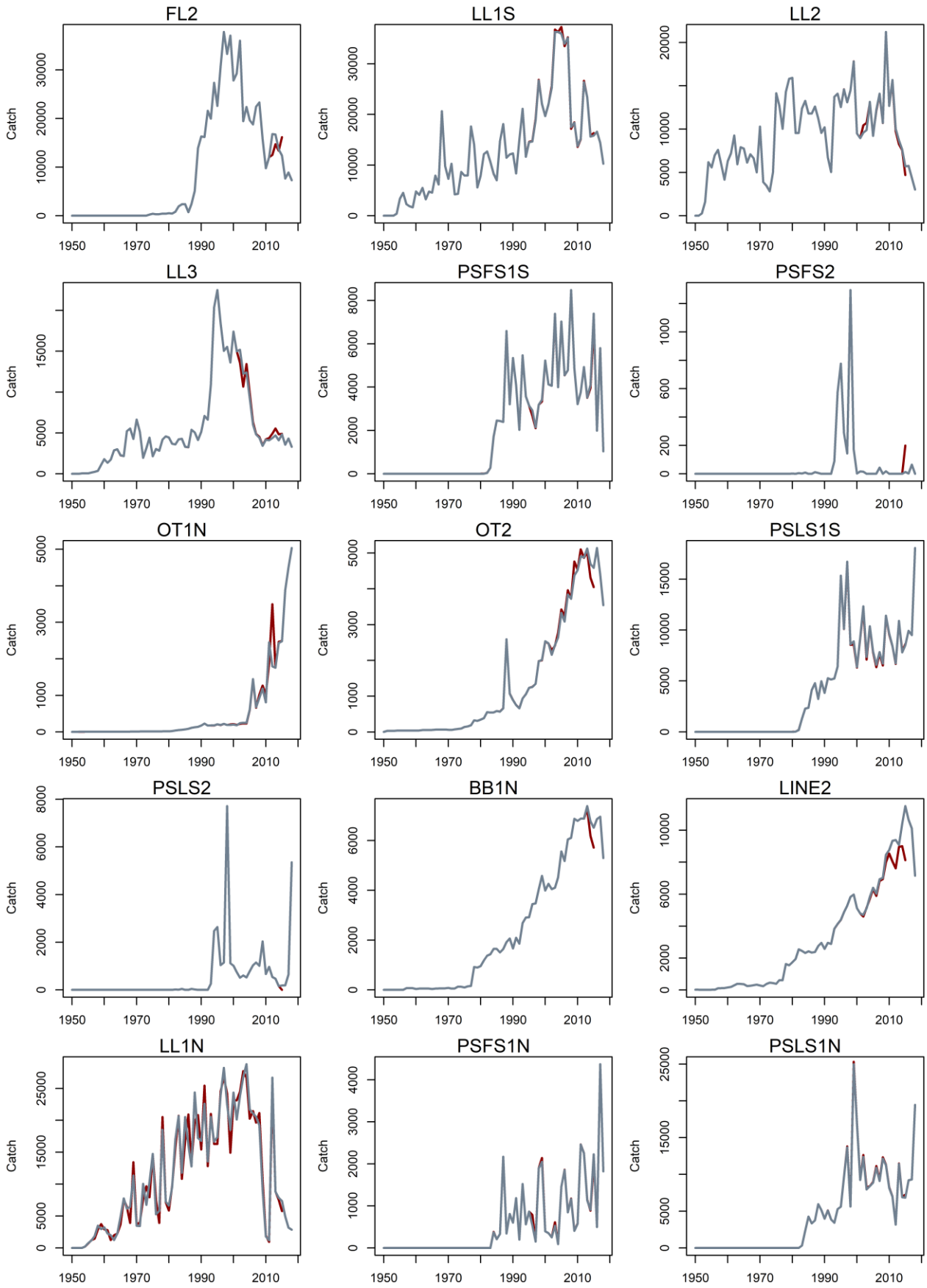

Figure 4: Fishery catches (metric tonnes) aggregated by year. Note the y-axis differs among plots. Red lines are catches used in the 2016 assessment.

2.5 CPUE indices

2.5.1 Longline CPUE

Standardised CPUE indices were derived using generalized linear models (GLM) from operational longline catch and effort data provided by Japan, Korea, Taiwan,China, and Seychlles (Hoyle *et al* 2019a, b). Cluster analyses of species composition data by vessel-month for each fleet were used to separate datasets into fisheries understood to target different species. Bigeye catch (numbers of fish) was the dependent variable of the positive catch model (lognormal error structure), while the presence/absence of bigeye tuna in the catch was the dependent variable in the binomial model. In addition to the year-quarter, models included covariates for vessel identity, 5° square location, number of hooks, and either cluster (for 3) or HBF (for regions 1N, 1S, and 2).

In 2019, several sets of CPUE indices were derived for each region based on alternative model configurations relating to treatment of vessel effects, targeting strategy, and discards. (Hoyle *et al* 2019a, b). The assessment modelling incorporated the *vessel_79nd* set of CPUE indices for the base case (Table 3). This sets of indices incorporated vessel effects for the period when individual vessel identifiers were available (1979–2018). The catch for the Twaiwanse fleet from 2005 to 2018 were adjusted for diccards estimated using commerical logbook records. However, the correction for discards is not expected to have a large impact on the inidces. (see Hoyle *et al* 2019a).

The previous assessment used the indices developed from the longer time series (1953–2015) but excluded the years prior to 1979 for a number of reasons: the decline in the indices during the late 1960s–early 1970s is inconsistent with the relatively low level of catch. The 2–3 fold increase in the indices during 1976–1978 was considered to be related to factors other than abundance (Kolody et al 2010, Langley et al 2013b, Langley 2016, Hoyle et al. 2017a).

The standardised quarterly CPUE indices are shown in Figure 5. The CPUE indices from the four regions exhibit broadly comparable trends, declining by about 65–75% from the early 1980s to 2010s. In the western equatorial region, the decline from 1979 to the early 2000s is slightly less in the southern subregion, but steeper in the northern subregion. The indices in both R1N and R1S peaked in 2011 when the main fleets returned to the main fishing ground but declined rapidly through to 2018 and is currently at the lowest level. In the eastern tropical region (R2) there is also a general decline in CPUE after 1980, with an increase in CPUE after 2010 that is much smaller than in the west. The CPUE in R2 is currently also close to the lowest level observed. For the temperate region (R3), the indices since 1990s are similar to the northern indices, with declining CPUE overall, but a suggestion of some increase since 2010. The indices were broadly similar to those used in the previous assessment except for R1N where the updated indices showed a steeper decline overall (Figure 5).

Langley (2016) showed there was some indication that the differential in CPUE in each region is correlated with the Indian Ocean Dipole Index (IODI): The strong positive IODI during 2006–2012 is correlated with the higher CPUE in region 1 (relative to region 2), while the sharp decline in CPUE in region 1 during 2013–2014 corresponded to generally negative IODI (see Langley 2016).

The CPUE indices from region 3 exhibit considerable seasonal variation, with lower CPUE in the first quarter (Jan–Mar) and relatively high CPUE in the third quarter (Jul–Sep). This seasonality is also somewhat reflected in the longline length samples, with large fish caught in the third quarter and smaller fish in the first and second quarter. Stock Synthesis does not have the flexibility to estimate seasonal catchability or movement dynamics when the model is configured based on a quarterly time step. Consequently, to account for the seasonal variation in the CPUE indices, the Region 3 CPUE indices were incorporated in the model as four separate sets of abundance indices (i.e. one series for each quarter). It might be useful to explore alternative temporal structures (e.g. year-season) in the future to

explicitly model seasonal dynamics (e.g. movement).

The very large recent spike in bigeye catch rates in the western tropical Indian Ocean 2011–12 has some similarities to the 1976–78 peak. It is believed to have occurred when vessels returned to the area that had been unfished for several years due to piracy. It may have reflected a major increase in catchability as a result of changes in population density, fishing effort, and/or fish behaviour (Hoyle et al. 2017a).

For the regional longline fisheries, a common catchability coefficient was estimated in the assessment model, thereby, linking the respective CPUE indices among regions. This significantly increases the power of the model to estimate the relative (and absolute) level of biomass among regions. However, as CPUE indices are essentially density estimates it is necessary to scale the CPUE indices to account for the relative abundance of the stock among regions. For example, a relatively small region with a very high average catch rate may have a lower level of total biomass than a large region with a moderate level of CPUE. The approach used was to determine regional scaling factors that incorporated both the size of the region and the relative catch rate to estimate the relative level of exploitable longline biomass among regions. The scaling factors used in the previous assessment were derived from the Japanese longline CPUE data from 1981–2000 (R1N 0.50, R1S 0.50, R2 0.87, R3 0.83).

Hoyle & Langley (2018) revised the estimates of regional weighing factors for IO tropical tuna spcies using a standardiation model based on aggretated longline catch effort data. The authors recommended the estimates by method ‘8’ for the period 1979–1994. The relative scaling factors calculated are R1N 0.63, R1S 0.80, R2 1.00, R3 0.63. The revised scaling factors were adopted for the current assessment.

For each of the principal longline fisheries, the GLM standardised CPUE index was normalised to the mean of the period for which the region scaling factors were derived (i.e. the GLM index from 1979–1994). The normalised GLM index was then scaled by the respective regional scaling factor to account for the regional differences in the relative level of exploitable longline biomass among regions.

Table 3: the individual sets of CPUE indices used for each model region for the base case model.

Region		Model variables	Indices series name
1N		No cluster, HBF	*Joint_regB3_R5_dellog_vesselid_79nd*
1S		No Cluster, HBF	*Joint_regB3_R1_dellog_vesselid_79nd*
2		No Cluster, HBF	*Joint_regB3_R2_dellog_vesselid_79nd*
3		cluster, HBF	*Joint_regB3_R3_dellog_ vesselid_79nd*

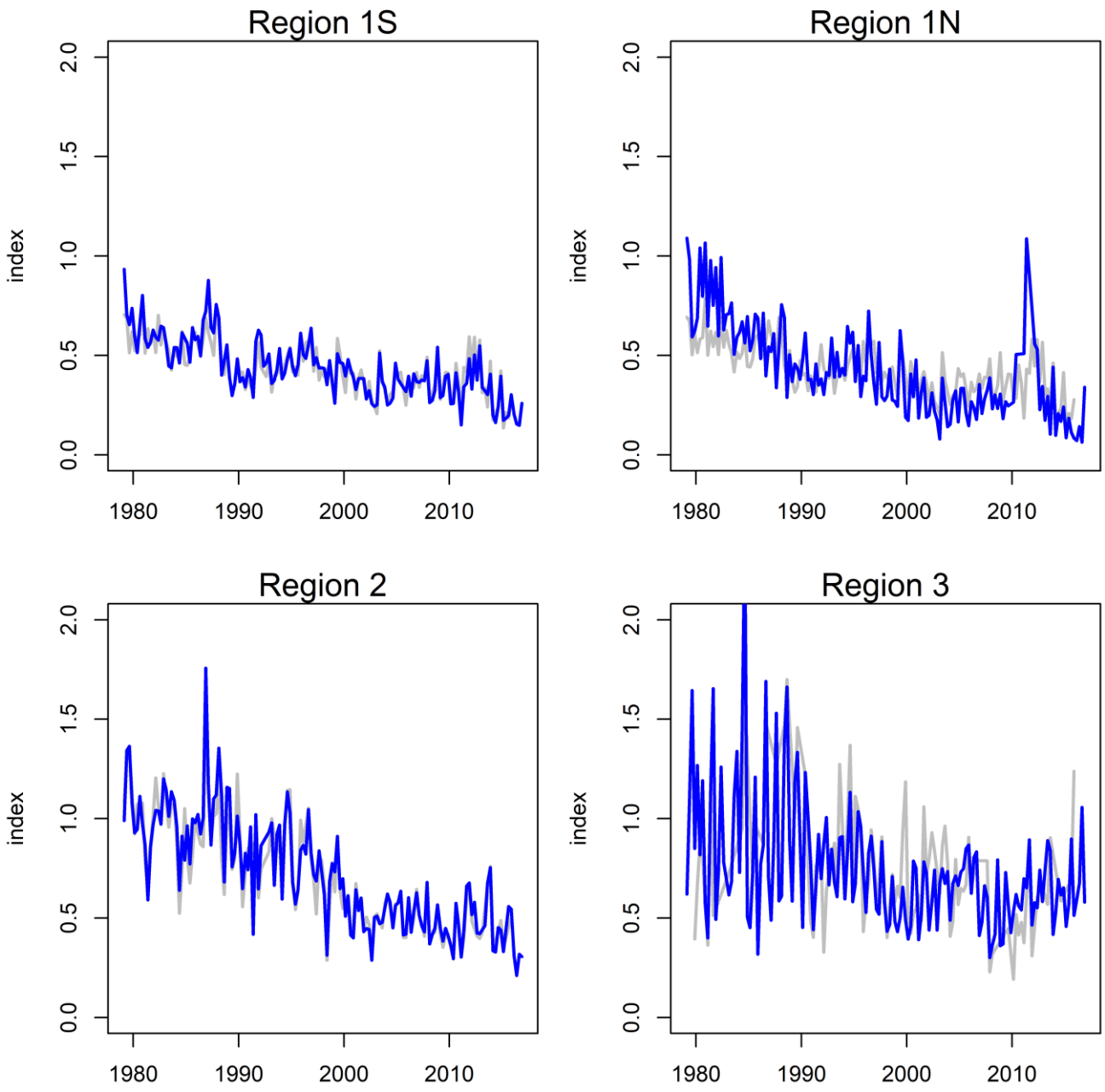

Figure 5: A comparison of the longline CPUE indices included in the 2016 stock assessment (grey line) and the 2019 stock assessment (blue line). The 2016 indices are rescaled to have the same mean of the 2019 indices for each region. The same indices were used for both region 1N and 1S in the 2016 stock assessment.

2.6 Length frequency data

Available length-frequency data for each of the defined fisheries were compiled into 95 2-cm size classes (10–12 cm to 198–200 cm) and were aggregated to provide a composite length composition for each year/quarter. Each length frequency observation for purse seine fisheries represents the number of fish sampled raised to the sampling units (sets in the fish compartment) while for fisheries other than purse seine each observation consisted of the actual number of bigeye tuna measured. Each aggregated length sample was assigned an initial sample size. The sample size was determined based on the number of fish included in the aggregated sample, up to a maximum of 1000. The sample size was then divided by 100 resulting in a maximum initial sample size of 10. Purse seine length samples were also assigned

an initial sample size of 10. A graphical representation of the availability of length samples is provided in Figure 6.

Longline, distant-water (LL 1–3). Size frequency data are available for the LL1−3 fisheries from 1965 to 2018. Prior to 1995, the length compositions were dominated by sampling from the Japanese longline fleet, while in the subsequent period the size data were increasingly dominated by data collected from the Taiwanese distant-water longline fleet. In recent years, length frequency data were also collected from locally based longline fleets (e.g. Seychelles).

Length and weight data were collected from sampling aboard Japanese commercial, research and training vessels. Weight frequency data collected from the fleet have been converted to length frequency data via a processed weight-whole weight conversion factor and a weight-length key. While in recent years most of the samples available have come from scientific observers on commercial vessels, in the past samples came from training and research vessels, and commercial vessels. Matsumoto (2016) suggested that length distribution was similar between sampling sources (commercial and non-commercial vessels) or platform (fishermen, scientists, observers) in the Indian Ocean. Length frequency data from the Taiwanese longline fleet are also available from 1980−2018. Length samples from this component come from commercial vessels and include lengths recorded by fishermen and, to a lesser extent, lengths measured by scientific observers on some of those vessels.

Previous assessments of IO bigeye tuna have highlighted the temporal variability in the length composition data from the main longline fisheries. Langley (2016a) examined the longline length data to investigate potential sources of variation in fish length. For the LL 1 area, there were marked differences in the sizes of fish sampled from the various longline fleets during the late 1980s and early 2000s. There were also divergent temporal trends in the lengths of fish sampled amongst the fleets (see Figure A1 of Langley 2016a). A similar trend is also apparent in the length composition data from the eastern equatorial region. Following Langley (2016a), the length data were restricted to the main area of catch from the bigeye tuna longline fishery (core area) for each model region. It was considered that restricting the sampling data to the core area would minimise potential variation in length composition attributable to the collection of length samples from the periphery of the fishery (Langley 2016a). The core areas for each region were defined as follows (there is a slight revision to the boundaries following the examination of the catch effort data).

LL1	Latitude range 10°S to 10° N, longitude 50° E to 70° E (inclusive)
LL2	Latitude range 15°S to 5° S, longitude 85° E to 110° E (inclusive)
LL3	Latitude range 35–25° S (inclusive)

The lengths of fish sampled from the Taiwanese fleet increased markedly during the early 2000s and the length compositions of the samples from catches of most fleets were comprised of larger fish during 2005–2015 (see Figure A1 Appendix 1 of Langley 2016). The increase in Taiwanese fish sizes during the period coincided with a large shift in the ratio of the Taiwanese bigeye and yellowfin longline catches in the region during the same period; the ratio of bigeye in the longline catch increased during the late 2000s and remained at a higher level in the subsequent years (Hoyle et al 2015, see Figure 20). A review of the recent Taiwanese length composition data by Geehan & Hoyle (2013) recommended "*excluding from stock assessments the size data for BET, YFT and ALB from the Taiwanese DWLL fleet after the early-2000s, until the cause of changes in the size frequency data have been determined by the WPTT*".

Based on that recommendation, the recent length frequency data from the Taiwanese longline logbooks were excluded from the final length frequency data sets. The period of data exclusion was also extended to 1997, encompassing the period of considerable change in the length composition from the region 1

longline fishery. The length data collected by scientific observers in the period 2005–2018 were included in the assessment.

For the final data sets, the length compositions of the LL1–3 fisheries are dominated by fish in the 90−150 cm length range (Figure 7). The aggregated length compositions are comparable for the three regions, although the average lengths of fish in the sampled catch fluctuated over the study period (Figure 8). For LL1N &1S, average fish length declined during the early 1990s. Limited samples were available from LL1 during 1997−2005 but fish sampled in the subsequent years (2006−2015) were considerably larger than sampled during the preceding period (Figure 8). Relatively few samples were available from LL2 and LL3 during the latter period.

Longline, fresh tuna fleet (FL2). Length and weight data were collected during the unloading of catches at several ports, primarily from fresh-tuna longline vessels flagged in Indonesia and Taiwan/China (IOTC-OFCF sampling). Length data from 1998−2008 were included in the previous assessment. But most samples were subsequently found to be biased (F. Fiorellato per. comm., IOTC Secretariat). For the current assessment, only nine years of data are included (2002, 2003, 2012–2018).

The composite length composition of the catch is similar to the distant water longline fleet (Figure 7) and remained relatively stable over the sampling period except in 2012 when there are larger fish in the samples (Figure 8).

Purse seine (PSFS1, PSFS2, PSLS1, PSLS2). Length-frequency samples from purse seiners have been collected from a variety of port sampling programmes since the mid-1980s. The samples are comprised of large numbers of individual fish measurements and represent comprehensive sampling of the main period of the fishery (Figure 6). Limited size data are available from the purse-seine fisheries within region 2.

The associated purse-seine fishery (PSLS) primarily catches smaller bigeye tuna, while the size composition of the catch from the free-school fishery is bimodal, being comprised of the smaller size range of bigeye and a broad mode of larger fish (Figure 7). There was a general decline in the average length of fish caught by the PSLS1 fishery from 1990 to 2018 (Figure 8). The average size of fish sampled from the free-school fishery was variable among quarters, although fish tended to be smaller during the late 2000s, increased during the early−mid 2000s and in more recent years. It is unknown whether the trends in the length composition of the purse seine catch are representative of the population or reflect changes in the operation of the fishery.

Baitboat (BB1). Limited length samples are available from the fishery (Figure 6) and the sampled catch was dominated by fish in the smaller length classes (50−70 cm) (Figure 7 and Figure 8).

Line (LINE2). Negligible length frequency data are available from the fishery although the available data indicate that the catch was predominantly composed of larger fish (Figure 7). Fish sampled from this fishery are considerably larger than the fish sampled from the other main longline fisheries.

Other (OT1 and OT2). While catches from the OT1 fishery are dominated by the Iranian driftnet fleet, there are no length samples available from this component of the fishery. Instead, the available OT1 length samples were collected from the 'other' fisheries that operated prior to 2005 (Figure 6). The aggregate length samples encompass a broad length range (Figure 7).

For the Other 2 (OT2) fishery, limited length samples were collected from the Indonesian small purse seine and troll fisheries (Figure 6). The aggregate length frequency data available include two size modes from the small scale purse seine samples (Figure 7). This is probably due to different sizes of fish taken by different modes of fishing (e.g. fishing at night with light, around anchored FADs, etc.).

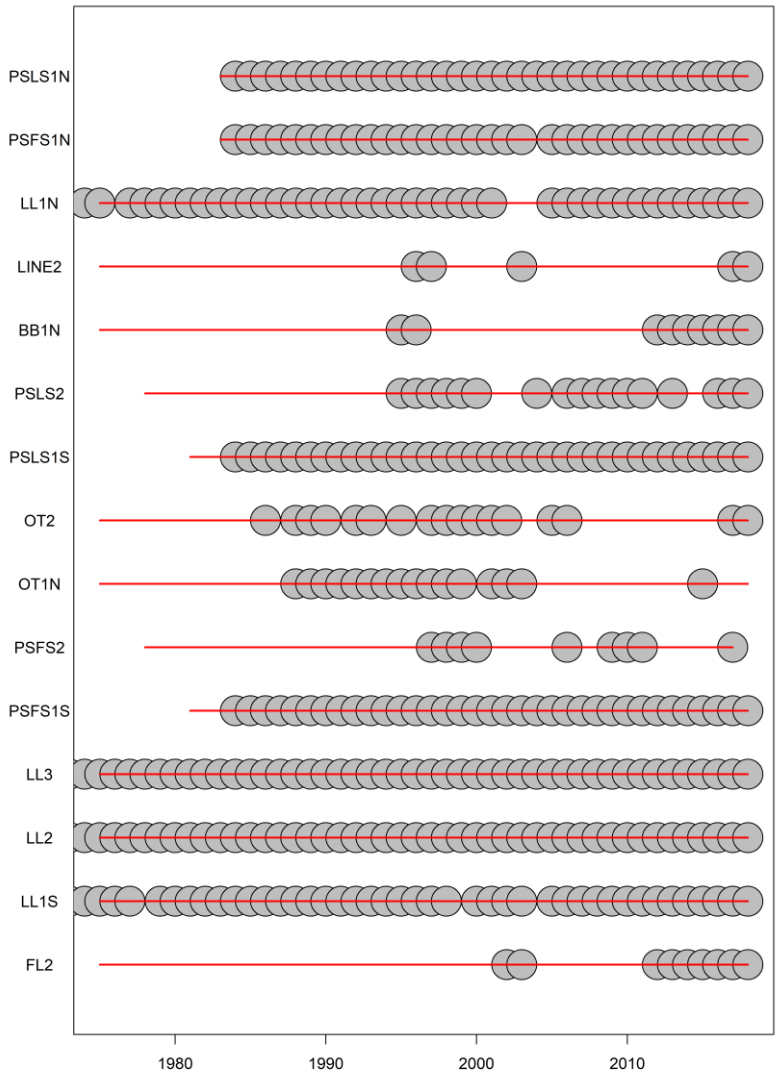

Figure 6: The availability of length sampling data from each fishery by year. The grey circles denote the presence of samples in a specific year. The red horizontal lines indicate the time period over which each fishery operated.

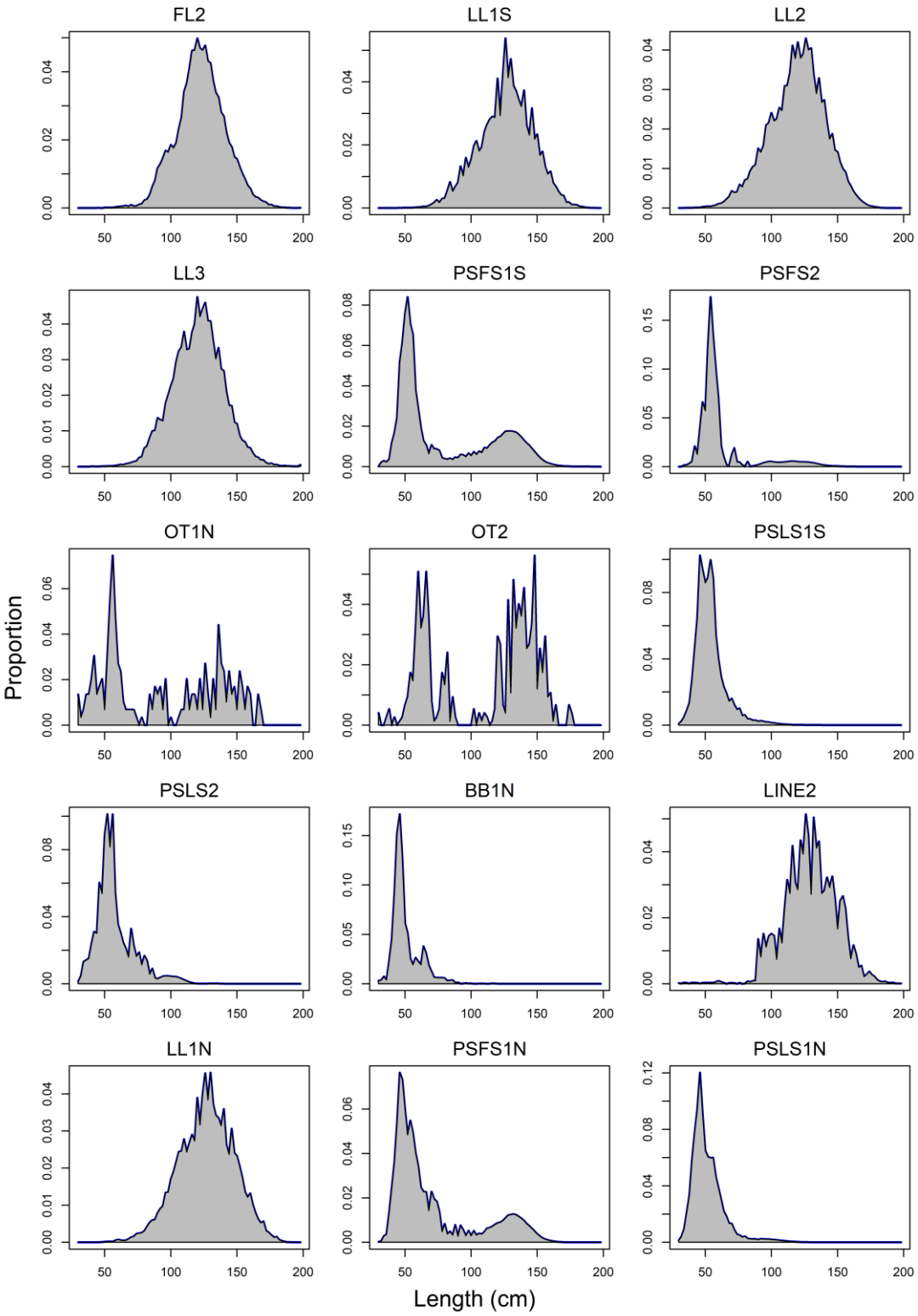

Figure 7: Length compositions of bigeye tuna samples aggregated by fishery.

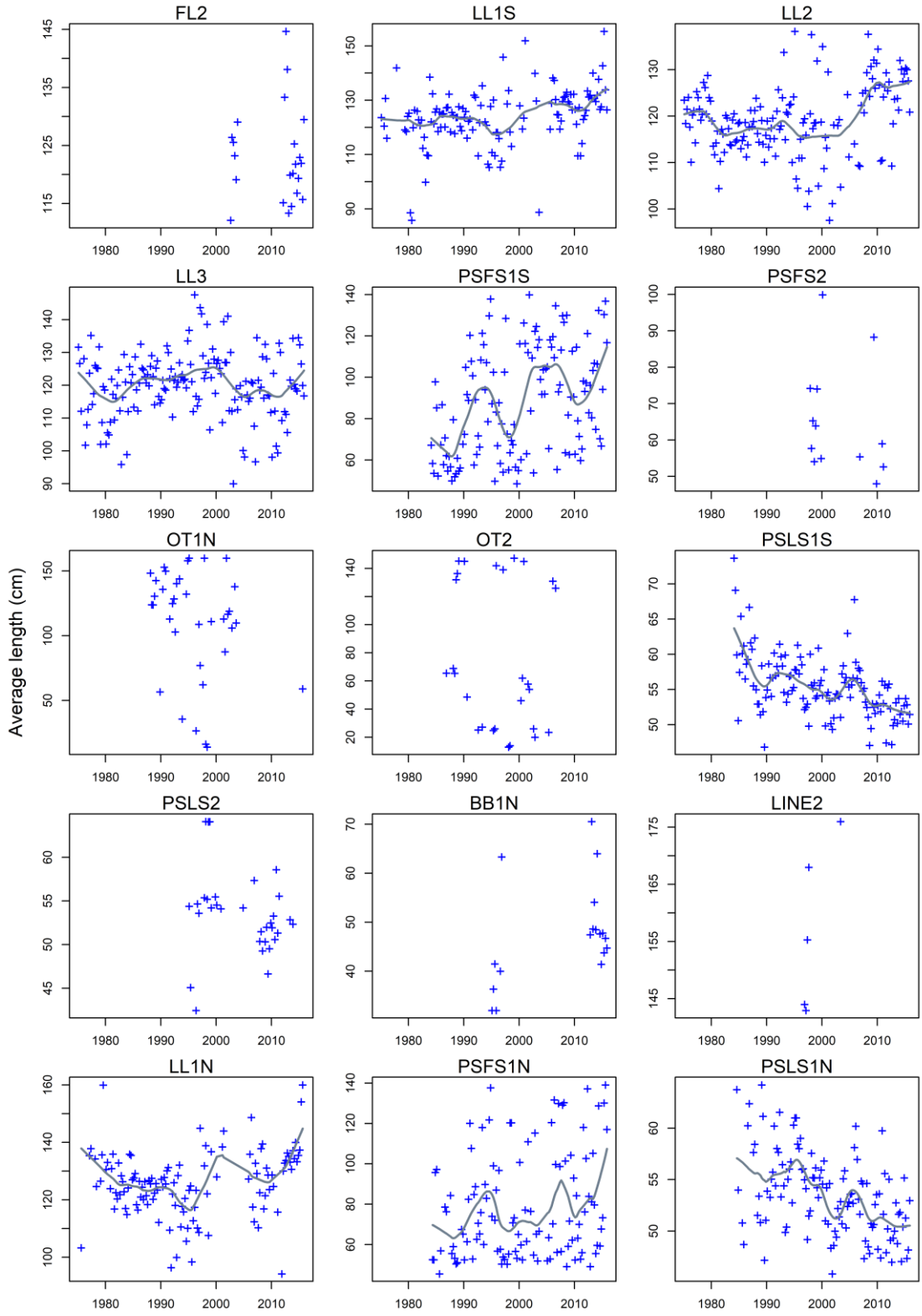

Figure 8: Mean length (fork length, cm) of bigeye sampled from the principal fisheries by year quarter. The grey line represents the fit of a loess smoother to each dataset.

2.7 Tagging data

A considerable amount of tagging data was available for inclusion in the assessment model. The data used consisted of bigeye tuna tag releases and returns from the Regional Tuna Tagging Project-Indian Ocean (RTTP-IO) phase of the Indian Ocean Tuna Tagging Programme (IOTTP). Tags were released during 2005–2007 and recoveries were monitored by the IOTTP during 2005–2009 and by the IOTC in the subsequent years.

A total of 34,478 bigeye tuna were released by the RTTP-IO program (removed tagged fish with unknown length). All the bigeye tag releases of the RTTP-IO occurred in a localized area off the Tanzania coast within the western equatorial region (region 1S) (Figure 9). Most of the releases occurred during the second and third quarters of 2006 and the third quarter of 2007 (Figure 10).

In total, 5674 tag recoveries (removed tags with unknown recovery dates) could be assigned to the fisheries included in the model. A relatively high proportion of tag recoveries occurred in the vicinity of the main release location (Figure 9). There was also a relatively large number of tags recovered from bigeye tuna catches from the Mozambique Channel. Overall, most of the tags were recovered in the home region, some recoveries occurred in adjacent regions, particularly region 1N. A very small number of tags were recovered in regions 2 and 3 (less than 1%) (Table 4).

Most of the tag recoveries occurred between mid-2006 and 2008 (Figure 11). The number of tag recoveries started to attenuate in 2009 although small numbers of tags were recovered up to the end of 2015. Most of the recaptures near main release locations were from purse seine associated sets during 2007 and were comprised of tagged fish at liberty for 6–12 months. Recoveries from the purse seine fishery for fish at liberty for at least 12 months were more evenly distributed over the main area fished by the purse seine fleet.

A significant proportion of the tag returns from purse seiners were not accompanied by information concerning the set type. These tag recoveries were assigned to either the free-school or FAD fishery based on the assumed age of the fish at the time of recapture; i.e. based on the age assigned to the release group and the period at liberty. Fish “older” than 12 quarters were assumed to be recaptured by the free-school fishery; “younger” fish were assumed to be recovered by the FAD set fishery.

Langley (2016) identified considerable differences in the recovery rate (number of tags per tonne of catch) from the PSLS fishery amongst latitudinal zones for tags at liberty for at least 12 months (Tag recovery rates from south of 2°S were consistently higher than from north of 2°S during the main recovery period). The difference in tag recovery rates between the two main areas of the fishery indicates that the dispersal of tagged bigeye during the 12 month “mixing period” was insufficient to redistribute tagged fish throughout the bigeye population resident within the western equatorial region (Region 1). Consequently, the distribution of PSLS fishery effort (and catch) would have strongly influenced the number of tags recovered from the fishery. Following Langley (2016), the western equatorial region has been partitioned into two regions (Region 1N and Region 1S) in the assessment model account for the potential incomplete mixing of tagged fish.

For incorporation into the assessment model, tag releases were stratified by release region, time period of release (quarter) and age class. The returns from each tag release group were classified by recapture fishery and recapture time period (quarter). The tag data were further adjusted for tag losses and reporting rates to minimize the bias on estimates of fishing mortality and abundance in the assessment model. The procedure is described in below.

Age assignment of tag release. In the previous assessment the numbers of fish in each age at release were determined by applying an age-length key to the length composition of the tagged fish. The age-length key was derived by assuming an equilibrium population age-length structure based on the age-

specific natural mortality, average length-at-age from the growth function (see Section 3.1.2) and the standard deviation of length-at-age (CV 0.1).

The age-length key approach intended to admit the uncertainty in the size distribution at age. However, the probabilistic conversion from age to length for individual tag observations could result in multiple realisations of the tagging datasets which have different recovery history for a given release age. Therefore, for the current assessment the age at release was assigned based on the mean growth function. The uncertainty arising from the length-age conversion is evaluated using a bootstrap approach through a model ensemble (n=10) in which the age at tag release is resampled from the underlaying age-length key for each of the models.

Tagging mortality. The number of tags in each release group was reduced by 30% to account for initial tag mortality. The initial tag mortality estimates of 20.5% was increased by a further 10% to account for an assumed level of tag mortality associated with the best (base) tagger (Hoyle *et al* 2015)**.**

Reporting rate. The results of the tag seeding experiments conducted during 2005–2008, have revealed considerable temporal variability in tag reporting rates from the IO purse-seine fishery (Hillary *et al.* 2008a). Reporting rates were lower in 2005 (57%) compared to 2006 and 2007 (89% and 94%). Quarterly estimates were also available and were similar in magnitude (Hillary *et al.* 2008b). This large increase over time was the result of the development of publicity campaign and tag recovery scheme raising the awareness of the stakeholders, *i.e.* stevedores and crew. SS3 assumes a constant fishery-specific reporting rate. To account for the temporal change in reporting rate, the number of tag returns from the purse-seine fishery in each stratum (tag group, year/quarter, and length class) were corrected using the respective estimate of the annual reporting rate (Langley 2016).

Following Kolody (2011), Fu (2017), and Fu et al. (2018), a slightly revised approach was used to correct for tag reporting from the Purse seine fishery: tags recovered at-sea are assumed to have a 100% reporting rate; tags recovered from landings in Seychelles were corrected for the quarterly estimates of reporting rates from Hillary *et al* (2008b). The tag recoveries were further increased by the proportions of EU PS catches landed outside the Seychelles, to account for purse-seine catches that were not examined for tags. For example, the adjusted number of observed recaptures for a PSLS fishery as input to the model, R'_L was calculated using the following equation:

$$R'_L = R_L^{sea} + \frac{R_L^{sez}}{P^{sez} r^{sez}}$$

where

R_L^{sea} = the number of observed recaptures recovered at sea for the PSLS fishery.
R_L^{sez} = the number of observed recaptures recovered in Seychelles for the PSLS fishery.
r^{sez} = the reporting rates for PS tags removed from the Seychelles
P^{sez} = the scaling factor to account for the EU PS recaptures not landed in the Seychelles.

The adjusted number of observed recaptures for a PSFS fishery was calculated similarly. A reporting rate of 94% was assumed for the correction of the 2009−2015 tag recoveries. The numbers of tag recoveries were also adjusted for long-term tag loss (tag shedding) based on an analysis by Gaertner and Hallier (2015). Tag shedding rates for bigeye tuna were estimated to be approximately 1.7% per annum.

A total of 34 427 releases were classified into 62 tag release groups. Most of the tag releases were in the 5−12 quarter age classes (Figure 10) A total of 5,701 actual tag recoveries were included in the tagging data set. The cumulative effect of processing the tag recovery data increased the number of recoveries to 6,788 tags.

Table 4: Tag recoveries by year of recovery (box), region of release (vertical), and region of recovery. Region of recovery is defined by the definitions of the fisheries included in the model.

Recovery year	Release region		Recovery region		
		1S	1N	2	3
2005	1S	6	5		
2006	1S	478	256	4	1
2007	1S	2407	613		3
2008	1S	1191	160		9
2009	1S	178	18	3	13
2010	1S	107	8	2	15
2011	1S	36	17	2	15
2012	1S	72	14		5
2013	1S	13			1
2014	1S	11			
2015	1S	10			1

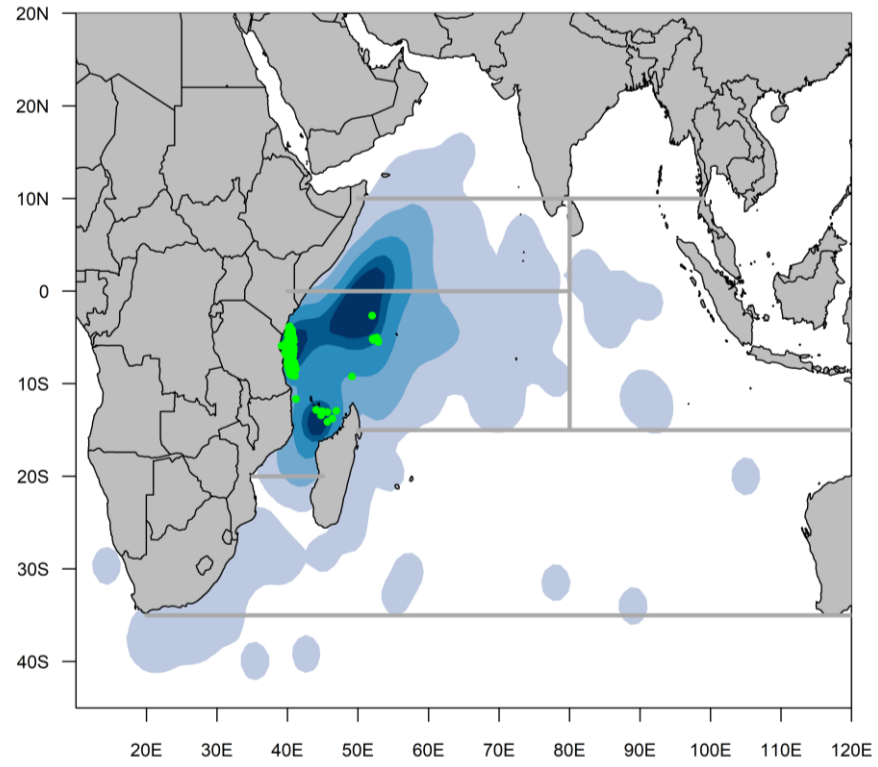

Figure 9: Location of releases (green) and density of recoveries for the bigeye tuna RTTO-IO tag Program

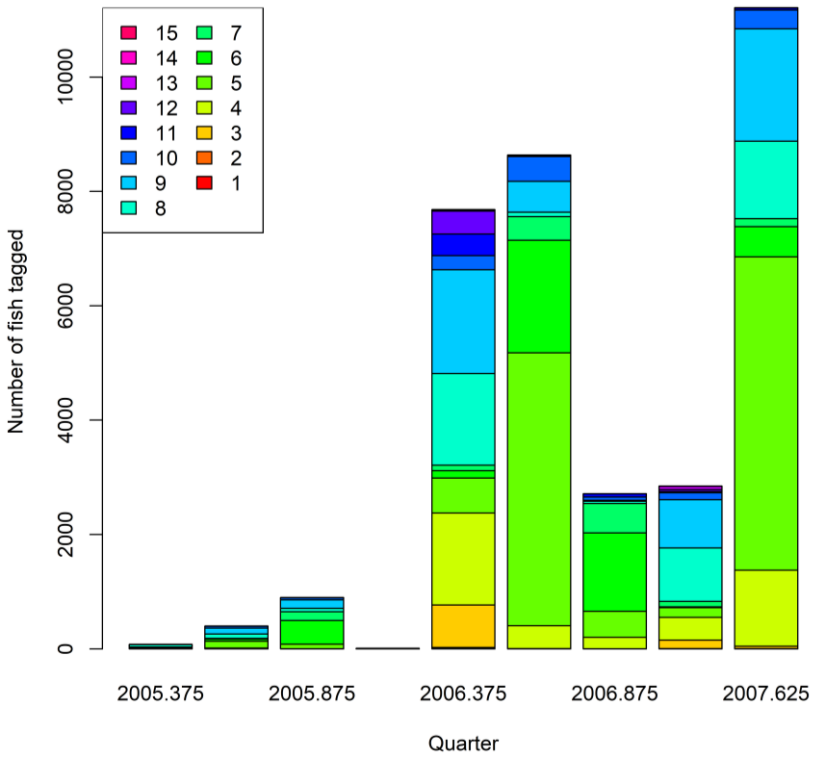

Figure 10 : Number of tag releases quarter and age class included in the assessment data set. Al tag releases occurred in region 1S. Ages were assigned based on the length.

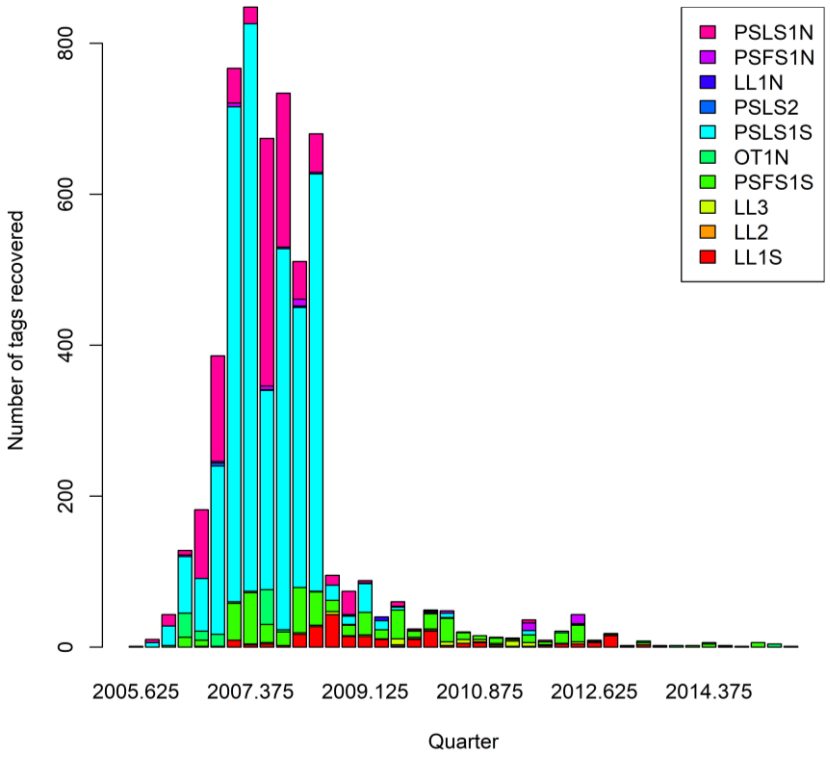

Figure 11: Bigeye tag recoveries by year/quarter and fishery included in the assessment model. Purse seine tag recoveries have not been corrected for reporting rate.

3. MODEL STRUCTURAL AND ASSUMPTIONS

3.1 Population dynamics

The model population structure is comprised of 41 quarterly age classes; the first age class represents fish aged 0–3 months (age 0) and the last age class accumulates all fish age 40+ quarters. The population is aggregated by sex and partitioned by region.

The model commences in 1975 and extends to the end of 2018 in quarterly intervals (176 time steps). The initial (1975) age structure of the population was assumed to be in an exploited, equilibrium state. The four main LL fisheries were operating prior to 1975 and initial fishing mortality parameters were estimated for each of these fisheries, based on early catches and size structure in the commercial catches in the early years. The resulting fishing mortality rates are applied to determine the initial numbers-at-age in each model region.

3.1.1 Recruitment

Recruitment of 0 age fish occurs in each quarterly time step of the model. Recruitment was estimated as deviates from the BH stock recruitment relationship (SRR) for 1985–2017 (132 deviates). The recruitment deviates were estimated for the period that corresponds to the operation of the PSLS fishery which provides catch and length data for the smaller fish and, hence, may be informative regarding the variation in recruitment. Recruitment deviates were assumed to have a standard deviation (σ_R) of 0.6. The final model options included three (fixed) values of steepness of the BH SRR (h 0.7, 0.8 and 0.9). These values are considered to encompass the plausible range of steepness values for tuna species such as bigeye tuna and are routinely adopted in tuna assessments conducted by other tuna RFMOs (Harley 2011, ISSF 2011).

The recruitment for bigeye remains uncertain as the areas where larvae and early juveniles are concentrated have never been sampled nor studied by scientists (Fonteneau 2004). As the temperate regions are generally believed to be feeding grounds, in the previous assessment recruitment was assumed to occur in the equatorial regions only. This means the model relies on migration to estimate pre-recruit to the southern region. In the current assessment, recruitment is assumed to occur in all regions (hence differentiating between recruitment into the population, vs. spawning).

The overall proportional distribution of recruitment among the four regions was estimated. There is little information to indicate that there are significant differences in the pattern of recruitment between the regions; i.e. the CPUE trends are broadly comparable between the equatorial regions and the length composition data from the longline fisheries do not appear to be informative regarding recruitment. Length composition data from the small fish fisheries are available from the western equatorial regions only. The relative distribution of recruitment between the four regions (1N, 1S, 2, 3) was initially assumed to be temporally invariant. However, regional recruitment distribution was allowed to vary for 2005–2018 in the reference model, to account for as the divergent regional CPUE trends in more recent years.

3.1.2 Growth and Maturation

Eveson *et al* (2012) derived estimates of Indian Ocean bigeye tuna growth from otolith age data and tag release/recovery. Growth estimates are available for both sexes combined (an updated analysis by Eveson *et al* (2015) estimated very similar growth parameters for males and females). The quarterly growth deviates from a von Bertalanffy growth function with considerably lower growth for quarterly age classes 4–8 (Figure 12–left). Maximum average length (L_∞) was estimated by Eveson *et al* (2012) at 150.9 cm (fork length). The growth model was unable to reliably estimate the standard deviation of length-at-age; however, the most appropriate level of variation in length for all age classes was considered to be represented by a coefficient of variation of 0.10 (P. Eveson, pers. comm.). The growth function was implemented in SS using age-specific deviates on the *k* growth parameter.

The size of sexual maturity was equivalent to that applied by Shono et al (2009) and used in the subsequent assessments. Female fish were assumed to attain sexual maturity from 100 cm (F.L.) with full sexual maturity at about 125 cm (Figure 12–right). In recent years, additional histological data have been collected from IO bigeye tuna and these data may enable a re-evaluation of the maturity ogive (Emmanuel Chassot *pers. comm.*)

The length-weight relationship in previous assessments (Shono *et al* 2009, Kolody *et al* 2010, Langley *et al* 2013, Langley 2016) were based on estimates derived by Nakamura and Uchiyama (1966) (Fish weight = a.length^b, a = 3.661 x 10^{-5} , b = 2.901 where weight is in kilograms and length is in centimetres). The current assessment used updated estimates by Chassot et al. (2016) a=2.217 x 10^{-5}, b= 3.01211). The effect of this change was assessed.

.

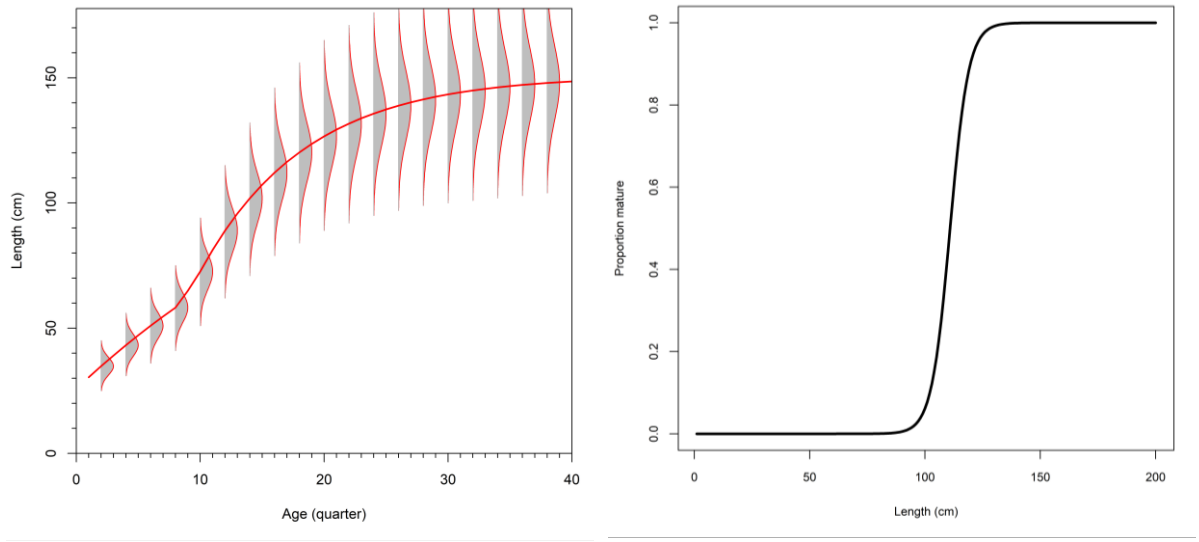

Figure 12: Fixed growth function for bigeye tuna following Eveson et al. 2012 (left) and length-based maturity Ogive following Shono et al (2009). For the growth function, the red line represents the estimated mean length (FL, cm) at age and the grey area represents the assumed distribution of length at age).

3.1.3 Natural mortality

Following Langley (2016), two alternative levels of age-specific natural mortality were considered in the assessment. The higher level of natural mortality is comparable to IATTC and WCPFC bigeye tuna stock assessments with relatively high natural mortality for the younger age classes and natural mortality of about 0.1 per quarter for the adult age classes (Figure 13). A lower level of natural mortality was proposed based on a Lorenz curve analysis with a lower natural mortality for the adult age classes (0.0625 per quarter) (Figure 13). This is comparable to the level of natural mortality assumed for Atlantic bigeye tuna in the recent ICCAT stock assessment by (ICCAT 2015). This relationship between M and age/size (high M for juveniles and low M for adults) are well established for tuna (Hampton 2000) and corresponds well with some of the biological factors contributing to the variability of natural mortality of tuna (Fonteneau & Pallares 2004).

From the RTTP, a considerable number of tagged fish were captured after 7–8 years at liberty, indicating a considerable proportion of the tagged fish had reached an age of 8–10 years; 8 tags were recovered after 10 years at liberty and a few tags were recovered during the most recent year (2015), corresponding to an age at recovery of 11–12 years. The higher level of natural mortality would result in a very small proportion of the tagged fish reaching 12 years of age, suggesting that the lower level of natural mortality may be more plausible. The lower level of M is also supported by the aging study of bigeye tuna in the eastern and western Australia water which suggested the longevity of bigeye is more than the 8–10 years which were the maximum age commonly thought (Farley et al. 2004)

Langley (2016) found that model options that included the lower level of natural mortality yielded lower tag likelihood values, indicating that the number of tag recoveries, primarily from the PSLS fishery, were more consistent with lower levels of *M*. Nonetheless, considerable caution should be placed on model based inferences of natural mortality due to potential biases in the tag recovery process, particularly related to the extent of tag mixing, and potential confounding between the estimation of natural mortality and other model parameters (especially selectivity, recruitment and movement). For the current assessment, the lower level of natural mortality was given priority based on the minimum estimates of longevity obtained from the maximum periods at liberty for tagged fish.

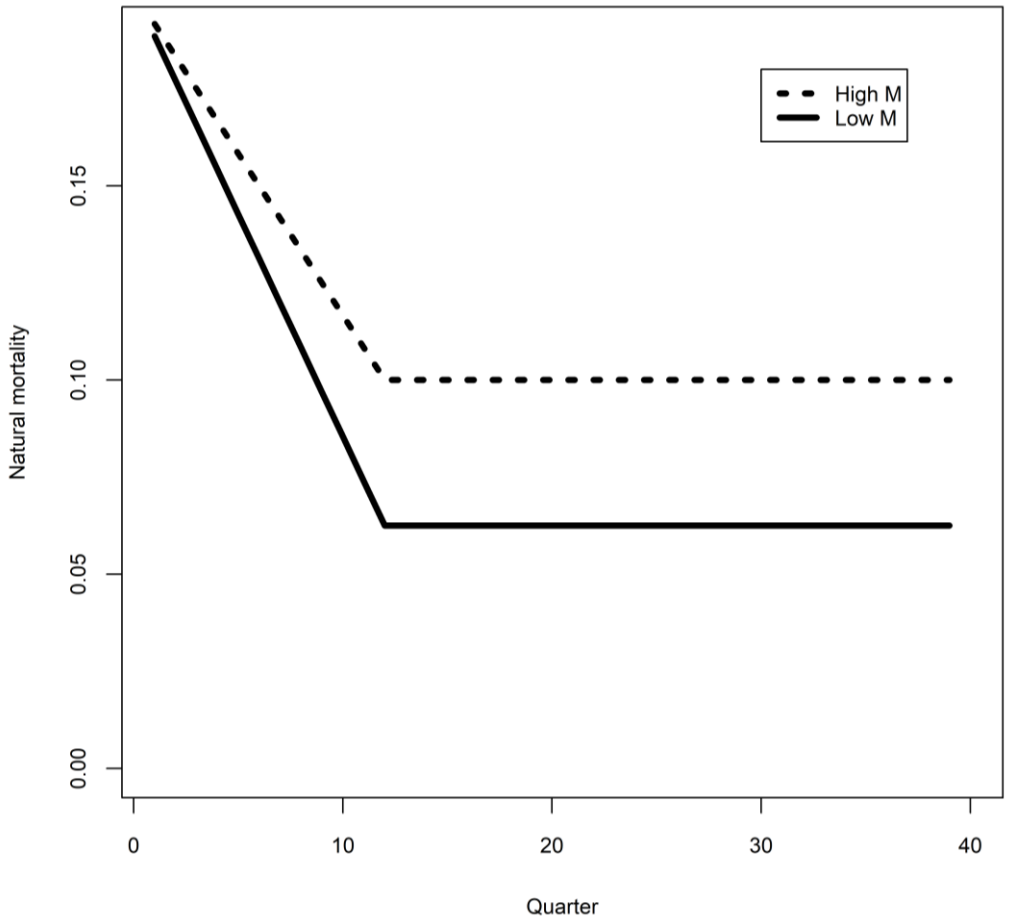

Figure 13: Age specific natural mortality (per quarter) patterns assumed for the highM and lowM assessment model options.

3.1.4 Movement

In Stock Synthesis, movement is implemented as the proportional redistribution of fish amongst regions, including the proportion remaining in the home region. The redistribution of fish occurs instantaneously at the end of each model time step (quarter).

Movement of fish was estimated amongst the four model regions. Movement was parameterised to estimate differential movement from young (8 quarters) to old (≥15 quarters) fish to approximate potential changes in movement dynamics associated with maturation. For each movement transition, two separate movement parameters were estimated (for young and older fish). A linear interpolation between the age specific movement rates was applied to determine movement of the intermediate age classes. Fish younger than age 3 quarters were assumed to remain within the natal region. Movement rates were assumed to be temporally invariant.

3.2 Fishery dynamics

Age based selectivity were assumed for all fisheries. Selectivity is more likely to be a length-based process for most gears. However, as the model has adopted a quarterly resolution, the age selectivity is considered adequate in approximating the length-based process. A common selectivity function was estimated for the four main longline fisheries (LL1N, 1S, 2, 3) using a logistic function. A logistic selectivity was also assumed for the FL2 longline fishery.

The selectivities of the PSLS and BB fisheries were estimated using a double normal functional form. Separate selectivity functions were estimated for the PSLS1N and PSLS1S fisheries. For the PSLS1N and PSLS1S fisheries, there was a marked shift in the length composition of the fishery catch in the mid-2000s. Langley (2016) explored the modelling option of accounting for the apparent change in the selectivity of the PSLS1 fishery by including two time blocks (1975–2005 and 2006–2015) for the estimation of the selectivity parameters related to the age of the peak selectivity and the width of the ascending limb of the selectivity. The temporal shift in selectivity was not included in the final model options.

To account for the bimodal length composition of the catch from the PSFS fishery, the selectivity was modelled using a cubic spline with 6 nodes. The selectivity of the PSFS1N and PSFS1S fisheries was assumed to be equivalent.

Limited data were available to estimate the selectivity of either the PSLS2 or PSFS2 fisheries. The selectivity of these fisheries was constrained to be equivalent to the corresponding fishery selectivity in the western equatorial region 1S.

Limited size data are available from the "Other" fisheries. During the previous assessment, attempts to estimate independent selectivities for these fisheries were not successful, partly due to the variability in the length composition between samples. In aggregate, the length compositions are bimodal and similar to the length composition from the PSFS fishery. On that basis, the selectivities for the two "Other" fisheries (OT1 and OT2) were assumed to be equivalent to the PSFS fishery. Similarly, limited length data are available for the LINE2 fishery and the selectivity was assumed to be equivalent to the main longline fishery.

Fishing mortality was modelled using the hybrid method that estimates the harvest rate using Pope's approximation and then converts it to an approximation of the corresponding *F* (Methot & Wetzel 2013).

3.3 Dynamics of tagged fish

3.3.1 Tag mixing

In general, the population dynamics of the tagged and untagged populations are governed by the same model structures and parameters. The tagged populations (tag groups) are monitored over time intervals following release. The predicted number of tags in each region and subsequent time intervals are derived based on the movement parameters, natural mortality and fishing mortality. For each time interval, the number of tags recovered by a specific fishery is predicted based the modelled number of tags in each age class in the region, the selectivity of the fishery and the fishing mortality of the specific fleet (fishery). The predicted number of tag recoveries is also moderated by the fishery specific reporting rate.

The assessment framework assumes that the probability of capturing a tagged fish is equivalent to the probability of catching an untagged fish. Violation of the assumption of homogeneous mixing of tagged fish at the relevant spatial scale (i.e. region) is likely to introduce a bias in the estimation of fish abundance. In Stock Synthesis, a mixing period is specified which partitions the tag data sets (by release group); tag recoveries (observed and predicted) from the mixing period are excluded from the tag likelihood and therefore do not influence the estimation procedure.

For bigeye tuna, almost all tags were released from a localised area of region 1S. The tagged bigeye were predominantly aged 4−8 quarters at release, while the selectivity of the PSLS1S is estimated to be 4−11 quarters. Consequently, there is likely to be a limited time period (4−8 quarters) during which most of the tagged fish would be available to the PSLS fishery. Thus, a mixing period of four quarters was chosen on the basis that sufficient numbers of tagged fish remained available to the PSLS fishery during the post mixing period, albeit for a relatively limited period.

An analysis of the spatial distribution of the tag recoveries from the purse-seine fishery (Appendix A) suggested that the four quarter mixing period may be sufficient to allow for a reasonable degree of mixing of tagged fish within the south-western equatorial region (Region 1S). The dispersal of tags into the north-western equatorial region (Region 1N) will be mediated by the estimated movement rates (from Region 1S), however, the distribution of tagged fish in this region is unlikely to be homogeneous and it is likely that tag densities would be higher in the southern area of Region 1N (i.e. closer to the release location). Consequently, tag recoveries from the region may be influenced by the spatial distribution of the catch from the fishery.

Specifying a mixing period of 12 months (4 quarters) in the stock assessment model will effectively exclude 76% of all the FAD tag recoveries, while retaining 69% of the free-school recoveries (reducing the total tag recoveries by 66%). This effectively reduces the potential bias introduced by the FAD tag recoveries while maintaining most of the free-school tag recoveries. The remaining FAD tag recoveries are predominantly comprised of fish larger than 80 cm and, arguably, these larger fish are likely to be more evenly distributed that the smaller size category.

3.3.2 Tag Reporting

The observed number of tag recoveries for the purse seine fisheries were already adjusted to account for the differential tag reporting rates. On that basis, the reporting rates for the purse seine fisheries were fixed at 1.0. The model also incorporates the tag recoveries from the other fisheries, most notably the LL fisheries. There are no external estimates of tag reporting rates available for the longline fishery and, hence, the fishery specific reporting rates were estimated based on uninformative priors and were assumed to be temporally invariant. Tag recoveries from the longline fishery will be considerably less informative about stock abundance.

3.4 Modelling methods, parameters, and likelihood

The total likelihood is composed of four main components: catch data, the abundance indices (CPUE), length frequency data and tag release/recovery data. There are also contributions to the total likelihood from the recruitment deviates and priors on the individual model parameters. The model was configured to fit the catch almost exactly so the catch component of the likelihood is very small. There are two components of the tag likelihood: the multinomial likelihood for the distribution of tag recoveries by fleets over time and the negative binomial distribution of expected total recaptures across all regions. Details of the formulation of the individual components of the likelihood are provided in Methot & Wetzel (2013).

The regional CPUE indices are assumed to represent the relative abundance (numbers of fish) of the proportion of the regional population that was vulnerable to the longline fishery. The weighting of the CPUE indices followed the approach of Francis (2011). A series of smoother lines were fitted to the CPUE index and the RMSE of the resulting fit to each set of CPUE indices was determined as a measure of the magnitude of the variation of each set of indices CPUE indices. The analysis performed to the annualised CPUE index (Hoyle et al. 2019) to remove the influence of seasonal variation in CPUE. On basis of the analysis, a CV of 0.2 was assigned to each set of CPUE indices in the base model, to ensure the stock biomass trajectories were broadly consistent with the CPUE indices while allowed for a moderate degree of variability in fitting to the indices.

The relative weighting of the tagging data was controlled by the magnitude of the over-dispersion parameters assigned to the individual tag release groups. Following Langley (2016), the over-dispersion parameters for all tag release groups were estimated within the assessment model assuming a relatively uninformative beta prior (mean 10, sd 3). This prior reflected the variability in the tag-recapture data (variance of the standardised residuals) as determined from preliminary model runs (Langley 2016).

For all fisheries, except for the PSLS fisheries, the individual length frequency observations were assigned an effective sample size (ESS) of 1. For the PSLS fisheries an ESS of 10 was assigned to all length observations. The higher weighting of the purse seine PSLS length frequency data reflects the comprehensive nature of the port sampling programme monitoring the catch. There is a high degree of variation in the length composition data from the PSFS fisheries which appears related to the bimodal structure in the fishery length compositions; variation in the individual length samples may be attributable to sampling different proportions of the catch from each length mode. Based on the apparent level of sampling error an ESS of 1 was assigned to the length samples from the PSFS fisheries.

The Hessian matrix computed at the mode of the posterior distribution was used to obtain estimates of the covariance matrix, which was used in combination with the Delta method to compute approximate confidence intervals for parameters of interest.

4. ASSESSMENT MODEL RUNS

A series of model runs were conducted for the current assessment. These included sequential updates of the base case from the 2016 assessment, exploratory models to investigate alterative assumptions, and the final model options to provide estimates of stock status. The assessment was conducted using the 3.24z version of the Stock Synthesis software under the Linux platform. The stock status was reported for the terminal year of the model (i.e. 2018).

4.1 2016 model continuity run

The 2016 assessment revealed that the magnitude of overall stock abundance was particularly sensitive to the treatment of the tagging data set. The final model options selected for management advice included two options for the weighting of the tagging data (tag lambda 0.1 and 1.0) with three alternative levels of steepness for the spawner-recruit relationship (0.7, 0.8, 0.9) representing a total of six model options. The model option with the tag lambda of 0.1 (representing the intermediate weighting of the tagging data) and steepness of 0.8 was considered as the reference model (Langley 2016).

The 2016 reference model was updated sequentially to ensure a level of continuity, and to assess the influence of the additional data available. The model structure was revised to extend the model period to include the 2016–2018 years. Incremental changes were made to the 2016 reference model (see Table 5 for details). Updates were also made to the model with high tag weighting option (tag lambda=1).

Table 5: Description of the sequence of model runs to update the 2016 base model.

Model	Description
TagLambda01	2016 final model with steepness = 0.8 and tag lambda =0.1
Update-1Catch	Model extended to include 2016–2018, with updated catches
Update-2LF	Revised and updated length composition data for 2015 – 2018
Update-3CPUE	Revised and updated Longline CPUE indices
Update-4MSY	Extend period of estimation for recruitment deviates (to 2017); Definition of F-age for determination of MSY (2016 – 2017);

4.2 Exploratory model runs

Further revisions were made to the updated model (Table 6). This revised model (e*Revised*) served as a starting point for the exploratory analysis. The exploratory phase investigated a range of model options examining assumptions related to the configuration of key data sets, biological parameters and model structure. The analysis complements the comprehensive suite of exploratory models conducted during

the previous assessment, with the aim of determining a suitable reference model. Table 6 provides a description of the range of alternative model options considered. As these model trials were completed prior to the finalisation of the catch and size data for 2016–2018, the fishery catches and length frequency data for the last three years were assumed to be equivalent to the 2015.

Table 6: Description of the exploratory runs for the 2018 assessment.

Model	**Description**
eRevised	Revised length-weight relationship (Chassot et al. 2016); LL CPUE regional weighting factors using the '*7994m8'* estimates from Hoyle & Langley (2018); recruitment assuming to occur in all regions with constant regional recruitment distribution.
Spatial structure	
eRegion-lambda01	A one-region model removing the spatial structure (Fleet/fishery structure remained unchanged); all LL CPUE indices were retained in the model; tag lambda = 1.
eRegion3	A three-region model with the north and south western equatorial regions (R1N and R1S) combined as one model region (R1); both R1N and R1S CPUE indices retained for region R1;
eRegion3MoveHigh	The three-region model but fixed the regional movement rates to a very high values (for fish aged 15 quarters and above). The tags recovered outside region 1 were removed and associated reporting rates were set to zero
CPUE	
eRecruitVar	Allow regional recruitment distribution to be temporally variant from 2005 to 2017 to account for the recent divergent regional LL CPUE trends.
eQhyper	Separate catchability Q for LL CPUE indices 2011–2018 for both R1N and R1S; and estimate a hyper depletion parameter for 2011–2018; a high CV (0.9) was assigned to the CPUE index in 2011 and 2012; regional recruitment distribution assumed to be temporally invariant.
Length data	
eSelLLRegion	Estimating separate LL selectivity by region and assuming a double normal, time-variant selectivity for LL2.
eDwPSLSLF	Down-weighting the PSLS Length data to the extent where it has almost no influence on the model; fixing the *PSLS* selectivity to the preliminary estimates
eDwLLLF	Down-weighting the LL Length data to the extent where it has almost no influence on the model; fixing the LL selectivity to the preliminary estimates
Tag data	
eTagNewProc	Tag data processed using the revised procedure as summarised in Section 2.7
eTagALK	An ensemble of models to evaluate the uncertainty in the age-length conversion using the Age-Length-Key through bootstraps (see Section 2.7)
Biological parameters	
eGrowthVB	Growth parametrized as a standard von-B growth function
eMhigh	Natural mortality of 0.1 per quarter for the adult age classes. Overall level of *M* approximately 60% higher than base level.
eMconst	Natural mortality of 0.0625 per quarter across all age classes

4.3 Reference cases and final model options

On basis of the exploratory analysis, a reference model was identified (see the details in Table 7). Further model options were configured to capture the uncertainty related to the recent longline CPUE indices, tagging dataset weighting, and stock-recruitment steepens assumptions, which are considered to contribute to the main source of uncertainty (Table 8). Thus, the final models involved running a full combination of options on CPUE (2 options), tag lambda weighting (2 weighting values), and steepness (3 values), with a total of 12 models.

Table 7: Main structural assumptions of the bigeye tuna *reference* model and details of estimated parameters. Changes to the 2016 base model are highlighted in red.

Category	Assumptions	Parameters
Recruitment	Occurs at the start of each quarter as 0 age fish. Recruitment is a function of Beverton-Holt stock-recruitment relationship (SRR). Regional apportionment of recruitment to R1N, R1S, R2, and R3. Temporal recruitment deviates from SRR, 1985–2016. Temporal deviates in the proportion of recruitment allocated to R1N, R1S and R2 from 2005–2016.	R_0 Norm(10,10); h = 0.80 *PropR2* Norm(0,1.0) *SigmaR* = 0.6. 140 deviates.
Initial population	A function of the equilibrium recruitment in each region assuming population in an initial, exploited state in 1975. Initial fishing mortality estimated for LL1N,1S,2,3 fisheries.	Norm(0.10,99)
Age and growth	40 quarterly age-classes, with the last representing a plus group. Growth based on VonBert growth model with age-specific k to approximate the mean length at age determined by Eveson *et al* (2012). SD of length-at-age based on a constant coefficient of variation of average length-at-age. Mean weights (W_j) from the weight-length relationship $W = aL^b$.	*Linfinity* = 150.913 cm, k (base) = 0.332, k deviates for ages 1,8,9,10. CV =0.10 a = 2.217e-05, b = 3.01211
Natural mortality	Age-specific, fixed. Ramp function Age 0-12, initial 0.2 at age 0. Constant age 12-40 at 0.0625	
Maturity	Length specific logistic function from Shono *et al* (2009). Mature population includes both male and female fish (single sex model).	Mat50_Fem 110.888 cm Mat_slope_Fem -0.25
Movement	Age-dependent with two blocks; age classes 3-8 and 15-40. Ramp function Age 8-15. No movement prior to age class 3. Constant among quarters.	12 movement coefs. Norm(0,4).
Selectivity	Age specific, constant over time. Principal longline fisheries (LL1N,1S,2,3) share logistic selectivity parameters. PSLS fisheries. Separate selectivity for PSLS1N, common selectivity PSLS1S and PSLS2 Common selectivity for all PSFS fisheries. LF2 fishery logistic selectivity. LINE2 share principal LL selectivity.	Logistic *p1* Norm(20,10), *p2* Norm(1,10) Double Normal Five node cubic spline

	BB fishery: double normal selectivity. OT 1 & 2 share PSFS selectivity. CPUE indices share principal LL selectivity.	
Catchability	Temporally invariant. Shared regional catchability coefficient. No seasonal variation in catchability for LL CPUE. LL2,3 CPUE indices have CV of 0.2; LL1N,1S CV 0.25.	Unconstrained parameter *LLq*
Fishing mortality	Hybrid approach (method 3, see Methot & Wetzel 2013).	
Tag mixing	Tags assumed to be randomly mixed at the model region level four quarters following the quarter of release. Accumulation after 28 quarters	
Tag reporting	Revised tag data processing (see details in Section 2.7) All (adjusted) reporting rates constant over time. Common tag reporting rate fixed for all PS fisheries. Non PS tag reporting rates uninformative priors.	PS RR 1.0 Other fisheries Norm(-0.7,5)
Tag variation	Over dispersion parameters estimated for each tag release groups.	beta prior (mean 10, sd 3)
Length composition	Multinomial error structure. PSLS length samples assigned maximum ESS of 10. PSFS length samples assigned maximum ESS of 1.0. LL and Other fisheries length samples assigned ESS of maximum 1.0.	

Table 8: Description of the final model options for the 2019 assessment. The final models consist of a full combination of options below, with a total of 12 models. The options adopted for the reference model is highlighted.

Model options	Description
CPUE	• **RecVar – Constant catchability for LL CPUE for both region 1N and 1S; estimating temporal variation in regional recruitment distribution from 2005–2018**
	• Qhyper – Estimating a separate catchability coefficient for LL CPUE before and after 2011, and a shape parameter for CPUE 2011–2018, for both region 1N and 1S; time-invariant regional recruitment distribution
Steepness	• h70 – Stock-recruitment steepness parameter 0.7
	• **h80 – Stock-recruitment steepness parameter 0.8**
	• h90 – Stock-recruitment steepness parameter 0.9
Tag weighting	• ***TagLamda01*** **– Tag lambda = 0.1 for both components of tag likelihood.**
	• *TagLamda1* – Tag lambda = 1 for both components of tag likelihood.

5. MODEL RESULTS

5.1 2016 model continuity run

Updating the 2016 base model with only the catch data yielded almost identical estimates of historical stock biomass (Figure 14). However, the inclusion of the revised and updated CPUE had an appreciable impact on the assessment model, with the overall stock biomass estimated to be about 10% - 18% lower than the 2016 base model (Figure 14, Table 9). The change is likely to be driven by the CPUE indices in region 1N, which had a steeper overall decline than the indices used in previous assessment (see Figure 5). Further model updates with additional length composition data and other model adjustments (e.g. reference years for the MSY calculation) had minimal impact on model estimates (Figure 14, Table 9). Overall the updated models estimated a lower level of stock productivity but did not change the conclusion of stock status (B_{2015}/B_{msy} and F_{2015}/F_{msy}) compared to the 2016 base model.

The model with the high tag lambda option (lambda=1) was also updated. With the higher tagging data weighting, the revised CPUE appeared to have less impact on estimates of absolute stock biomass. The results probably highlighted the conflict between the tag data set and CPUE indices, as revealed in the previous assessment: the influence of CPUE on the assessment model was mitigated by the weighting placed on the tagging data likelihood.

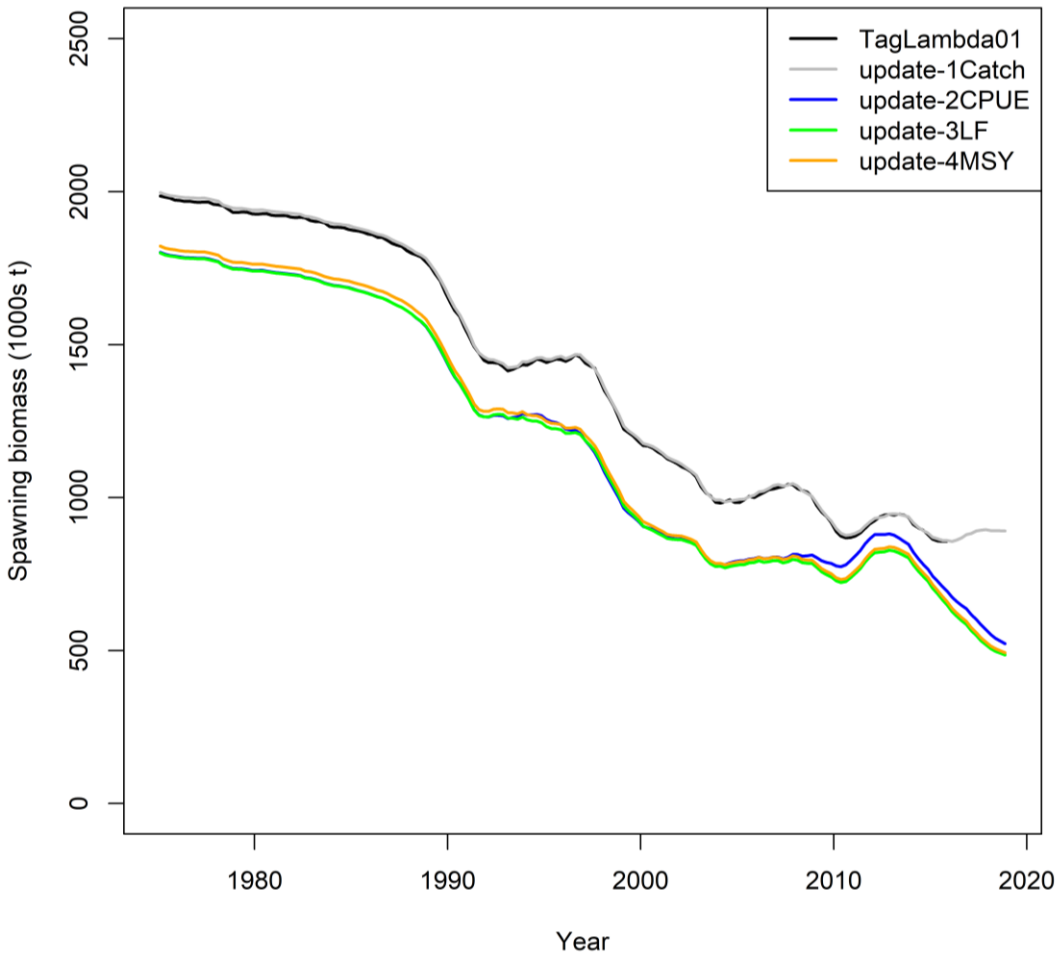

Figure 14: Spawning biomass trajectories for IO bigeye tuna from the step-wise model updates for 2018. (from the 2016 assessment reference model 'TagLambda01')

Table 9: Estimates of management quantities for the step-wise updates of the 2016 stock assessment reference model (*TagLambda01*).

Option	SB_0	SB_{MSY}	MSY	SB_{2015}	SB_{2018}	SB_{2015}/SB_{MSY}	SB_{2018}/SB_{MSY}	F_{2015}/F_{MSY}	F_{2018}/F_{MSY}
2016 model	2,102,400	614,278	115,786	859,204		1.40		0.59	
Update-1Catch	2,113,660	620,783	116,476	863,877	536,483	1.39	1.44	0.61	1.11
Update-2CPUE	1,915,310	395,200	92,424	718,299	536,483	1.82	1.36	0.72	1.15
Update-3LF	1,915,180	473,664	88,046	675,972	495,135	1.43	1.05	0.82	1.29
Update-4MSY	1,937,620	498,034	90,352	687,266	503,322	1.38	1.01	0.86	1.36

5.2 Exploratory models

The exploratory models investigated alternative options relating to parameter and structural assumptions and aimed to identify potential revisions to the assessment model. Key results of the exploratory runs are given in Appendix C and are also summarised below.

Revisions to the updated 2016 model

A number of revisions were made to the updated 2016 reference model (eRevised). The new length weight relationship represented a small increase in weight for fish over 150 cm but had almost no effect on model results. The incorporation of revised regional scaling factor to the longline CPUE distributed more biomass to region 1S relative to region 2 compared to the previous assessment (Figure B1) but had little effect on the overall biomass estimates.

Treatment of LL CPUE

The previous assessment assumed that the regional recruitment distribution was time invariant, based on the consideration that there was little data to inform the recruitment distribution. The intention was to produce a more parsimonious model. However, the new CPUE indices exhibited divergent trends amongst regions for the period 2012–2018, with a sharp decline in R1S and R1N, a moderate decline in R2, and a relatively flat trend in R3. The differences cannot be explained by the respective catch removals in each region for this period. Consequently, model predicted CPUE were poor for some regions (i.e. R2 and R3, see Figure B2).

Model *eRecruitVar* allowed the regional recruitment distribution to be time variant for the period 2005 – 2018. This enabled the model to reconcile the differences in regional CPUE by allowing more recruits into region 3 and less recruits into region 1 for recent years. The large decline of the CPUE indices from 2011 to 2018 in region 1 also resulted in the overall recruitment over the last 10 years to be estimated much lower than the average (Figure B3 – left), implying a potential regime shift.

It is also possible that the large decline in recent CPUE have reflected somewhat rapid changes in catchability of the longline fleets (see Discussions). On that basis, model *eQhyper* split the LL CPUE indices in both region 1N and 1S into two series (pre and after 2011), each with a separate catchability. An additional shape parameter was estimated for each of the LL1N and LL1S indices 2011–2018, effectively allowing them to have a non-linear relationship with the underlying abundance. Model *eQhyper* also predicted CPUE well for all regions, without relaxing the constant recruitment distribution assumption. Estimated overall recruitment for 2008 – 2018 is close to the long-term average (see Figure B3– left).

Both models estimated similar stock biomass– about 10% higher than that estimated by model eRevised (Figure B3–right). As expected, model *eRecruitVar* estimated a sharp decline in stock biomass for 2011–2018 whereas model *eQhyper* estimated a moderate decline (Figure B3–right). Both model options were included in the final model ensemble as they provided alternative yet plausible explanations to the regional CPUE trends.

Length composition data

Model *eLLSelRegion* relaxed the constraint of shared selectivity among regional LL fisheries and assumed a time-varying, dome shaped selectivity for LL2. The average fish length from the LL2 length samples appeared to be lower than other regions, particularly for the period 1980–1990 (see Figure 8). Model *eLLSelRegion* estimated a significant reduction in selectivity of fish older than 13–15 quarters for 1980–1990, resulting in an improvement in fits to the mean length (Figure B4). However, the reason for the predominance of smaller fish in the longline samples in the 1980s and 1990s remains unknow. It may have been related to sampling bias (i.e. samples were taken primarily from vessels targeting

albacore tuna), and also a number of other factors that may have degraded the longline size data (Hoyle et al. 2019a). The option of adopting regional-specific LL selectivity was not considered further for the assessment.

Model *eDwLLLF* and *eDwPSLF* explored the information content of the LL and PSLS length data. Downweighting LL length data (likelihood lambda set to zero and LL selectivity fixed) appeared to have little effect on the estimation of recruitment strength and/or abuance (Figure B5), probably because the longline length samples consisted of predominantly large fish (80 cm above) and did not exhibit any major trend over the long term. In contrast, the PSLS length data appeared to have contributed to the estimation of low recruitment in the 1990-2000 and the more recent high recruitment (Figure B5 – left). The declining trend in the mean fish length of the PSLS samples appeared to have provided the model with some abundance signals. The influence of the length composition data on the assessment model is further elaborated through the ASPM analysis (see Section 5.5.2).

Tag data

Processing the tag data using the revised procedure (see Section 2.7 for details) did not have any appreciable impact on model estimates (Table B1). The revised procedure aimed to harmonise the processing of tag data for inclusion into the SS3 assessment model for the main tropical tuna species.

eTagALK explored the uncertainty associated with length-age conversion for tag at release. *eTagALK* consists of a group of models (n=10) in which the age at tag release represents a random permutation of the age distribution for a given length. These models yielded almost identical biomass estimates (results not shown).

Biological parameters

Model *eGrowthVB* explored the possibility of simplifying the complex parameterisation of base growth function (i.e. age-specific K, see Figure 12) by using a standard VonB function. The reparametrized VonB growth was able to approximate the base growth for age 20 quarters and above (it's not possible to approximate the full age/length range due to the constraint of standard VonB function). The reparameterization led to significant deterioration in the fits the length data (log likelihood increased by about 100 point, see Table B2). Further analysis suggested that the base growth function is more consistent the modal progressions exhibited in the PSLS LF data for the younger fish.

The high M option (*eMhigh*) yielded much lower estimates of stock biomass (SSB0 is about 40% lower than the low M option). Another model (*eMconst*) assuming a constant M for all ages (even lower M for juveniles than the low M option) estimated a slightly higher biomass (SSB0 is about 15% higher than the low M option). Although the likelihood appeared to be in favour of the low M option (see Table B2), there is no discernible difference in model fits to observational data among these models. However, model predictions appeared to suggest that the high M option led to a lack of large fish (100 cm above) in the population relative to the Observed LL size data (Figure B6).

Almost all bigeye tuna caught from the purse seine FAD fishery are less than 80 cm (fish caught by longliners are generally greater than 100 cm). The question of the impact of these catches of small tuna on other tuna fisheries is frequently raised in fishery management meetings (Hampton 2002). The reduction in stock biomass as induced from fishing can be evaluated through the impact analysis (Minte-Vera et al. 2016). The analysis performed to the bigeye assessment model showed that the relative impact attributed to different fishing sectors is sensitive to the natural mortality assumption, e.g. the PSLS will have a much larger impact than the longline fishery if the juveniles experience a much lower natural mortality, (see Figure B8). The analysis indicated that a better understanding of the natural mortality of various life stages will have important management implications for the bigeye tuna stock.

Spatial structure

The 4-region spatial partitioning in the assessment model was to accommodate the distribution of fleets, differences in regional abundance trends, and the incomplete mixing of tags in the main area of recovery. The model requires a relatively large number of movements to be estimated. There is probably limited information to estimate movement rates within the model: all tags releases are limited to one region (R1S), the size structures in the commercial catches are similar among regions.

Models with simplified regional structure (1-region and 3-region) were briefly explored. The 1-region model (eRegion1-lamba1) estimated a much lower overall biomass than the 4-reginal model with equivalent, native tag weighting (Figure B8–left). This illustrated the potential bias that may arise when the model failed to account for the incomplete tag mixing via appropriate spatial partitioning of the tagging data.

The 3-region model accounted for incomplete mixing outside the main purse seine fishery area but ignores the inadequate diffusion of tags into the northern area of western equatorial region. The model significantly over-predicted the tag recoveries from the PSLS1N fishery (see Figure B9) and estimated somewhat higher stock biomass than the 4-region model (Figure B8–right). Similar to the 4-region model, movement rates estimated within the 3-region model were very low (Figure B10–left).

An alternative 3-region model in which movement rates were fixed at arbitrarily high levels (Figure B10–right) estimated a similar level of stock biomass (Figure B8–right). The model resulted in some deterioration in the fits to the CPUE and length data (Table B2) probably because it was difficult for the model to reconcile the differences in observed abundance trends and size structure amongst regions when a high degree of mixing was assumed.

5.3 Reference model

Exploratory model *eRecruitVar* was chosen as a reference model (see more details in Table 7). The reference model provided one possible explanation to the steep decline in the CPUE indices in region 1N and 1S for the period 2011 – 2018 (i.e. below average recruitment) and is used to further evaluate model fits and diagnostics (sections below). An alternative model *rQhyper* (based on model *eQhyper*), which allowed the LL CPUE 2011 – 2018 in region 1 to be non-linearly related to abundance is also briefly summarised. The reference model and model *rQhyper* adopted the revised tag processing procedure and has downweighted the tag dataset within the model (lambda=0.1). Both models were included in the final model assemble (see Section 5.4).

5.3.1 Model fits

The reference model fits the CPUE indices for the three main fisheries (LL1N, LL1S & LL2) and the seasonal CPUE indices from LL3 well (Figure 15). The trends in the LL1N&S and LL2 CPUE indices deviate during 1998–2017 and the model is able to accommodate the differences in these regional indices via varying levels of recruitment into these regions for more recent years. The residuals did not reveal any obvious patterns except this is a slight upward trend for region 1S (Figure 16) as the model has little flexibility to account for the differences in the CPUE trend for the early years. Overall, the variation in the residuals (RMSE 0.23, 0.32, 0.31, and 0.27 for LL1N, LL1S, LL2, LL3) was broadly comparable to the S.E. initially assigned to the CPUE indices.

Model *rQhyper* can also simultaneously fit the regional CPUE indices (Figure 17Figure 18). The CPUE shape parameter was estimated to be 2.2 for the LL1S indices and 4.7 for the LL1N indices, indicating a high degree of hyperdepletion between CPUE and abundance in both regions for 2011 – 2018. Consequently, the biomass trends in region 1N and 1S were largely determined by their respective catch removals (and migration)

Overall, there was a good fit to the aggregated length frequency data for most of the main fisheries with comprehensive sampling (Figure 19). However, the model fits to the length composition data from the Region 2 longline fishery (LL2) were poor. The model predicts considerably larger fish in the catch from the fishery than was observed. There is a reasonable fit to the average length over time for all fisheries (Figure 20). There are poor fits to the data from key fisheries during certain time periods. Most notably, the average length of fish from LL2 is over-estimated by the model throughout the 1980s and 1990s, and from LL1N and 1S is under-estimated from the 2000s to the present (Figure 20, also see Figure D2 in Appendix D). Although a time-varying, dome shaped selectivity can considerably improve the fits to the LL 2 length frequency data (as in model *eSelLLregion*), the option was not adequately justified. The model did not fit well the LINE fishery catch samples given that the selectivity was assumed to be the same as the longline fishery. Estimating a sperate selectivity did not work well due to the paucity of samples from this fishery.

The model also fits the PSLS LF reasonably well (Figure 19 & Figure 20). However, the strong temporal trend in the length of fish from PSLS1S and PSLS1N catch from 1990 onwards was not fully captured by the model (see Figure D2 in Appendix D). The PSLS1S length frequency data showed some noticeable mode progression between 2008 and 2013, with new recruits appearing to occur in the fourth quarter, progressing through to the first and second quarter of the following year, and the model tracked these observed modes reasonably well (Figure 21). The PSLS LF data has some strong influence on the estimates of recruitment strength.

The average length of fish sampled from the PSFS is highly variable (FigureFigure 20) probably reflecting the proportion of the catch sampled from the smaller and larger modes of the combined length composition. The model prediction of average length represents the length of fish in the intermediate length range (80–100 cm) (FigureFigure 20).

The fit to the observed number of tag recoveries was examined for those fisheries which accounted for most of the tag returns (e.g. PSLS1S). The fit to the number of tag recoveries was examined by recombining the tags into individual release periods (i.e. aggregating the releases by age class) and excluding those recoveries that occurred during the mixing period. The fit to the tag recoveries was examined by time period (quarters) and by age at recovery, and by time at liberty (quarters) for the individual release periods and the aggregated data set (all releases combined).

The number of tag recoveries varied considerably amongst the release periods (Figures C1 – C4). The tags released in 2005 and the first quarter of 2006 had very low recoveries, probably due to the small number of releases and high tag mortality in the initial phase of the program.

Overall, there was a reasonable fit to the tag recoveries from the LL1S fishery during the main tag recovery period (to 2011) but the model over-estimates the number of longer term tag recoveries from the older age classes (at recovery), i.e. those fish at liberty for a longer period (Figure), this may reflected variable tag reporting over time or mis-specification of natural mortality. The model predicted the recoveries for the LL2 fishery poorly, as the recoveries were only observed for a very short period.

Most of the observed tag recoveries in the post mix period were from the PSLS1S fishery and a high proportion of the total recoveries occurred during the first four quarters following the mixing period (Figure 23). Nonetheless, overall the model under-estimated the number of tag recoveries in the four-quarter period (Figure). Longer-term recoveries were less vulnerable to the PSLS1S fishery (due to the age specific selectivity) and, hence, numbers of recoveries declined considerably (Figure).

There was also a poor fit to the tag recoveries from the PSLS1S fishery by age class (at recovery) (Figure 23). The model under-estimated the overall number of tags recovered from the fishery in the older age classes (11–14 quarters) (Figure 23). This result indicates that the age-specific recoveries are inconsistent with the fishery selectivity functions. The tag recoveries from the PSLS fishery included a significant proportion of fish above 80 cm which generally were not vulnerable to the commercial fishery. Limited numbers of tags were also recovered by the PSFS1S and LL1S fisheries after longer periods at liberty (compared to PSLS1S). The model tends to underestimate the number of tag

recoveries throughout the age classes from the PSFS1S fishery. This may be indicating inadequate mixing of the tags with the fish population vulnerable to the PSFS fishery (Figure 23).

Tag recoveries were also aggregated by region of recovery and time period (Figure 24). The model provides a poor fit to the number of tags recovered from Region 1S during the initial recovery period, reflecting the poor fit to the PSLS1S tag recoveries. The smaller number of longer-term recoveries from Region 1S is reasonably well estimated by the model except for recoveries made after 2011 (Figure 24). The model also provides a reasonable fit to the long-term tag recoveries from Region 1N. The model provides a reasonable prediction of the tag recoveries from Region 3 from the LL3 fishery. A small number of tags were intermittently recovered in Region 2 by the LL2 fishery and the model predicts a correspondingly low number of tag recoveries from the region (Figure 24).

Not surprisingly, the model with a higher (lambda 1.0) weighting to the tagging data generally exhibit a better fit to these data, particularly for the PSLS1S fishery. The model improved the fit to the older (11–14 quarters) age classes (at recovery), with a shift in PSLS1S selectivity towards larger fish (70–100cm). The model with the higher weighting of the tag data resulted in a worse fit to the PSLS length composition data.

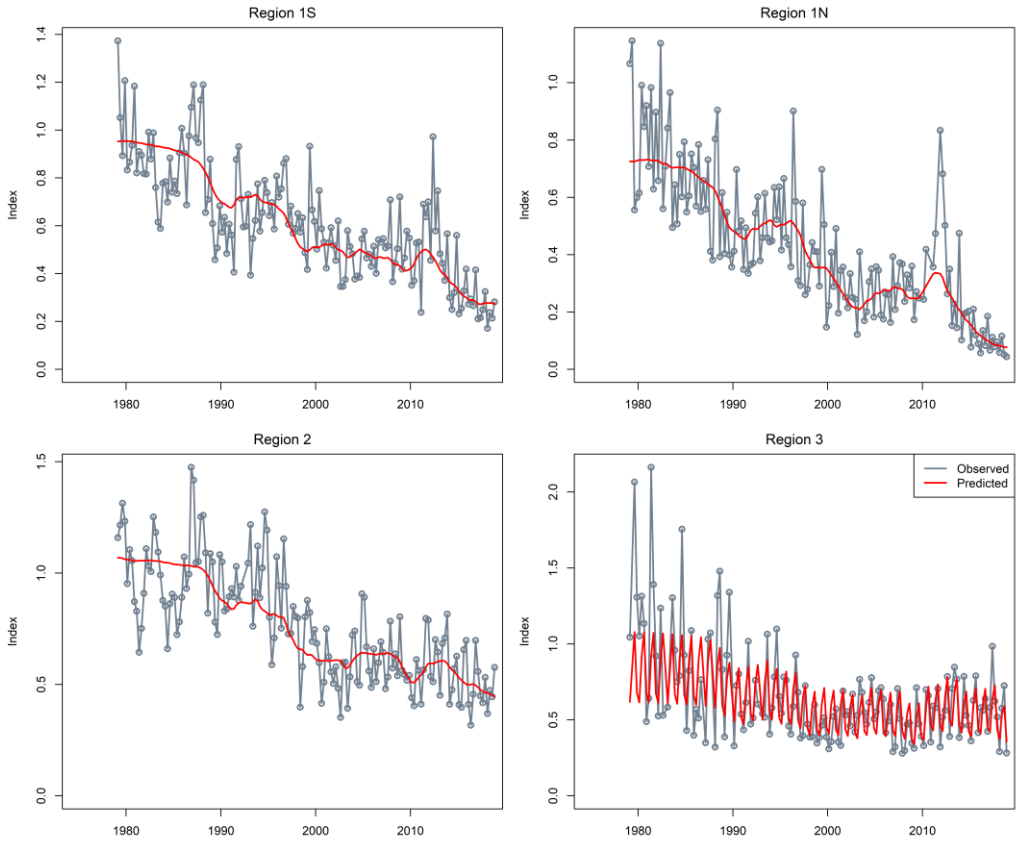

Figure 15: Fit to the regional longline CPUE indices, 1979–2018 from the reference model.

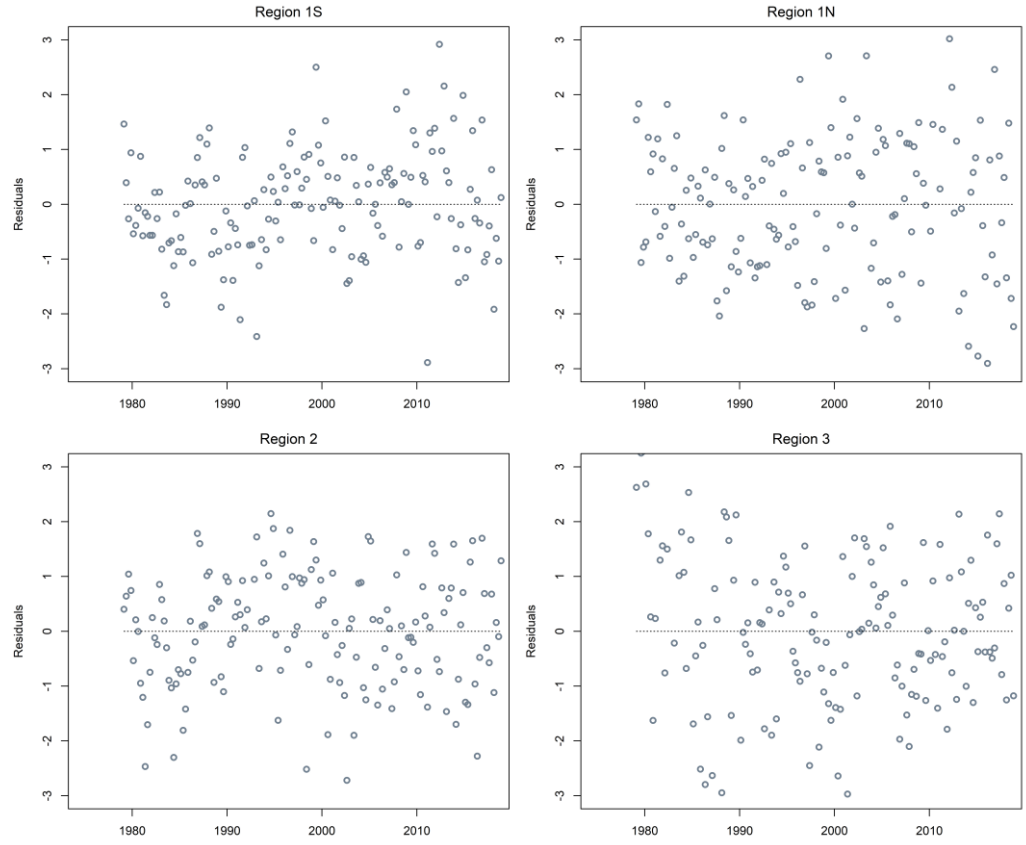

Figure 16: Standardised residuals from the fits to the CPUE indices from the reference model.

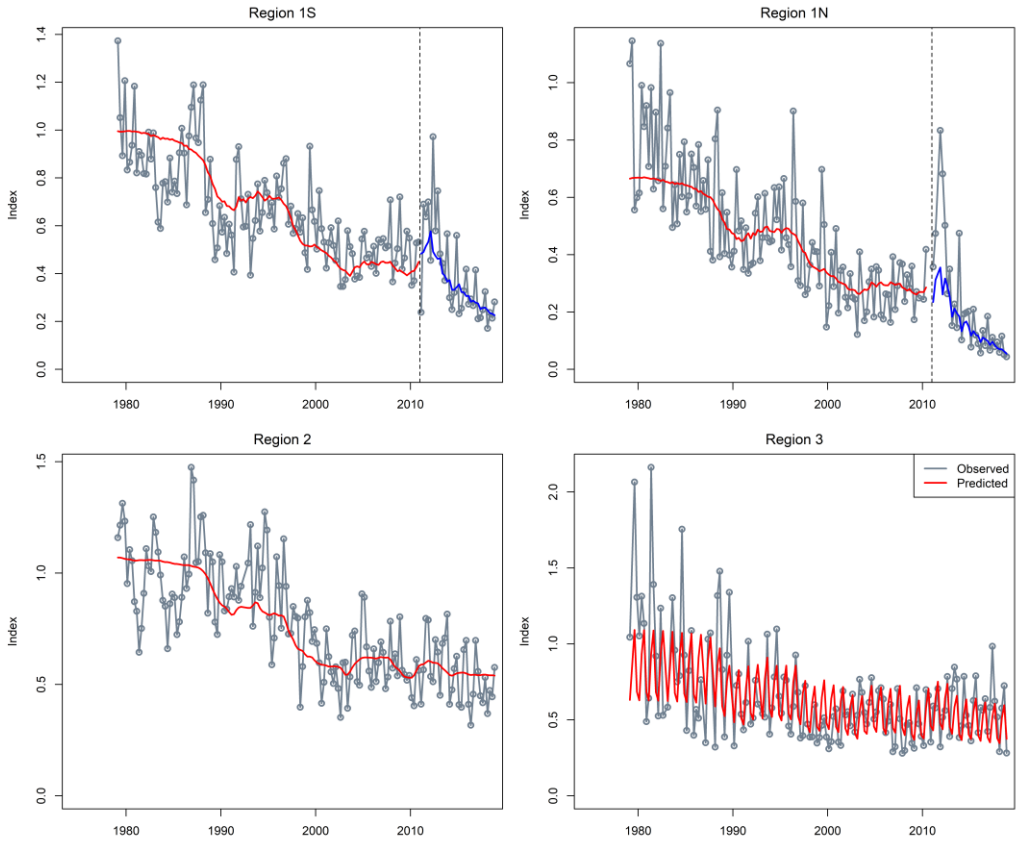

Figure 17: Fit to the regional longline CPUE indices, 1979–2018 from model rQhyper.

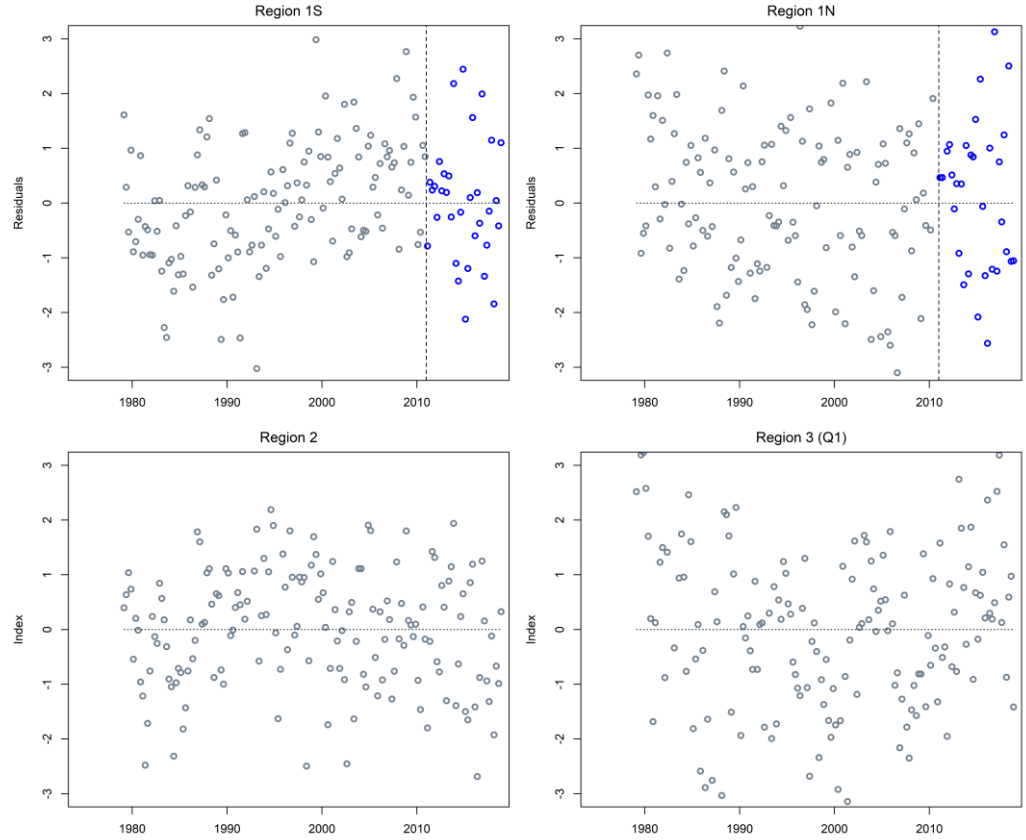

Figure 18: Standardised residuals from the fits to the CPUE indices from model rQhyper.

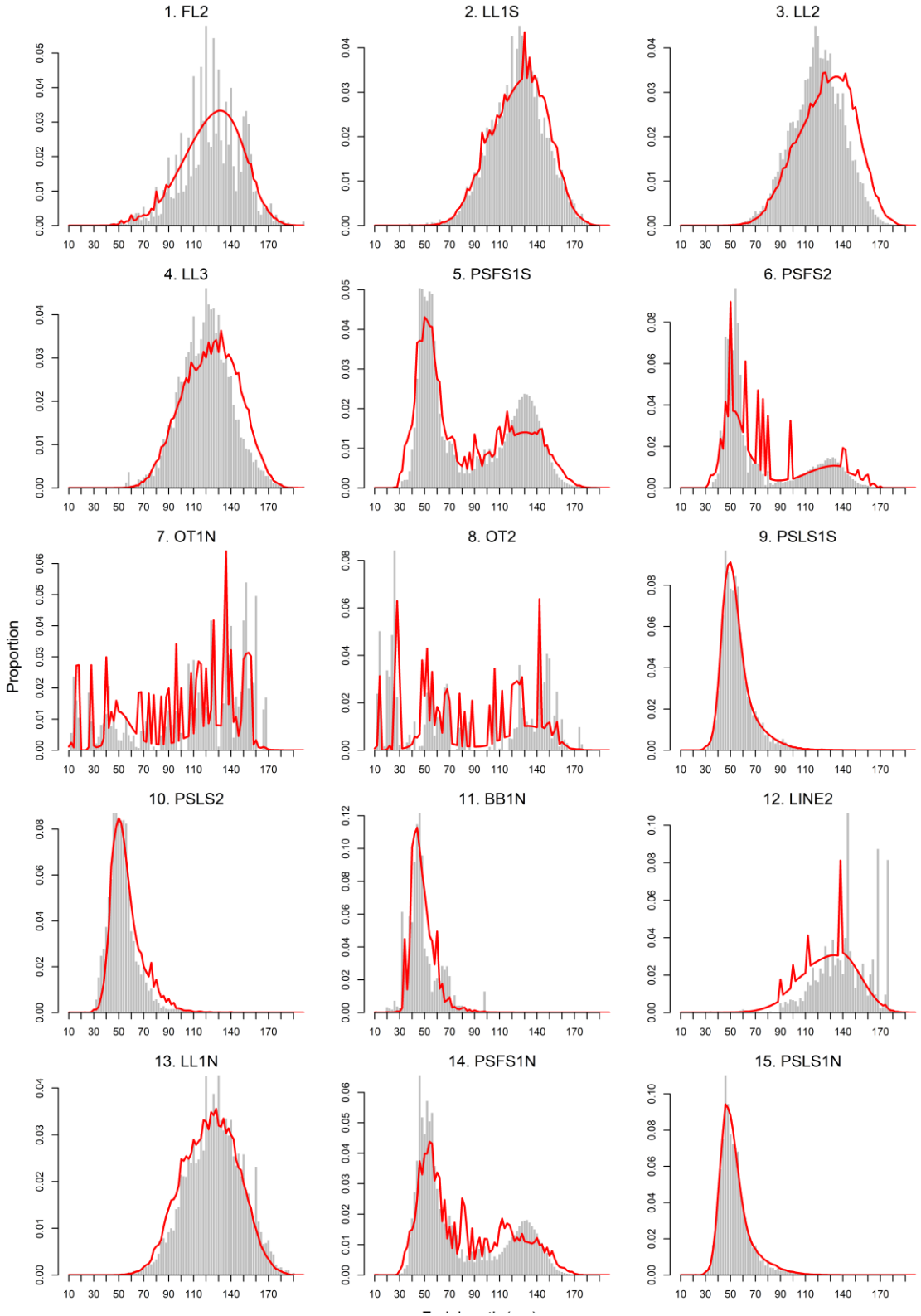

Figure 19: Observed (grey bars) and predicted (red line) length compositions (in 2 cm intervals) for each fishery of bigeye tuna aggregated over time for the reference model.

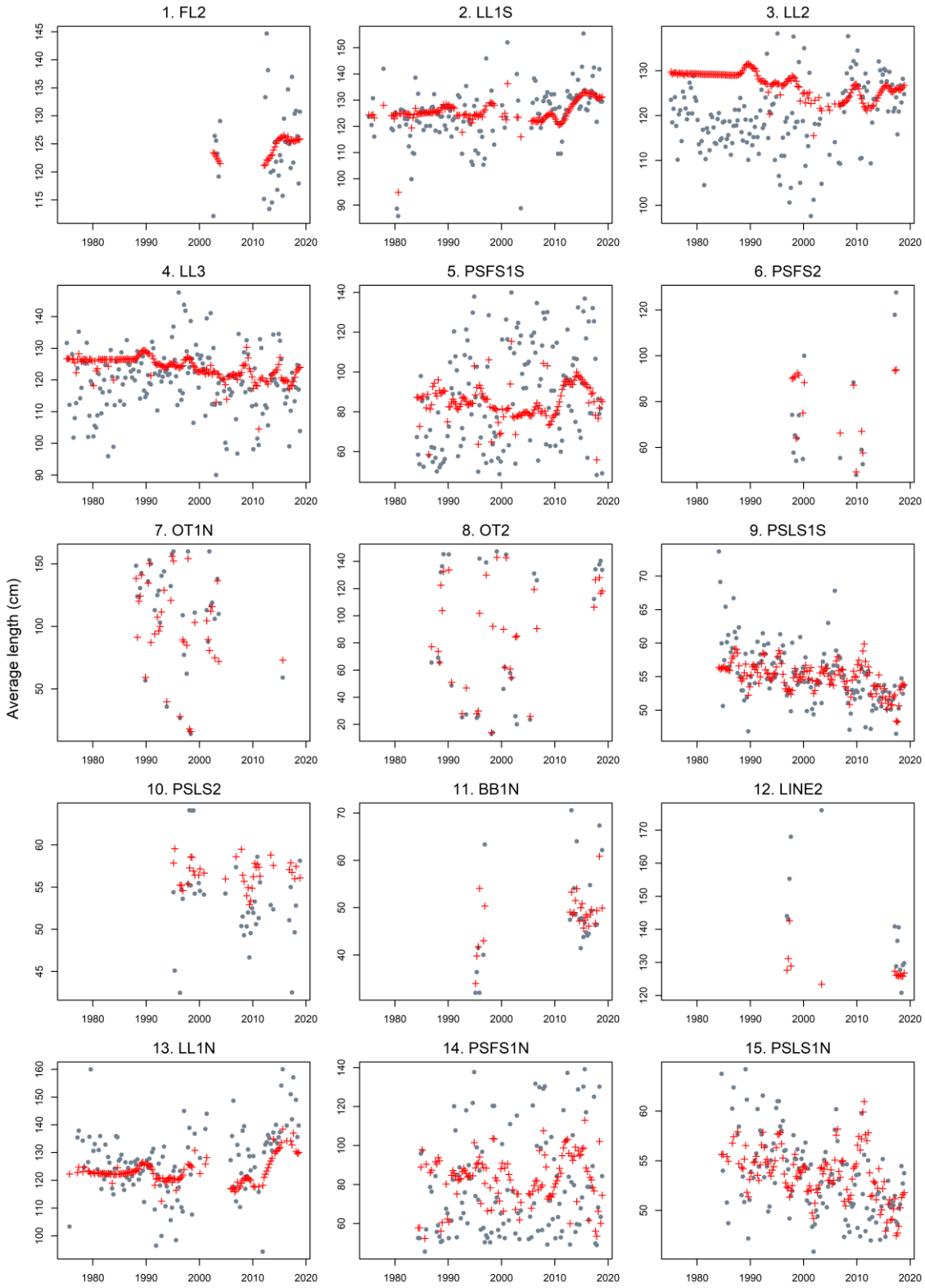

Figure 20: A comparison of the observed (grey points) and predicted (red points and line) average fish length (FL, cm) of bigeye tuna by fishery for the main fisheries with length data for reference model.

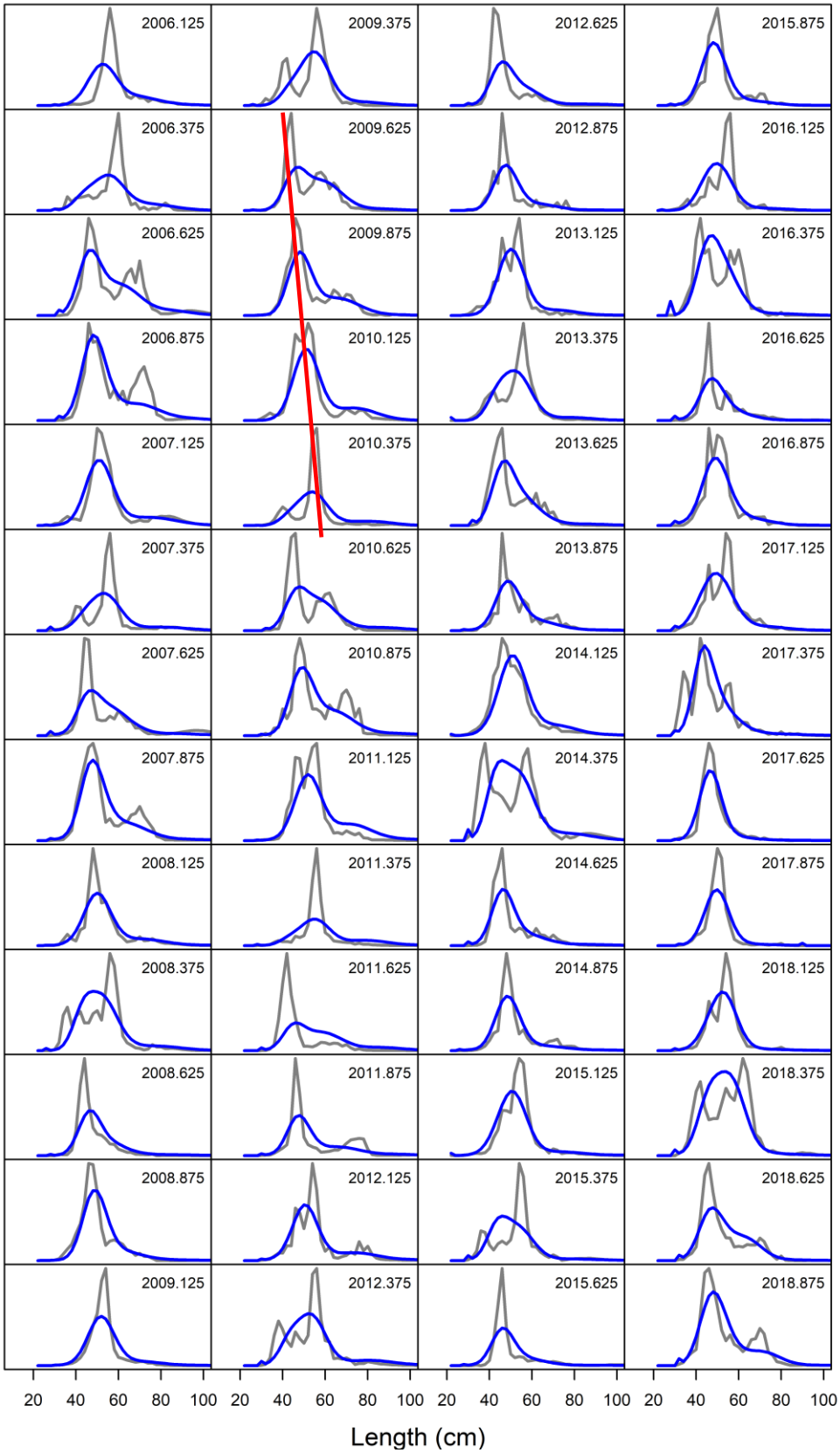

Figure 21: Observed (grey) and predicted (blue line) length compositions for the PSLS 1S fishery by year quarter 2006–2018 for reference model. The red line indicates a example of mode progression in the data.

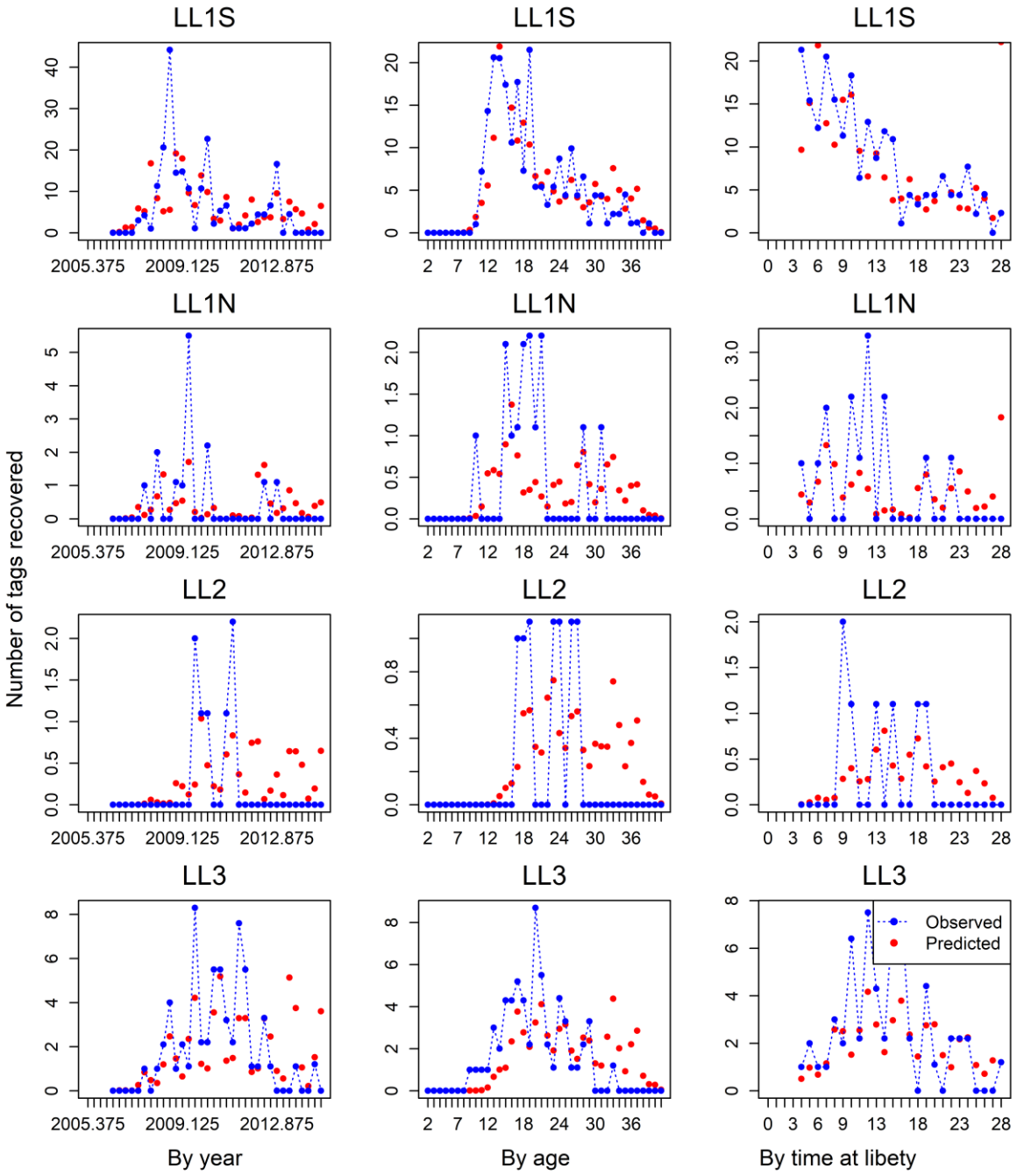

Figure 22: Observed and predicted number of tags recovered by year/quarter time-period (left), by age (mid), and by time at liberty (in quarters, right) for main longline fisheries and regions (LL1N, 1S, 2, 3) from the reference model. Only tags at liberty after the four-quarter mixing period are included. Tag recoveries are aggregated for each of the regional fisheries.

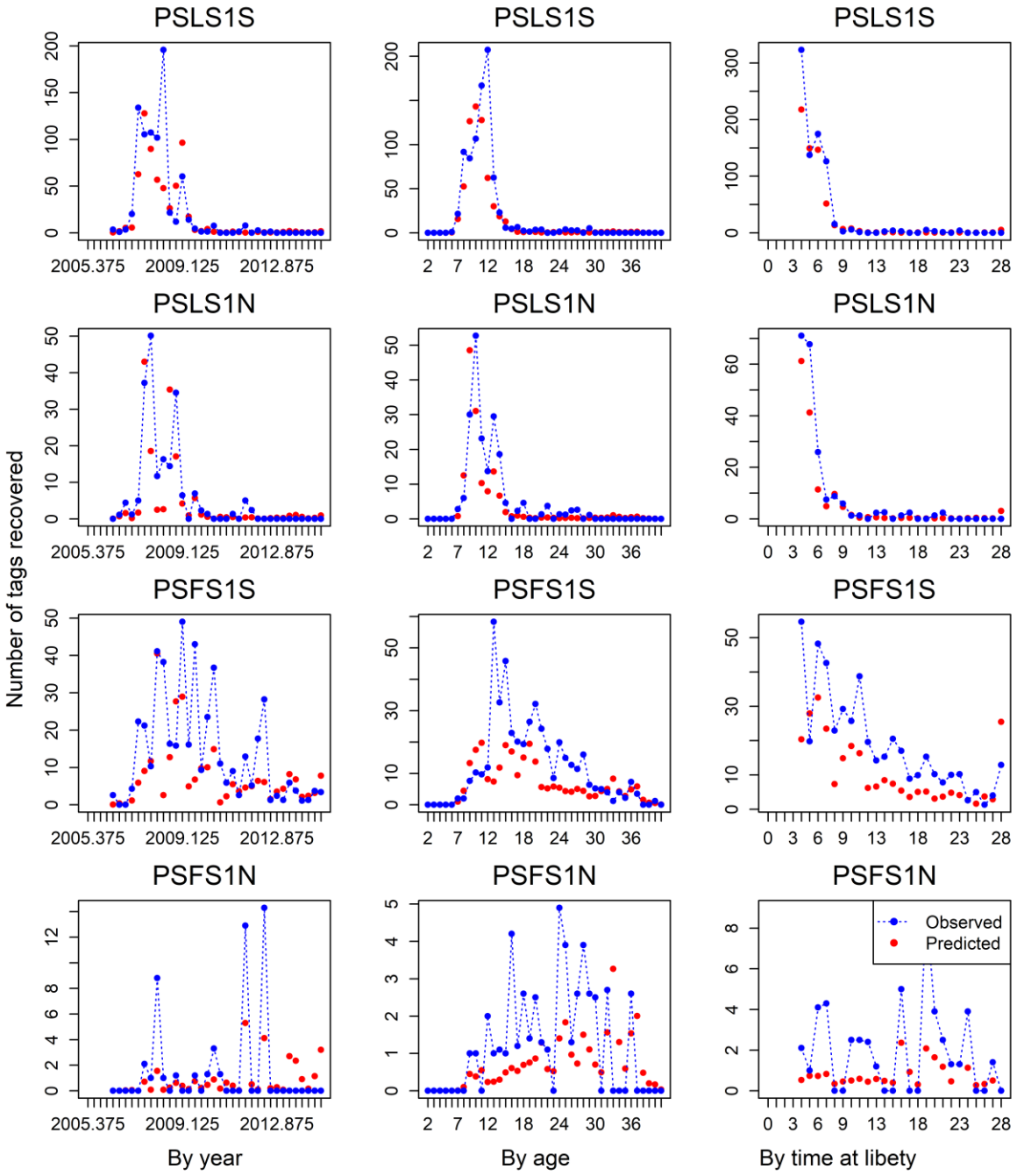

Figure 23: Observed and predicted number of tags recovered by year/quarter time-period (left), by age (mid), and by time at liberty (in quarters, right) for main purse seine fisheries and regions (PSLS1S, 1N, PSFS 1S, 1N) from the reference model. Only tags at liberty after the four-quarter mixing period are included. Tag recoveries are aggregated for each of the regional fisheries.

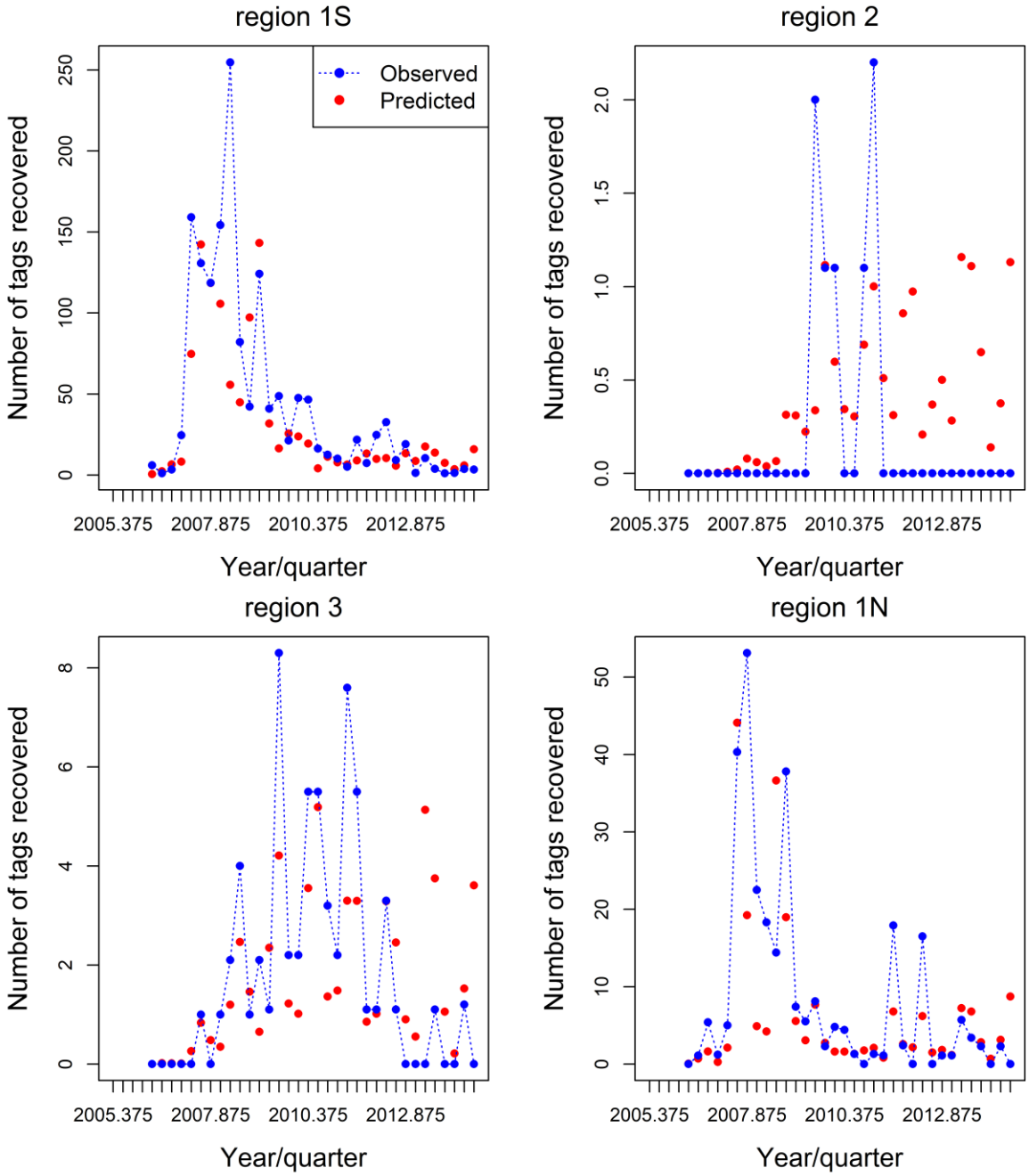

Figure 24: Total observed and predicted the number of tag recoveries by region (all regional fisheries combined) by quarter following the mixing period from the reference model.

5.3.2 Model estimates

The estimated parameters in the reference model include: the overall population scale parameter *R0*, the time series of recruitment deviates, the distribution of recruitment among regions, age specific movement parameters, the fishery selectivity parameters, fishery tag reporting rates and the catchability parameters for the CPUE indices. Model *rQhyper* also estimated a shape parameter for the LL1S and LL1N CPUE series 2011–2019 seperately.

The age-specific selectivity functions are presented in Figure 25. For the main longline fisheries (LL1N,1S,2,3), full selectivity is attained at about age 18 (quarters). Peak selectivity for the PSLS1N and PSLS1N fisheries occurs at ages 5–8 quarters. (Figure 25). For the PSFS fisheries, selectivity was estimated to be bimodal with a similar level of selectivity for the younger and older modes.

Recruitment deviates were estimated for the quarterly time steps from 1985–2016. There are longer term trends evident in the recruitment deviates with higher than average recruitment estimated for the late 1990s–early 2000s and lower recruitment during the mid-2000s (Figure 26). These trends correspond to period of higher and lower catches from the PSLS fishery. Recruitment for 2010–2016 was estimated to be much lower than the long-term average (Figure 26), driven by the decline in the CPUE indices (Figure 27). The recruitment for this period was estimated higher by model *rQhyper*. Both models estimated a recruitment pulse towards the end of the timeseries, which corresponds to the significant increase of catches from the PSLS fishery in 2018. Tag weighting also has an appreciable impact on recruitment deviations during 2005-2007, a time period immediately prior to the main tag recovery period (Langley 2016).

Recruitment was assumed to occur in the all regions and the distribution of recruitment was estimated to be apportioned 34% to Region 1N, 28% Region 1S, 24% to Region 2, and 14% to region 3. The reference model estimated a decreasing level of recruitment into region 1N for 2008–2014 (Figure 28).

Movement rates were estimated amongst the model regions. The model estimates low movement rates of mature fish amongst the regions, with some reciprocal movement between Region 1S and Region 3 (Figure 29). Limited mixing was estimated to occur between Regions 1N and 1S for the reference model, but the mixing was estimated higher for model *rQhyper*. This suggested the movement rates were probably not well informed by the data, and estimates are probably more influenced by other model option (e.g. recruitment dynamics). Exploration models showed that biomass estimates are not sensitive to the assumed level of mixing amongst regions.

Tag reporting rates were estimated for the non purse seine fisheries. For some of these fisheries, the estimated reporting rates are unlikely to be influential in the overall assessment as the reported tags were predominately recovered during the tag mix period. However, a considerable proportion of the tag recoveries from the LL1S and LL3 fisheries occurred during the post mixing phase and, hence, the tag reporting rates will have some influence in the model likelihood. For these fisheries, tag reporting rates were estimated at 0.21 and 0.52, respectively (Figure 30), while the reporting rate for the LL1N fishery was estimated to be considerably lower (0.05). The estimates for the LL2 and LL3 fisheries are associated with high uncertainty, and probably have reflected the large inter-annual variabilities in the tag recoveries (and reporting) from these fisheries.

For the reference model, Regions 1N&1S accounted for about 45% of the initial biomass (Region 2, 35%; Region 3, 20%). These estimates are somewhat different to the previous assessment due to revised regional scaling factors (Hoyle & Langley 2018). Relative trends in stock biomass are similar for Regions 1N, 1S and 2, while the overall level of depletion was much lower for Region 3 (Figure 31).

The spawning biomass declined through to the 1990s and early 2000s, followed by a relatively flat trend in the 2000s (Figure 32). The biomass increased slightly in 2011–12 and declined rapidly to the historical low in 2018. Model *rQhyper* estimated similar spawning biomass overall except for 2011 – 2018 where a moderate decline was predicted, with the biomass in 2018 estimated to be at a similar level to 2010 (Figure 32).

The estimates of fishing mortality were relatively low for the fisheries within Region 2 and Region 3 (Figure 33). Fishing mortality rates for the LL1N and LL1S fisheries were comparable to the longline

fishing mortality rates in the two other regions. By comparison, fishing mortality rates for the PSLS fisheries were estimated to be relatively high in Region 1N and Region 1S from the mid-1990s, with a significant increase in 2018 (Figure 33).

The recent (2016–17) pattern of age specific fishing mortality reveals higher levels of fishing mortality for the age classes (4–9 quarters) vulnerable to the PSLS fisheries (Figure 34). Langley (2016) showed that the estimated level of fishing mortality for these younger age classes was similar amongst different levels of weighting for the tagging data set as these younger cohorts were not included within the portion of the population included in the tag release/recovery programme, whereas the estimated fishing mortality rates for the age classes vulnerable to the longline fishery (20+ quarters) were sensitive to the relative weighting of the tagging data set.

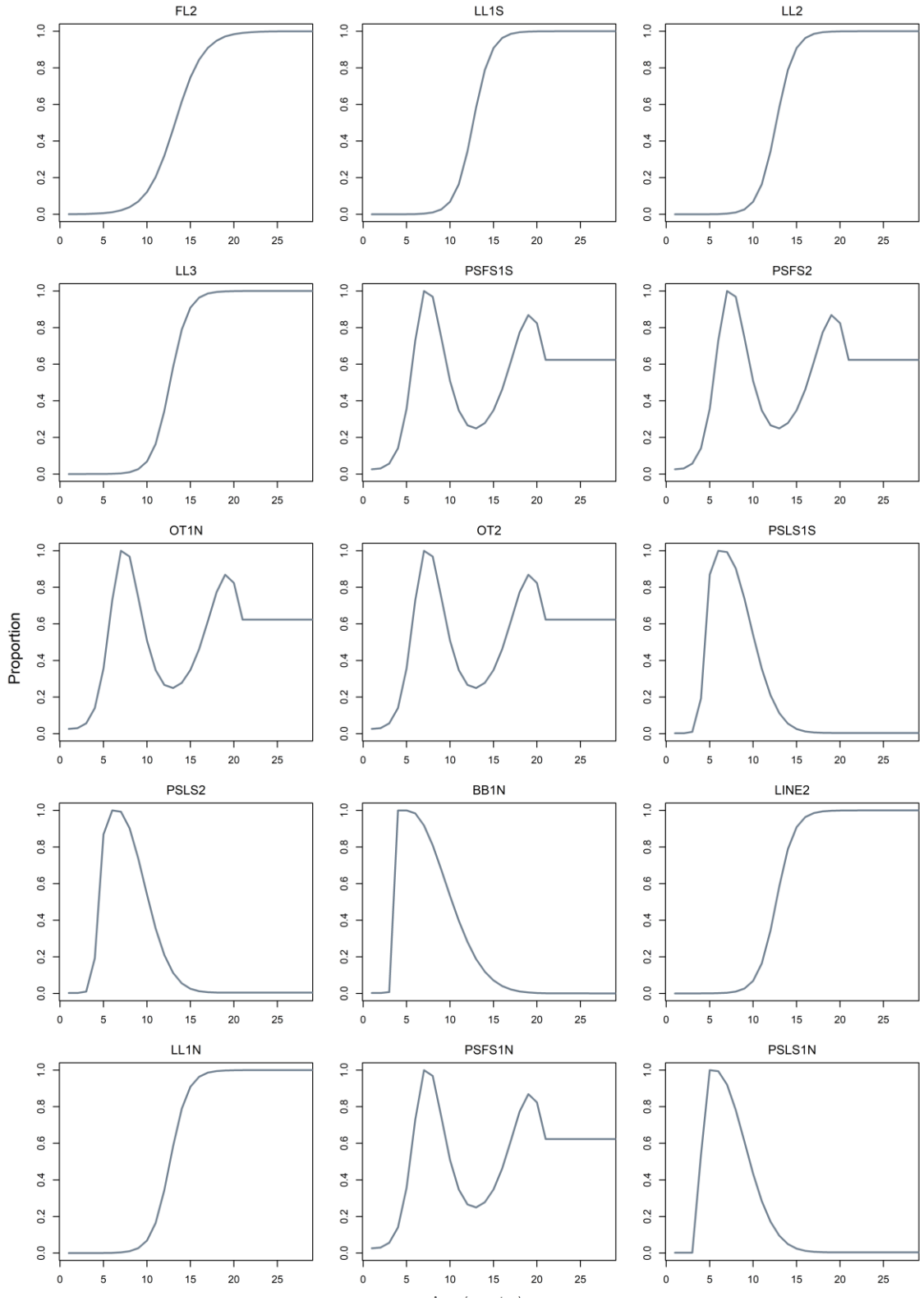

Figure 25: Age specific selectivity by fishery from the reference model.

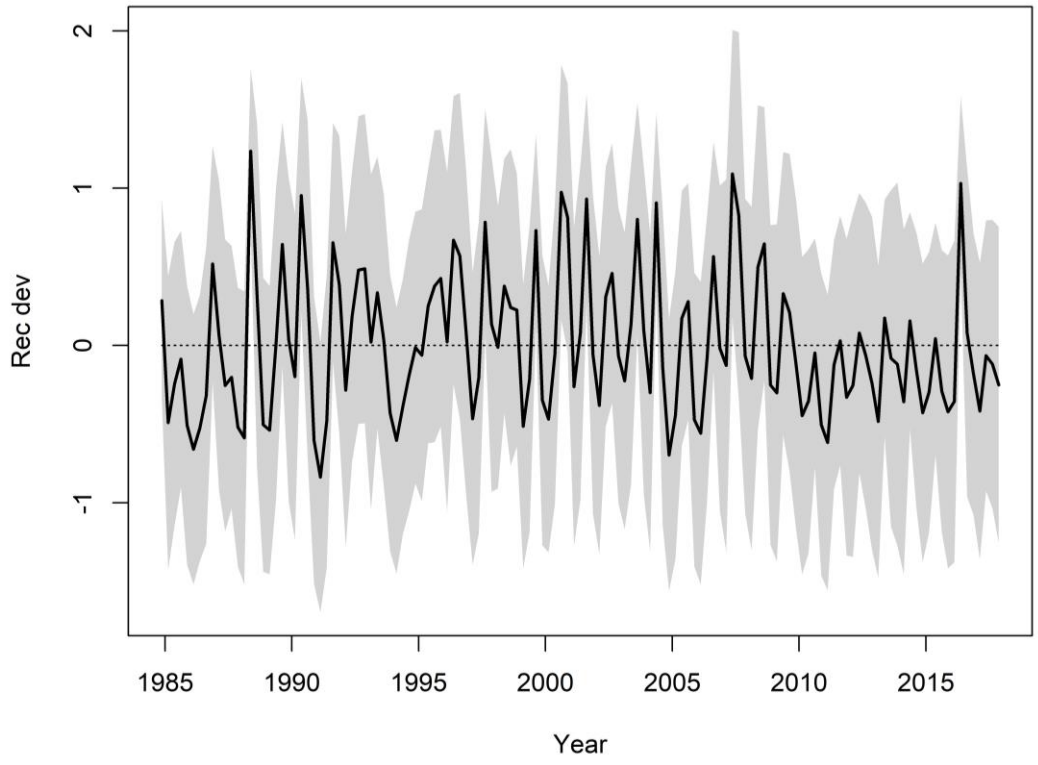

Figure 26: Recruitment deviates from the SRR with 95% confidence interval from the reference model

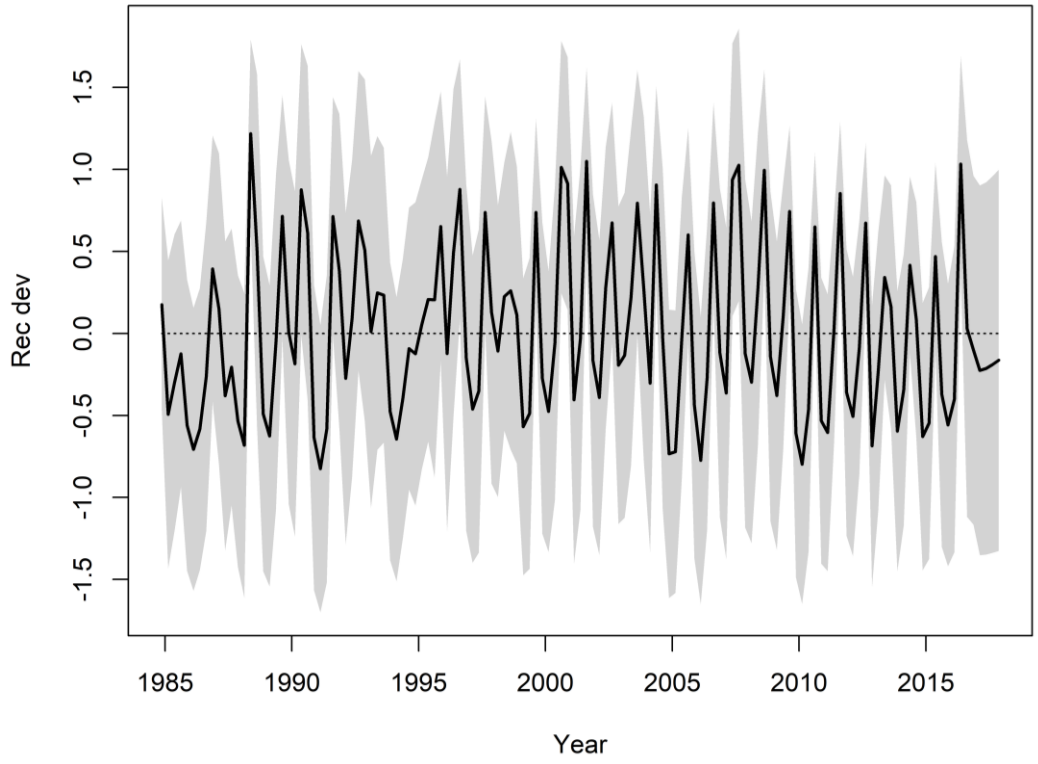

Figure 27: Recruitment deviates from the SRR with 95% confidence interval from model rQhyper.

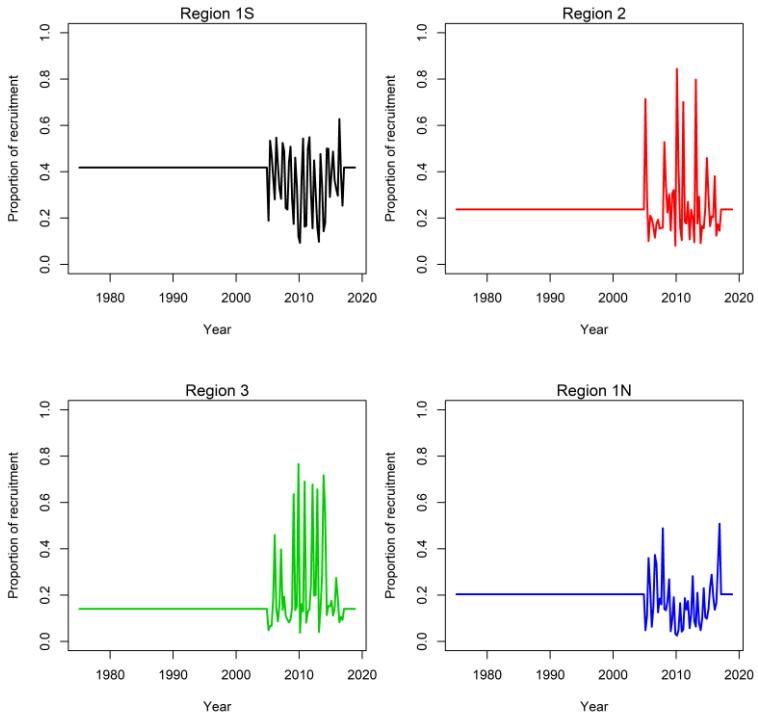

Figure 28: Proportion of the total quarterly recruitment assigned to each region for the reference model.

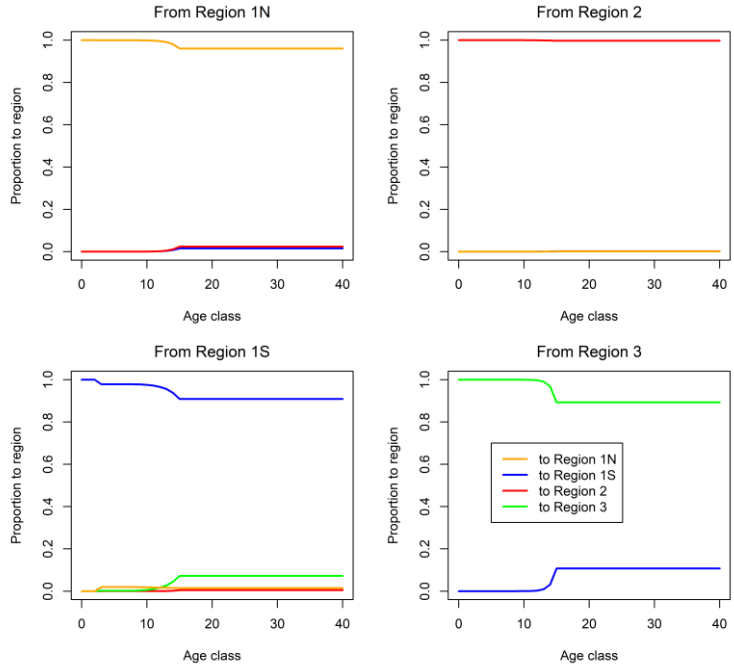

Figure 29: Estimated age specific movement parameters for the reference model.

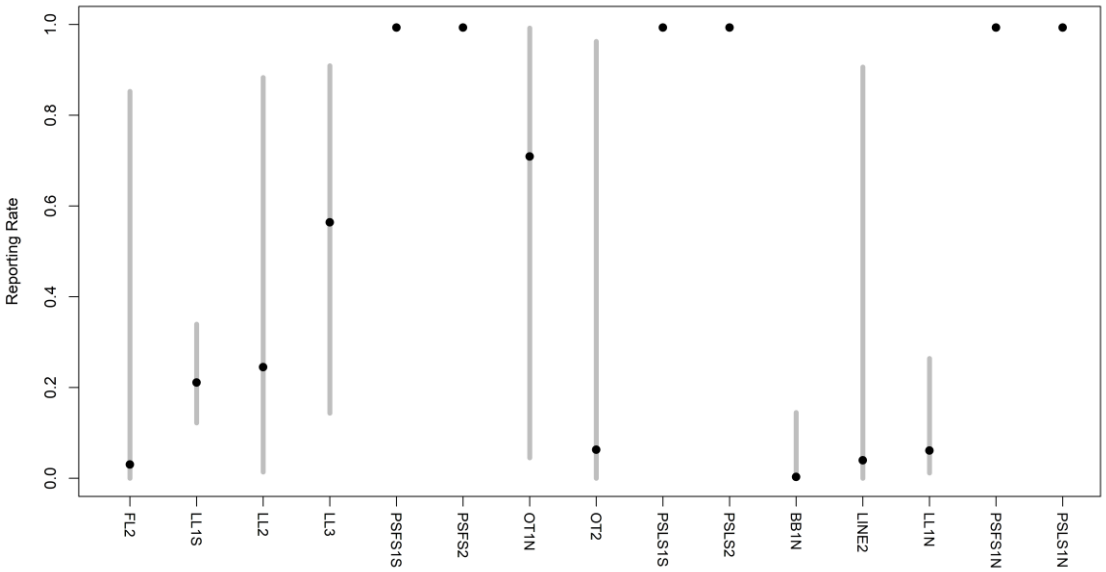

Figure 30: Tag reporting rates for each fishery from the reference model. Purse seine reporting rates were fixed at a value of 1.0. Reporting rates for the other fisheries were estimated. The grey lines represent the 95% confidence interval for the estimated values.

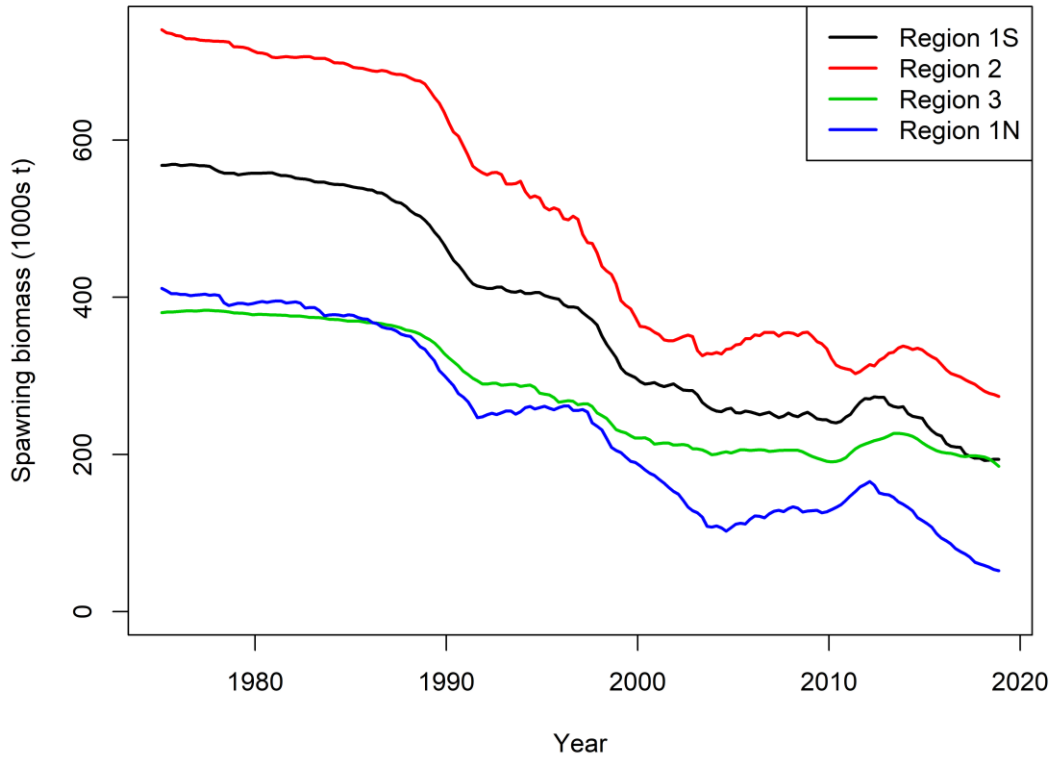

Figure 31: Estimated spawning biomass trajectories for the individual model regions from the reference model.

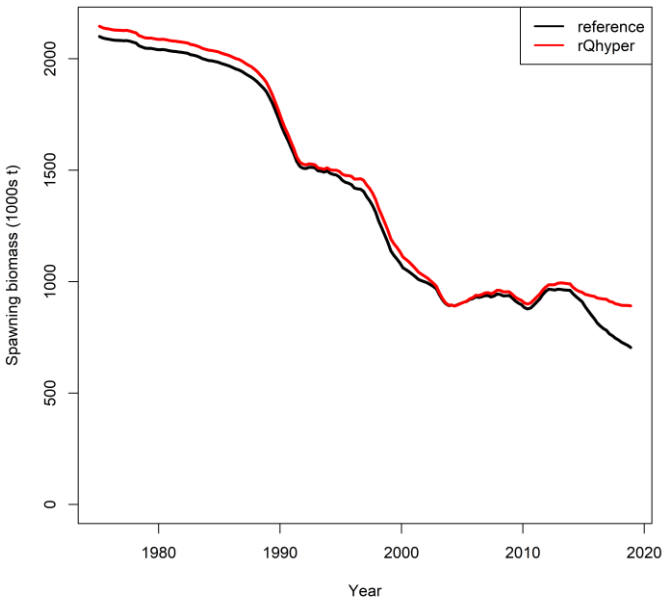

Figure 32: A comparison of estimated spawning biomass from the reference model and model rQhyper.

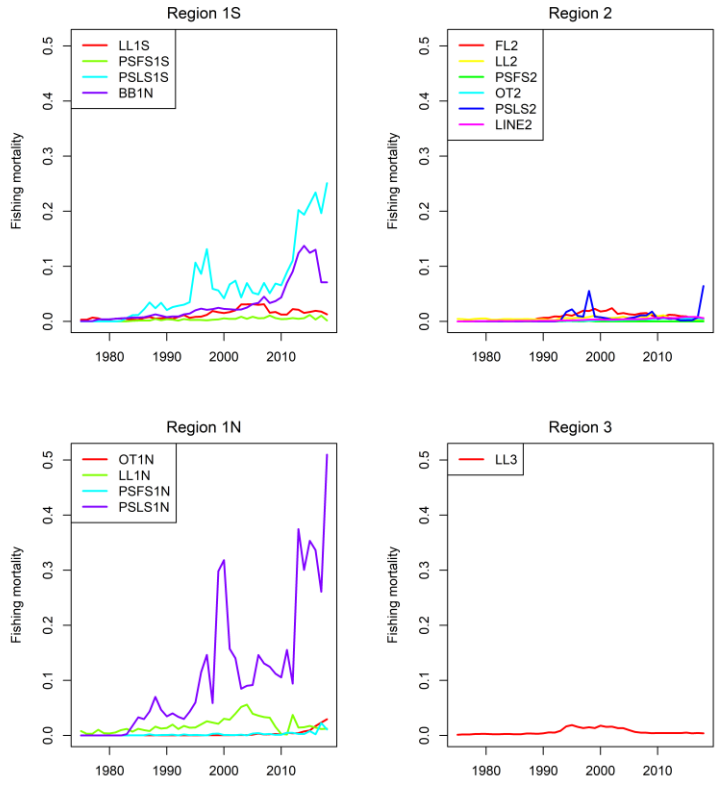

Figure 33:Trends in fishing mortality (quarterly) by fleet for reference model.

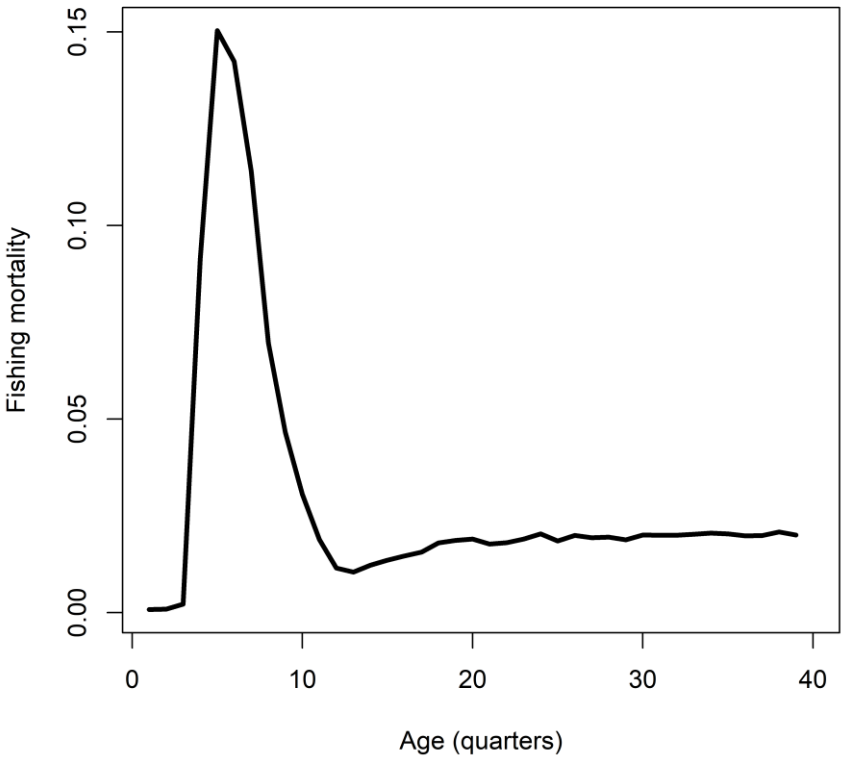

Figure 34. Fishing mortality (quarterly, average) by age class and region for the period used to determine the total F-at-age included in the calculation of MSY based reference points (2016 and 2017) for the reference model.

5.4 Final model options

The reference case and Model *Qhyper* was aimed to capture the uncertainty in recent stock trend relating to interpretation of the LL CPUE in the western equatorial regions for the period 2011-2018. For both models, tag lambda was set at 0.1, which represents an intermediate level of weighting of the tagging data between two extremes. Levels of weighting higher or lower than the current intermediate level of weighting will result in biomass levels that are closer to the lower or high levels of biomass, respectively. Thus, following the 2016 assessment, a tag lambda of 1.0 representing the native weighting of the tag recovery data (giving the tagging data a relatively high weighting) was also included in the final model options.

The reference model assumed a steepness of 0.8. The final model options also included two alternative values of steepness of the BH SRR (*h* 0.7 and 0.9). These values are considered to encompass the plausible range of steepness values for tuna species such as bigeye tuna and are routinely adopted in tuna assessments conducted by other tuna RFMOs.

The final model ensemble corresponds to a full combination of the two CPUE options, two tag lambda weighting, and three steepness values, with a total of 12 models (see Table 8). These models encompass a wide range of stock trajectories, with high tag lambda and steepness values generally yielding lower estimates of biomass (Figure 35). The data included in the stock assessment models are uninformative regarding SRR steepness, although there was generally a small improvement in the total model likelihoods with the higher levels of steepness (Table 10).

Table 10: Details of objective function components for the final set of stock assessment models.

Model	TOTAL	CPUE	Length_comp	Tag_comp	Tag_negbin	Recruitment	Parm_priors	Parm_devs	Catch
RecVar-TagLambda01-h70	1374.9	-496.5	1342.0	322.2	196.7	-26.7	24.7	12.0	0.04
RecVar-TagLambda01-h80*	1372.8	-496.7	1347.0	321.8	194.3	-29.6	22.7	12.9	0.04
RecVar-TagLambda01-h90	1371.5	-497.5	1347.8	321.6	193.4	-29.9	22.7	12.9	0.04
RecVar-TagLambda1-h70	5846.4	-461.9	1370.1	3121.3	1729.8	-0.2	74.8	11.6	0.45
RecVar-TagLambda1-h80	5897.6	-433.5	1375.5	3139.7	1731.1	-3.4	75.4	11.1	1.32
RecVar-TagLambda1-h90	5888.1	-435.5	1375.2	3138.7	1724.5	-4.0	75.4	12.1	1.36
Qhyper-TagLambda01-h70**	1409.3	-472.6	1360.1	324.5	195.8	-22.8	23.1	0.0	0.79
Qhyper-TagLambda01-h80	1440.5	-471.6	1356.9	332.6	199.2	-16.6	39.6	0.0	0.01
Qhyper-TagLambda01-h90	1442.0	-472.8	1361.1	333.3	204.0	-18.5	34.5	0.0	0.01
Qhyper-TagLambda1-h70	5895.6	-405.9	1385.2	3111.7	1729.1	-4.0	77.2	0.0	1.75
Qhyper-TagLambda1-h80	5874.8	-423.6	1386.2	3115.7	1724.3	-5.4	75.2	0.0	1.95
Qhyper-TagLambda1-h90	5943.2	-410.0	1392.7	3137.7	1730.7	9.9	79.1	0.0	2.76

* reference case
** model *rQhyper*

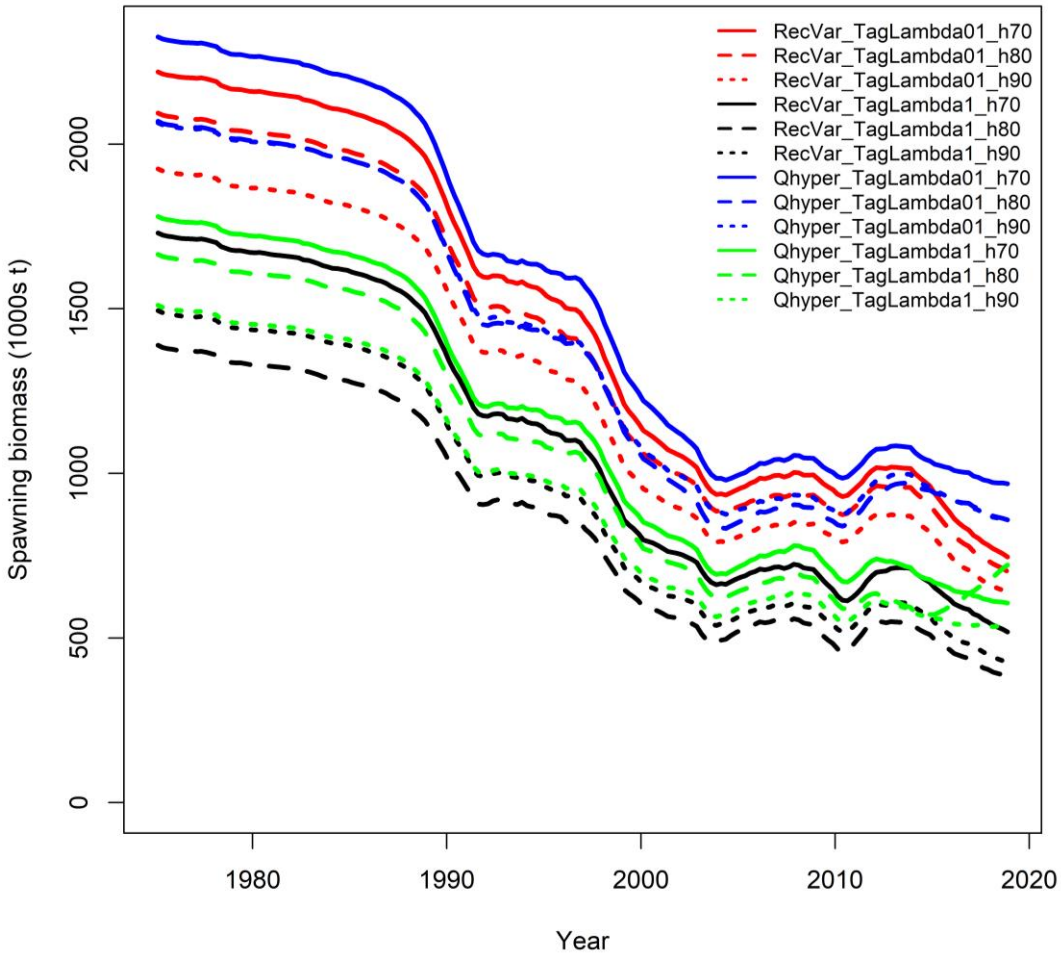

Figure 35: Spawning biomass trajectories from the final model options (details in Table 8).

5.5 Diagnostics

Several diagnostic tools were run for the reference model, including likelihood profiling, ASPM analysis, and retrospective analysis. Further diagnostics using the "run" test (a tool developed by Henning Winker and Felipe Carvalho to evaluate random or systematic pattern in the residuals.) is provided in Appendix D (for model rQhyper only).

5.5.1 Profile likelihood

The likelihood profile on the population scaling parameter (R0) did not show major conflicts between datasets (Figure 36). Overall the CPUE and size data appeared to have provided information on both the upper and lower bounds for the stock abundance. The tagging data has a rather flat likelihood surface in favour of a smaller R0. Increasing the tag weighting (lambda=1) will produce a tag likelihood profile that is slightly more informative (i.e. U-shaped). The total likelihood is also strongly driven by the recruitment penalty function which penalises large recruit anomalies (required to support the catch history for a small R0. An additional jittering analysis suggested the model has attained the minimum in the likelihood surface examined.

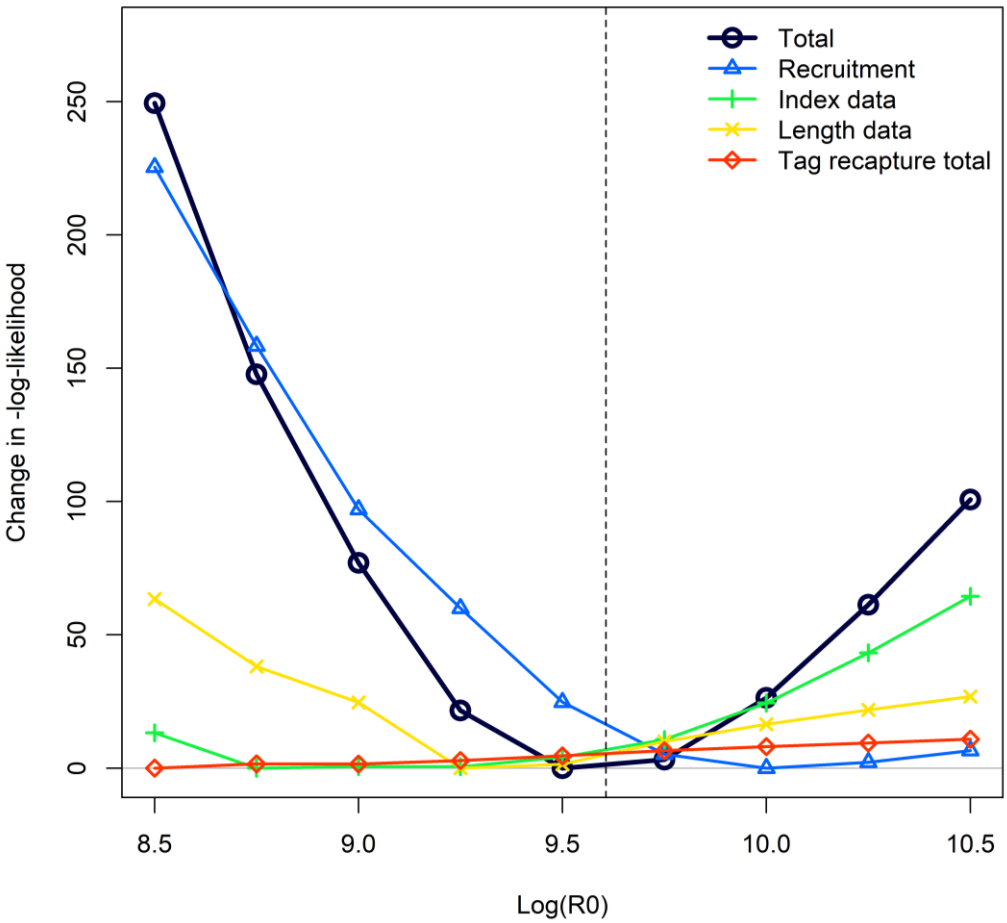

Figure 36:Likelihood profile including total and component likelihood function values for reference model.

5.5.2 ASPM analysis

The Age Structured Production Model (ASPM) analysis (Maunder & Piner 2015) was used to illustrate what is the main driver of the population trend, and whether the composition data has an undue influence on the estimates of abundance. The ASPM analysis involved running two variations of the reference model: *ASPMfixed* – where the length composition data were removed from the model (selectivity parameters fixed) and recruitment deviates were fixed to be zero; and *ASPMdev* – the same as *ASPMfixed* except that fixed recruitment deviates (estimates from the reference model) were added back.

The stock biomass from the two ASPM model runs are shown in Figure 37. The analysis indicated that there is remarkable consistency between the catches and abundance indices for the bigeye tuna stock, i.e. the catch alone is able to explain well the historical trend in the CPUE indices until around 2011–12. However, the model requires lower than average recruitment to accommodate the CPUE trend for 2011–2018 (therefore it is important to examine alternative interpretation of the CPUE trend). The analysis also suggested the length composition data has some influence on the estimate of the population scaling parameter.

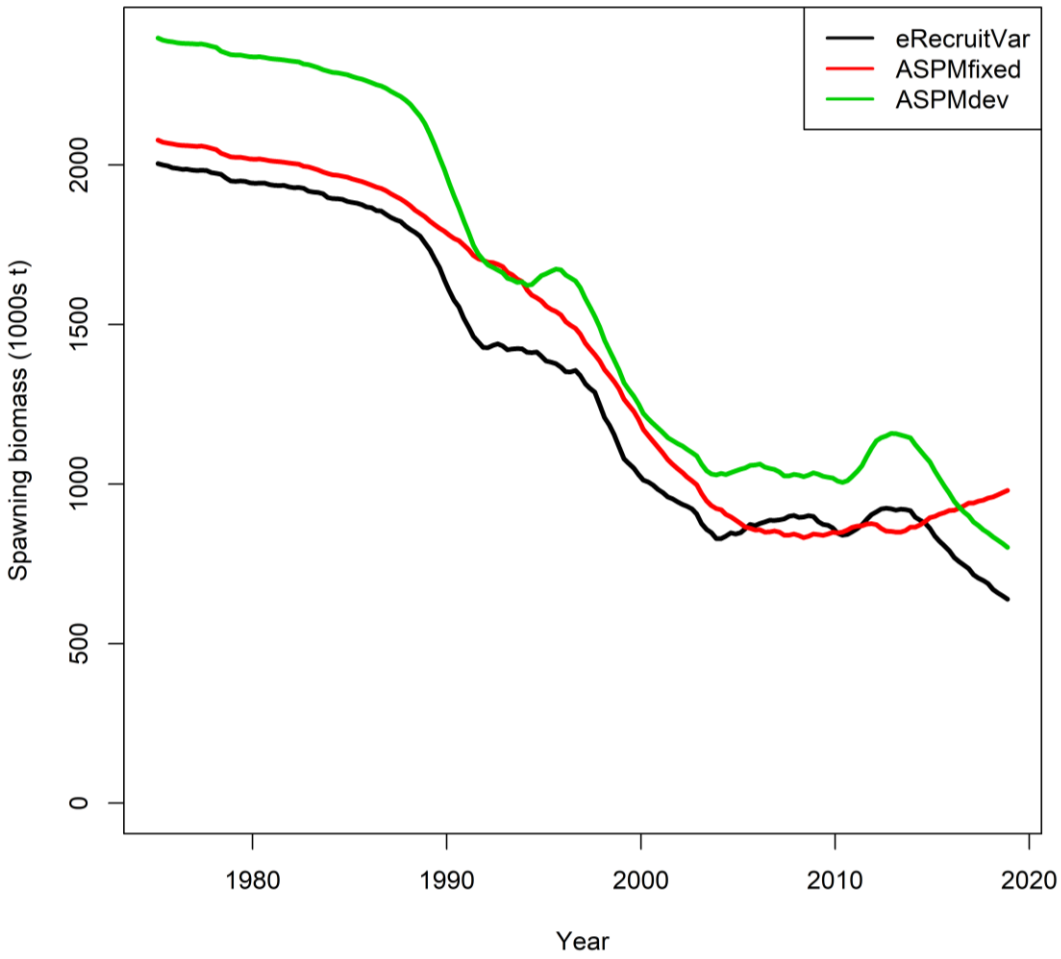

Figure 37: ASPM analysis for the reference model: ASPMfixed (no recruitment deviations), and ASPMdev (recruitment deviates from the reference model added back). Both runs excluded the length composition data and fixed the selectivity parameters.

5.5.3 Retrospective analysis

Retrospective analysis is diagnostic approach to evaluate the reliability of parameter and reference point estimates and to reveal systematic bias in the model estimation. It involves fitting a stock assessment model to the full dataset. The same model is then fitted to truncated datasets where the data for the most recent years are sequentially removed. The retrospective analysis was conducted to the reference model for the last 5 years of the assessment time horizon to evaluate whether there were any strong changes in model results. The selected period was intended to avoid removing any tag recovery data. The analysis involves sequentially removing 4 quarters of data at each trial.

The analysis conducted to the reference model indicated there is no apparent retrospective pattern for SSB estimates and the ratio SSB over SSB_0 and there appears to be some retrospective pattern for the ratio of F over F_{msy} (which may have been related to the sequential change in the reference year used for defining the selectivity pattern). Overall the very low level of retrospective pattern provided some confidence on the robustness of the model with respect to the inclusion of recent observational data.

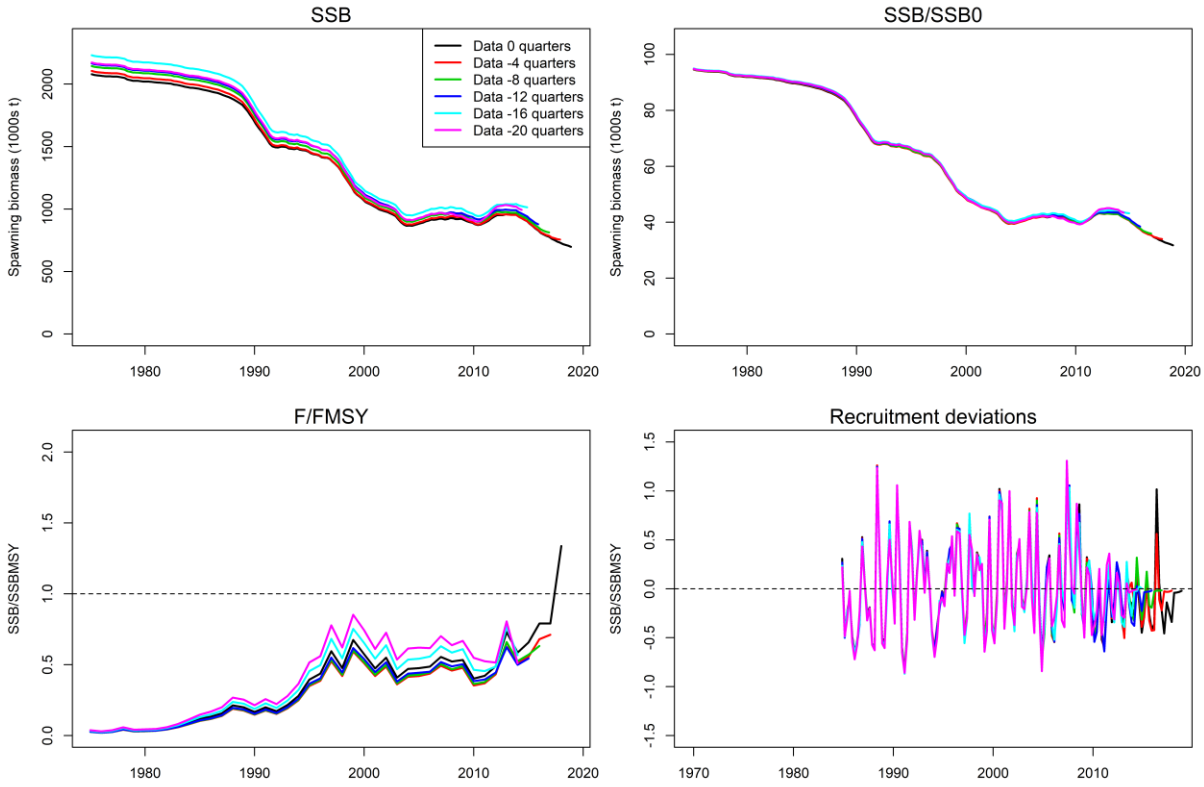

Figure 38: Retrospective analysis summary for the reference model.

6. STOCK STATUS

6.1 Current status and yields

MSY based estimates of stock status were determined for the final model options, including alternative assumptions on CPUE catchability, alternative values of SRR steepness and the alternative higher (native) weighting of tag dataset. Stock status was determined for individual models (Table 11), as well as the for all (12) models combined incorporating uncertainty from individual models based on estimated variance-covariance matrix of parameters (Table 12).

MSY based reference points were derived for the model options based on the average F-at-age matrix for 2016–17 (Figure 34). The period was considered representative of the recent average pattern of exploitation from the fishery. However, it is important to note that recent fishery catches from the fishery have been quite variable (PSLS catches doubled in 2018); variation in the proportion of catches between the main fishing gears (LL and PSLS) are likely to influence the F-at-age matrix and, hence, *MSY* based indicators.

For the selected model options, point estimates of *MSY* ranged from 70,430 mt to 117,530 mt (Table 11) compared to most recent annual catches of about 92,000 mt (Table 2). The lower range of *MSY* values (70–83 k t) were derived from model option *RecVar* with high tag weighting, while the model option *Qhyper* with low tag weighting yielded higher *MSY* estimates closer to or above 10 k t. Model options with higher steepness generally yielded comparatively higher estimates of *MSY*.

For the reference model, fishing mortality rates have remained well below the F_{MSY} through to 1990s and 2000s, increased significantly after 2010 (Figure 39). Biomass was estimated to have declined considerably from the late 1990s before stabilizing through the 2000s and declined rapidly following the increase in 2011–12 (Figure 39). Current fishing mortality (F_{2018}) was estimated 32% higher than F_{MSY}, and current biomass (SSB_{2018}) 29% higher than SSB_{MSY} (Table 11, Figure 40). Stock status estimates for model *rHyper* were slightly more optimistic (Figure 41), with SSB_{2018} estimated to be 39%

higher than SSB_{MSY}, and F_{2018} about 20% higher than F_{MSY} (Table 11, Figure 42). Both models estimated that fishing mortality exceeded F_{MSY} in 2018.

In general, current stock status relative to the *MSY* based benchmarks are not fundamentally different for the range of model options, although the proximity to the *MSY* benchmarks is sensitive to the different of model assumptions. The levels of stock depletion and current fishing mortality were sensitive to the CPUE options; i.e. depletion levels and fishing mortality were considerably higher for the model with CPUE option "*RecVar"* (Table 11). The levels of stock depletion and current fishing mortality were also sensitive to the relative weighting of the tagging data. Clearly, the levels of stock depletion and current fishing mortality derived from the model options with the intermediate level of weighting of the tagging data set will have been influenced by the arbitrary selection of the relative weighting of these data (lambda =0.1). A lower or higher weighting of these data would have resulted in more or less optimistic estimates of stock status and yield. Current (2018) fishing mortality was estimated to be above the F_{MSY} level ($F_{2018}/F_{MSY} > 1.0$) except for one model; current spawning biomass was estimated to be above the SB_{MSY} level ($SB_{2018}/SB_{MSY} > 1.0$) except for three models (they are all associated with high tag weighting option).

Estimates were combined across from the 12 models to generate the final KOBE stock status plot (Figure 43). For individual models, the uncertainty is characterised using the multivariate lognormal Monte-Carlo approach (Walter et al. 2019, Walter & Winker 2019, Winter et al. 2019), based on the maximum likelihood estimates and variance-covariance of the untransformed quantities F/F_{MSY} and SSB/SSB_{MSY}. Thus, estimates of stock status included both within and across model uncertainty. Combined across the model ensemble, SSB_{2018} was estimated to be of 1.30 SSB_{MSY} (0.76– 1.84), and F_{2018} was estimated 1.55 F_{MSY} (0.84–2.26) (Table 12). Thus, the stock is considered not to be overfished, and but is subject to overfishing in 2018.

.

Table 11: Estimates of management quantities for the stock assessment model options. Current yield (mt) represents yield in 2018 corresponding to fishing mortality at the FMSY level.

Option	SB_0	SB_{MSY}	SB_{MSY}/SB_0	SB_{2018}	SB_{2018}/SB_0	SB_{2018}/SB_{MSY}	F_{2018}/F_{MSY}	MSY
RecVar-TagLambda01-h70	2 337 420	692 626	0.30	759 505	0.32	1.10	1.69	79 362
*RecVar-TagLambda01-h80**	2 212 620	555 249	0.25	714 158	0.32	1.29	1.32	86 236
RecVar-TagLambda01-h90	2 043 040	343 297	0.17	647 444	0.32	1.89	1.00	91 755
RecVar-TagLambda1-h70	1 848 300	597 453	0.32	529 104	0.29	0.89	2.39	77 853
RecVar-TagLambda1-h80	1 505 460	448 052	0.30	389 863	0.26	0.87	2.46	70 430
RecVar-TagLambda1-h90	1 611 460	428 792	0.27	433 046	0.27	1.01	1.87	83 792
Qhyper-TagLambda01-h70	2 443 230	717 022	0.29	970 772	0.40	1.35	1.16	96 762
*Qhyper-TagLambda01-h80***	2 186 170	620 862	0.28	864 944	0.40	1.39	1.20	101 012
Qhyper-TagLambda01-h90	2 181 640	366 524	0.17	862 631	0.40	2.35	0.73	117 532
Qhyper-TagLambda1-h70	1 896 960	617 933	0.33	609 052	0.32	0.99	1.95	83 254
Qhyper-TagLambda1-h80	1 782 350	532 257	0.30	703 864	0.39	1.32	1.23	96 276
Qhyper-TagLambda1-h90	1 627 200	425 854	0.26	536 102	0.33	1.26	1.46	91 602

* reference model
** reference model rQhyper

Table 12: Estimated Status of bigeye tuna in the Indian Ocean from the model ensemble.

Catch in 2018:	93 515
Average catch 2014–2018:	92 138
MSY (1000 t) (plausible range):	90 (73 –106)
F_{MSY}	0.23 (0.15–0.31)
SB_0(1000 t) (80% CI):	1975 (1580–2370)
SB_{2018} (1000 t) (80% CI):	668 (438–899)
SB_{MSY}	526 (370–685)
SB_{2018}/SB_0 (80% CI):	0.33 (0.27–0.40)
SB_{2018} / SSB_{MSY}	1.30 (0.76–1.84)
F_{2018} / F_{MSY}	1.55 (0.84–2.26)

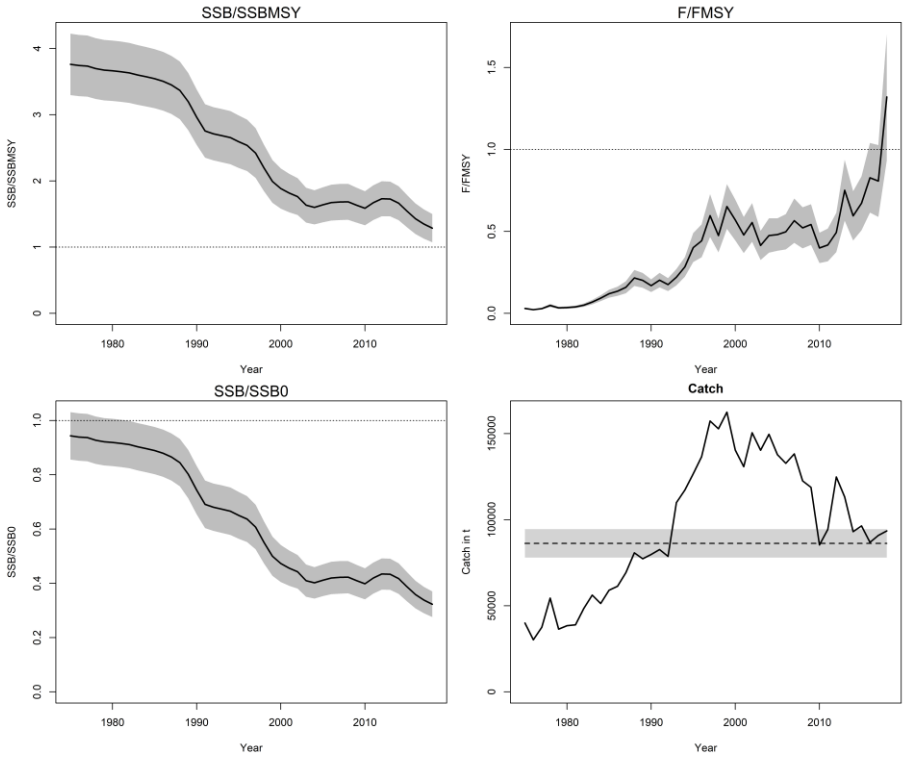

Figure 39: Estimated stock trajectories for the Indian Ocean bigeye tuna from the reference model. Thick black lines shaded areas represent 5th and 95th percentiles. In the catch plot, dotted lines represent estimate of MSY, the shaded area represents 5th and 95th percentiles.

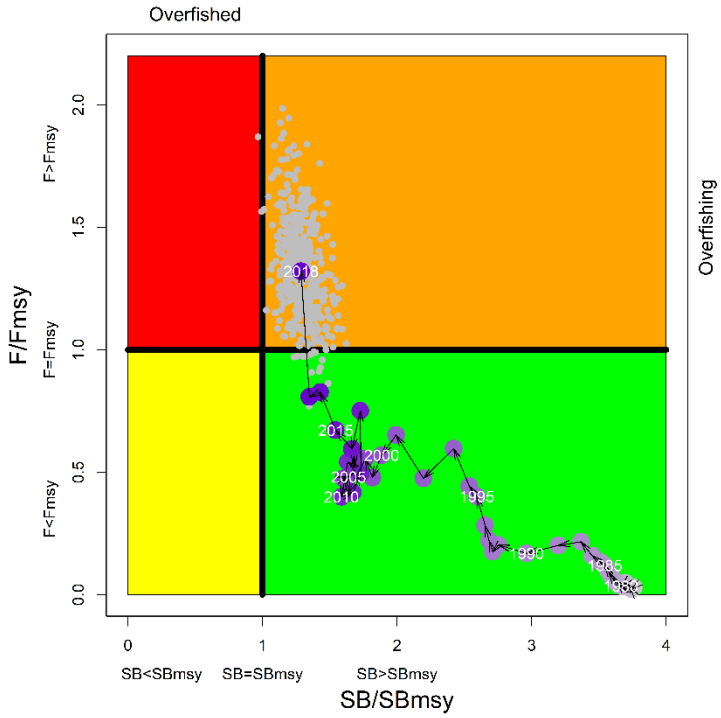

Figure 40: Annual stock status, relative to SB_{MSY} (x-axis) and F_{MSY} (y-axis) reference points from the reference model. The grey dots represent the uncertainty generated using the delta-MVLN estimator (Walter & Winker 2019).

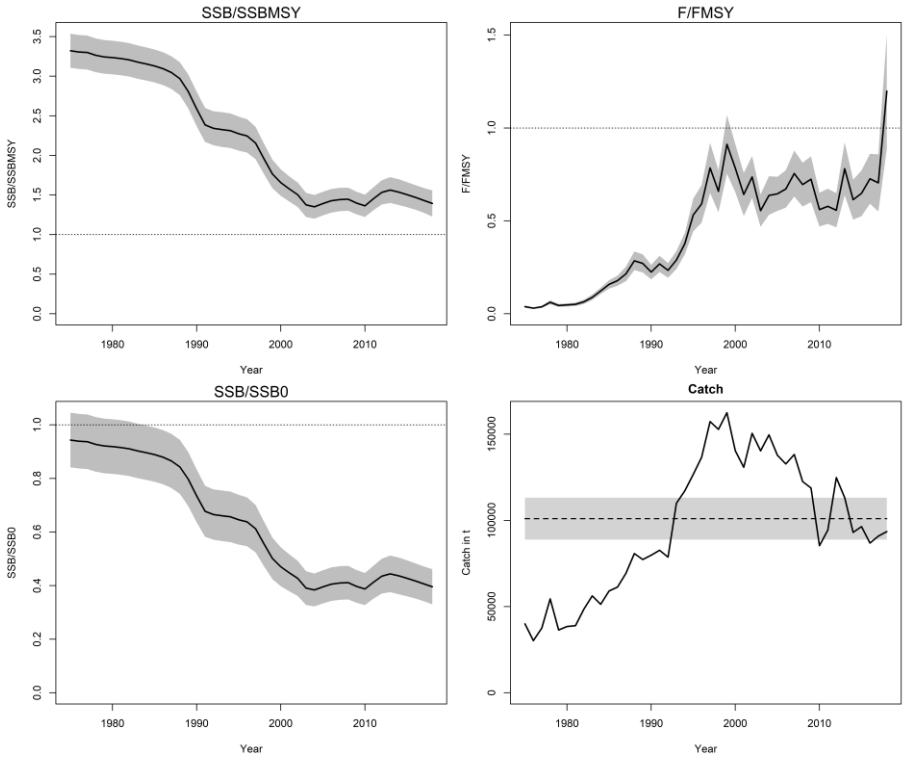

Figure 41: Estimated stock trajectories for the Indian Ocean bigeye tuna from the model rQhyper. Thick black lines shaded areas represent 5th and 95th percentiles. In the catch plot, dotted lines represent estimate of MSY, the shaded area represents 5th and 95th percentiles

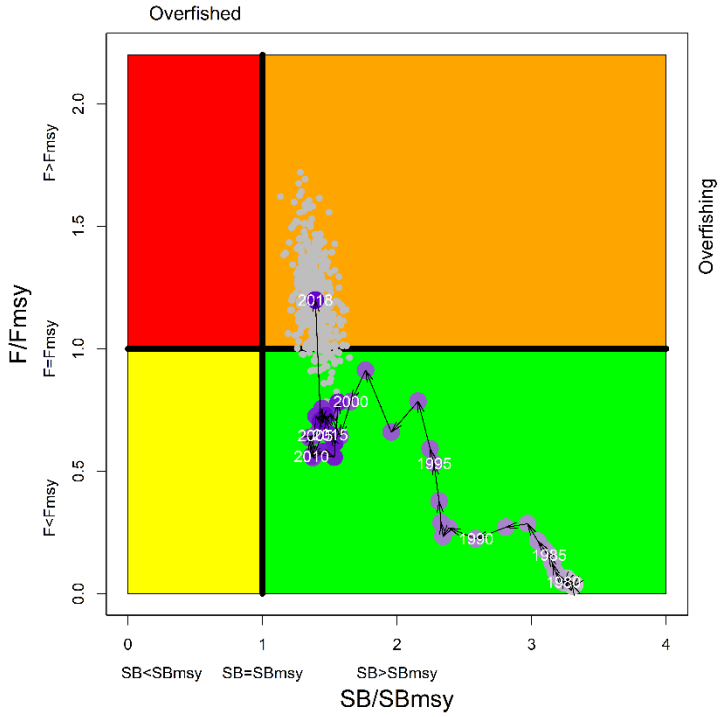

Figure 42: Annual stock status, relative to SB_{MSY} (x-axis) and F_{MSY} (y-axis) reference points from model rQhyper. The grey dots represent the uncertainty generated using the delta-MVLN estimator (Walter & Winker 2019).

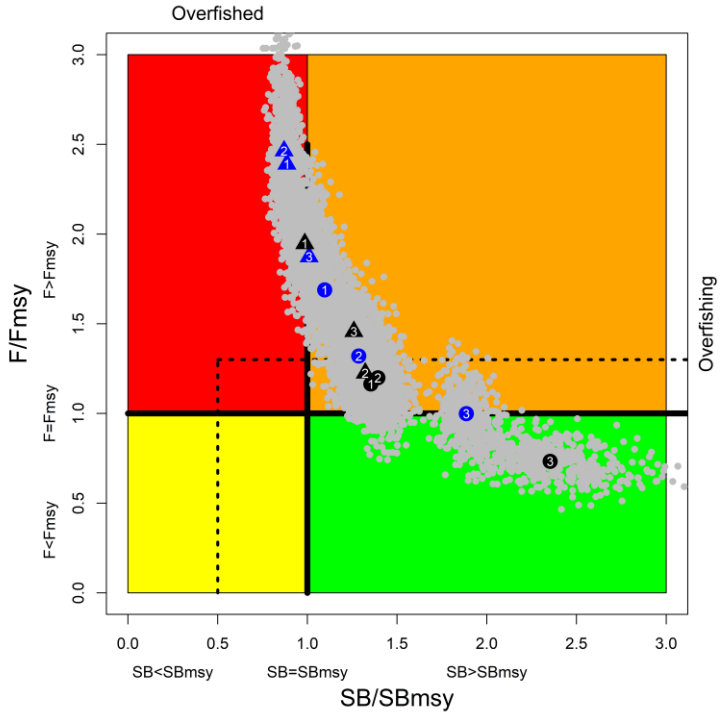

Figure 43: current stock status, relative to SB_{MSY} (x-axis) and F_{MSY} (y-axis) reference points for the final model options. Coloured symbols represent MPD estimates from individual models (Triangles and dots represents CPUE options RecVar and Qhyper respectively; black and blue represents tag weighting option lambda=0.1 and lambda=1 respectively; 1,2,3 represents steepness values of 0.7,0,8, and 0.9 respectively). Grey dots represent uncertainty from individual models. The dashed lines represent limit reference points for IO bigeye tuna (SB_{lim} = 0.5 SB_{MSY} and F_{lim} = 1.4 F_{MSY}).

6.2 Projection

Stock projections were tentatively conducted for the *reference* model and model *rQhype*. The projections were conducted for a 10-year period (2019–2028) at a constant level of catch set as a multiple of the fishery catches in 2018. Seven levels of catch were investigated representing 60% to 120% (in incremental of 10%) of the 2015 catch level. Recruitment during the projection period was at the equilibrium level. The uncertainty associated with the projected biomass was derived from the covariance matrix. For each stock scenario, the probability of the biomass being below the SB_{MSY} level was determined after 3 years (2021) and 10 years (2028).

The uncertainty associated with the projected biomass propagates rapidly, reflecting the uncertainty associated with the equilibrium recruitment level. For the *reference* model, the recent recruitment has been much below the average, the stock continues to decline in the short term. With the significant increase of catches from the PSLS fishery in 2018, current levels of catch are higher than the equilibrium surplus production and the stock biomass is projected to decrease over the longer period, with a relatively high probability of dropping below the SB_{MSY} level (Table 13). Catch reduction of 20% or more will result in the biomass being maintained at or above the SB_{MSY} for the longer term (with over 50% probability).

The projection for model *rQhyper* is more optimistic: the current level of catch will result in biomass dropping just below SB_{MSY}. Catch reduction of 10% will result in the biomass being maintained above the SB_{MSY} for the longer term.

It is important to note that the assumed catch distribution in the projection is based on the 2018 catches, which consisted of a significant PSLS component targeting almost exclusively on juvenile fish. Conceivably, assuming alternative catch distributions (e.g. from 2014 – 2017) that distribute more fishing pressure towards adult is expected to yield more optimistic projection results.

Table 13: Projected stock status: spawning biomass relative to SB_{MSY} and the probability of being below SB_{MSY} and 0.5SSB in 3 and 10 years for seven alternative levels of catch relative to 2018 (93 515 mt) for the reference and rQhyper model.

		3 years (2021)			10 year (2028)		
Model option	**Catch**	SB/SB_{MSY}	$Pr(SB<SB_{MSY})$	$Pr(SB<SB_{0.5MSY})$	SB/SB_{MSY}	$Pr(SB<SB_{MSY})$	$Pr(SB<SB_{0.5MSY})$
reference	60%	1.14	0.14	0.00	1.58	0.03	0.00
	70%	1.11	0.17	0.00	1.31	0.16	0.01
	80%	1.09	0.25	0.00	1.02	0.51	0.03
	90%	1.06	0.33	0.00	0.80	0.87	0.05
	100%	1.03	0.42	0.00	0.67	0.93	0.20
	110%	1.00	0.54	0.00	0.54	0.98	0.42
	120%	0.96	0.60	0.00	0.46	1.00	0.59
		SB/SB_{MSY}	$Pr(SB<SB_{MSY})$	$Pr(SB<SB_{0.5MSY})$	SB/SB_{MSY}	$Pr(SB<SB_{MSY})$	$Pr(SB<SB_{0.5MSY})$
rQhyper	60%	1.58	0.00	0.00	1.89	0.00	0.00
	70%	1.55	0.00	0.00	1.66	0.02	0.00
	80%	1.53	0.00	0.00	1.42	0.10	0.00
	90%	1.50	0.00	0.00	1.18	0.26	0.01
	100%	1.47	0.00	0.00	0.97	0.56	0.02
	110%	1.44	0.00	0.00	0.83	0.81	0.04
	120%	1.41	0.00	0.00	0.71	0.93	0.13

7. DISCUSSION

This report presents a preliminary stock assessment for Indian Ocean bigeye tuna using a spatially explicit, age structured model. It represents an update and revision of the 2016 assessment model with newly available data. There are no fundamental changes in the structure of the current assessment models compared to the previous assessment (Langley *et al* 2016a), with most revisions concerning observational data, e.g. the inclusion of revised regional LL CPUE indices, the adoption of a new regional weighting scheme, and a refined procedure to process the tag data that is more consistent with recent practice. A range of exploratory models are also presented to explore the impact of key data sets and model assumptions.

As earlier assessments, the models presented here, while providing a reasonable fit to some key data sets (e.g., the CPUE indices), also show some signs of poor fit (e.g. LF data). There are conflicts amongst observational datasets, noticeably between the CPUE and tag data, and the model estimates are sensitive to the relative weighting of these data. Estimates of movement rates were probably more influenced by model configurations than tag data. The nature and extent of the dispersal of tagged fish remains a key uncertainty in the assessment.

The overall stock status estimates obtained from a range of model options do not differ substantially from the previous assessment: current spawning biomass remained to be above SSB_{MSY} (SSB_{2018}/SSB_{MSY} = 1.30). However, fishing mortality is estimated to be above F_{MSY} (F_{2018}/F_{MSY} = 1.55), mostly reflecting the significant increase of the catches from PSLS fishery. Current (2018) catches are higher than the estimated MSY from the final model ensemble and are likely to drive the stock to be below SSB_{MSY} in the long term. The retrospective analysis provided some confidence on the robustness of the model with respect to recent data, yet the uncertainly on levels of recent recruitment may undermine the predictive capabilities of the model.

One of the major uncertainties in the assessment model was related to the interpretation of the Longline CPUE in the western equatorial regions in the post-piracy period (2011 – 2018). Although the recent low catch rates were corroborated by the anecdotal evidence from commercial fishers, the extent of the decline appear to be inconsistent with the catch history. The LL CPUE in region 1 implied a rapid decline in stock abundance in recent years, as driven by a prolonged period of below average recruitment. Model options that provides alternative interpretation on the recent CPUE indices yielded more optimistic stock trend.

Historically, there was somewhat similar discontinuities in the longline indices, notably in the 1976–78. Hoyle et al. (2017b) found the discontinuities during the late 1970s exists for multiple fleets in multiple oceans and the marked change in the magnitude of the CPUE indices between the two periods corresponds to a large shift in the gear configuration of the longline fleets in the equatorial regions during this period (Hoyle & Okamoto 2015). The 2011–12 spike in the western tropical region coincided with the period when vessels returned to the old fishing ground that had been avoided for several years due to the threat of piracy. The spike was considered to be related to a combination of factors including increase in abundance and major changes in catchability (Hoyle et al. 2017a). Consequently, the rapid decline of indices in the years that followed may not fully conform to the population dynamics, implying a possible non-linear relationship between CPUE and abundance.

Another source of uncertainty is related to the discards. Unaccounted discards introduce bias to catch and length composition data and undermine the interpretation of CPUE. There was evidence that indicated that discards of small bigeye and yellowfin tuna may be more common in the Longline fishery than previously thought. Regulations of catch limit and changes in market conditions can create incentives to retain larger, high value bigeye tuna and to discard smaller ones (Nóbrega, et. al. 2014). However reliable estimates of discards for tropical tuna in the Indian Ocean is not available. Herrera (2018) suggested that the vanishing of smaller fish sampled for lengths from the Taiwanese commercial logbooks since 2000s was possibly the results of fish discards not being recorded in the logbook. Hoyle et al. (2019b) estimated the discards rates of bigeye tuna for 2002 – 2018 from the Taiwanese longline commercial logbooks, and the discard number/rate of bigeye tuna was very low except for 2005 when the catch limit (35000 t) was imposed. These estimates were considered to be biased low given potential under-reporting. Using observer data, Huang & Liu (2010) estimated an overall discard rate of about 4.7% for bigeye (the discard rate was estimated to be as high as 38% for some fleets). It is important to quantify the scale and trend of discards from available data sources, as discard rates are also likely to be subject to high variability depending on how stock abundance/catchability changed over time.

The assessment model adopted a 4-region spatial structure. Movement rates between regions were estimated to be very low. There is very little information on the movement dynamics of bigeye tuna and a low level of mixing among subpopulation may be possible. Alternative models assuming hypothetical high mixing rates did not yield very different estimates of stock abundance but was not consistent with the extent of spatial heterogeneity as observed in the regional CPUE indices. Models with less disaggregated regional partitioning (e.g. three regions) reduce the complexity of movement dynamics but is likely to introduce bias if the incomplete tag dispersal within the main tag recovery region is not adequately accounted for.

Another aspect of modelling that is yet to be fully explored is related to the recruitment bias adjustment. In the assessment model, the full log-bias adjustment factor is applied to the recruitment deviates (as recruitment variability is assumed to be lognormally distributed, see Methot et al. 2013). However, underestimation of recruitment variability (due to data period with low information) implies the need for further bias correction (Methot et al. 2013) to ensure that the population scaling parameter R0 represent the long-term average recruitment. The degree of bias correction can be determined from the relationship between the assumed and estimated recruitment variability (Methot and Taylor 2011). The initial investigation suggested that the bias correction factor should be lower than what is currently assumed but the value varied between model configurations (sensitive to the assumed CV of the CPUE indices, sample size of the length composition data, etc). Applying the bias correction factors resulted in lower estimates of stock productivity but made no appreciable difference to the stock status in relative terms. Nonetheless, the application of recruitment bias correction requires further exploration in future assessments.

8. ACKNOWLEDGMENTS

I am grateful to the many people that contributed to the collection of this data historically, analysts involved in the CPUE standardization, and developers for providing the SS3 software, and in particular to Adam Langley who conducted the previous assessments, and to Henning Winker who provided the scripts for calculating the delta-MVLN estimator and performing the “run” test.

9. REFERENCES

Appleyard SA, RD Ward, PM Grewe. 2002. Genetic stock structure of bigeye tuna in the Indian Ocean using mitochondrial DNA and microsatellites. J. Fish Biol. 60: 767- 770.

Basson, M., Dowling, N. 2004. Standardisation of size-based indicators for bigeye and yellowfin tuna in the Indian Ocean. IOTC-WPTT-2004-15.

Chassot E, Assan C, Esparon J,, Tirant A, Delgado d, Molina A, Dewals P, Augustin E, Bodin N. 2016. Length-weight relationships for tropical tunas caught with purse seine in the Indian Ocean: Update and lessons learned. IOTC-2016-WPDCS12-INF05.

Eveson, P., Million, J., Sardenne, F., Le Croizier, G. 2012. Updated growth estimates for skipjack, yellowfin and bigeye tuna in the Indian Ocean using the most recent tag-recapture and otolith data. IOTC-2012-WPTT14-23.

Eveson, P., Million, J., Sardenne, F., Le Croizier, G. 2015. Estimating growth of tropical tunas in the Indian Ocean using tag-recapture data and otolith-based age estimates. Fisheries Research 163, 58–68,

Fu, D. 2017. Indian ocean skipjack tuna stock assessment 1950-2016 (stock synthesis). IOTC–2017–WPTT19–47_rev1.

Fu, D., Langley, A. Merino, G., Ijurco, A.U. 2018. Preliminary Indian ocean yellowfin tuna stock assessment 1950-2017 (Stock Synthesis). IOTC–2018–WPTT20–33.

Hampton. J. 2000. Natural mortality rates in tropical tunas: size really does matter. Can. J. Fish. Aquat. Sci. 57: 1002–1010 (2000).

Harley, S.J. 2011. Preliminary examination of steepness in tunas based on stock assessment results. WCPFC SC7 SA IP-8, Pohnpei, Federated States of Micronesia, 9–17 August 2011.

Hillary, R.M., Million, J., Anganuzzi, A., Areso, J.J. 2008a. Tag shedding and reporting rate estimates for Indian Ocean tuna using double-tagging and tag-seeding experiments. IOTC-2008-WPTDA-04.

Hillary, R.M., Million, J., Anganuzzi, A., Areso, J.J. 2008b. Reporting rate analyses for recaptures from Seychelles port for yellowfin, bigeye and skipjack tuna. IOTC-2008-WPTT-18.

Hoyle, S.D., Leroy, B.M., Nicol, S.J., Hampton, J. 2015. Covariates of release mortality and tag loss in large-scale tuna tagging experiments. Fisheries Research 163, 106-118.

Hoyle, S.D., Kitakado, T., Matsumoto, T., Kim, D.N., Lee, S.I., Ku, J.E., Lee, M.K., Yeh,Y., Chang, S.T., Govinden, R., Lucas, J., Assan, C., Fu, D. 2017a. IOTC–CPUEWS–04 2017: Report of the Fourth IOTC CPUE Workshop on Longline Fisheries, July 3th–7th, 2017. IOTC–2017–CPUEWS04–R. 21 p.

Hoyle, S., Satoh, K., Matsumoto, T. 2017b. Exploring possible causes of historical discontinuities in Japanese longline CPUE. IOTC–2017–WPTT19–33 Rev1.

Hoyle, S., Gorka, M., Murua, H., Yeh, Y.M., Matsumoto, T., Satoh, K., Kim, D.N., Lee, S.I., Fu, D. 2019a. IOTC–CPUEWS–06 2019: Report of the Sixth IOTC CPUE Workshop on Longline Fisheries, May 28th–June 1st, 2019. IOTC–2019–CPUEWS06–R[E]: 27 pp.

Hoyle, S., Gorka, M., Murua, H., Yeh, Y.M., Matsumoto, T., Satoh, K., Kim, D.N., Lee, S.I., Fu, D. 2019b. Collaborative study of bigeye tuna CPUE from multiple Indian Ocean longline fleets in 2019. IOTC–2019–WPM09–xx.

Hoyle, S.D., Okamoto, H. (2015). Descriptive analyses of the Japanese Indian Ocean longline fishery, focusing on tropical areas. IOTC-2015-WPTT17-INF08.

Hoyle, S.D., Langley, A. 2018. Indian Ocean tropical tuna regional scaling factors that allow for seasonality and cell areas. IOTC-2018-WPM09-13.

IOTC–WPTT18 2016. Report of the 18th Session of the IOTC Working Party on Tropical Tunas.

Seychelles, 5–10 November 2016. IOTC–2016–WPTT18–R. 126 pp.

IOTC–WPTT20 2018. Report of the 20th Session of the IOTC Working Party on Tropical Tunas. Seychelles, 29 October – 3 November 2018. IOTC–2018–WPTT20–R. 127 pp.

IOTC 2018. Review of the statistical data and fishery trends for tropical tunas. IOTC-2018-WPTT20-07 Rev_1. IOTC-2004-WPTT-INF04.

Farley, J.H., Clear, N.P., Leroy, Bruno., Davis, T.L.O., McPherson, G. 2004. Age and growth of bigeye tuna (Thunnus obesus) in the eastern and western AFZ.

Fonteneau, A., Pallares, P. 2004. Tuna natural mortality as a function of their age: the bigeye tuna case. IOTC-2004-WPTT-INF02.

Fonteneau, A., Ariz, R., Delgado, A., Pallares, P., Pianet, R. 2004. A comparison of bigeye stocks and fisheries in the Atlantic, Indian and pacific oceans. IOTC-2004-WPTT-INF03.

Gaertner, D., Hallier, J.P. 2015. Tag shedding by tropical tunas in the Indian Ocean and other factors affecting the shedding rate. Fisheries Research. 2015/163.

Geehan, J. 2018. Revision to the IOTC scientific estimates of Indonesia's fresh longline catches. IOTC-2018-WPDCS14-23.

ISSF (2011). Report of the 2011 ISSF stock assessment workshop. Technical Report ISSF TechnicalReport 2011-02, Rome, Italy, March 14-17, 2011.

IOTC–WPTT18 2016. Report of the 18th Session of the IOTC Working Party on Tropical Tunas. Seychelles, 5–10 November 2016. IOTC–2016–WPTT18–R[E]. 126 pp.

Kolody, D., Herrera, M., Million, J., (2010). Exploration of Indian Ocean Bigeye Tuna Stock Assessment Sensitivities 1952-2008 using Stock Synthesis (updated to include 2009). IOTC-2012-WPTT10-4.

Kolody, D. 2011. Can length-based selectivity explain the two stage growth curve observed in Indian Ocean YFT and BET. IOTC–2011–WPTT13–33.

Langley, A.; Million, Julien. 2012. Determining an appropriate tag mixing period for the Indian Ocean yellowfin tuna stock assessment. OTC–2012–WPTT14–31.

Langley, A.; Herrera, M.; Sharma, R. 2013a. Stock assessment of bigeye tuna in the Indian Ocean for 2012. IOTC-2013-WPTT15-30.

Langley, A.; Herrera, M.; Sharma, R. 2013b. Stock assessment of bigeye tuna in the Indian Ocean for 2012. IOTC-2013-WPTT15-30-Rev_1.

Langley, A. 2016. Stock assessment of bigeye tuna in the Indian Ocean for 2016 — model development and evaluation.

Matsumoto, T. 2016. Consideration on the difference of average weight by estimation method for tunas caught by Japanese longline in the Indian Ocean. IOTC-2016-WPDCS12-16.

Method, R.D., Taylor, I.G. 2011. Adjusting for bias due to variability of estimated recruitments in fishery assessment models. Can. J. Fish. Aquat. Sci. 68: 1744–1760.

Methot, R.D. 2013. User manual for Stock Synthesis, model version 3.24f.

Methot, R.D., Wetzel, C.R. 2013. Stock synthesis: A biological and statistical framework for fish stock assessment and fishery management. Fisheries Research 142 (2013) 86–99.
Maunder. A concise guide to developing fishery stock assessment models.

Maunder, M.N., Piner, K.R., 2015. Contemporary fisheries stock assessment: many issues still remain. ICES J. Mar. Sci. 72, 7–18, http://dx.doi.org/10.1093/icesjms/fsu015.

Minte-Vera, G.A., Maunder, M.N. Aires-da-Silva, A.M. Satoh, K., Uosaki, K. 2017. Get the biology right, or use size-composition data at your own risk. Fisheries Research 192 (2017) 114–125.

Minte-Vera, G.A., Aires-da-Silva, Alexandre, Maunder., M. N. 2016. Status of yellowfin tuna in the eastern pacific ocean in 2016 and outlook for the future. SAR-18-2-YFT-assessment-2016. IATTC.

Shono, H., K. Satoh, H. Okamoto, and T. Nishida. (2009). Updated stock assessment for bigeye tuna in the Indian Ocean up to 2008 using Stock Synthesis III (SS3). IOTC-2009-WPTT-20.

Nóbrega, C.C., Mendes, P.P., Mendes, E.S. 2014. Factors that determine the quality of bigeye tuna, caught in the western tropical Atlantic Ocean. Arq. Bras. Med. Vet. Zootec., v.66, n.3, p.949-958.

Vincent, M. T., Pilling, G.M., Hampton, J. 2018. Incorporation of updated growth information within the 2017 WCPO bigeye stock assessment grid, and examination of the sensitivity of estimates to alternative model spatial structures. WCPFC-SC14-2018/ SA-WP-03.

Waterhouse, L, Sampson DB, Maunder M, Semmens BX. 2014. Using areas-as-fleets selectivity to model spatial fishing: Asymptotic curves are unlikely under equilibrium conditions. Fisheries Research. 158:15-25.

Walter, J., Hiroki, Y., Satoh, K., Matsumoto, T., Winker, H., Ijurco, A.U., Schirripa, M., 2019. Atlantic bigeye tuna stock synthesis projections and kobe 2 matrices. Col. Vol. Sci. Pap. ICCAT 75, 2283–2300.

Walter, J., Winker, H., 2019. Projections to create Kobe 2 Strategy Matrices using the multivariate log-normal approximation for Atlantic yellowfin tuna. ICCAT-SCRS/2019/145 1–12.

Winker, H., Walter, J., Cardinale, M., Fu, D. 2019. A multivariate lognormal Monte-Carlo approach for estimating structural uncertainty about the stock status and future projections for Indian Ocean Yellowfin tuna. IOTC–2019–WPTT21–xx.

APPENDIX A: SPATIAL DISTRIBUTION OF TAG RECOVERIES

Following the approach of Langley & Million (2012), the duration of mixing period was investigated using the spatial distribution of tag recoveries from the purse seine fishery. The tag recovery data from individual year/quarters and by set type are presented as a series of maps that overlay the *tag mark rate* (number of tags per metric tonnes of yellowfin caught) and the catch distribution for the set type. The number of tag fish recovered per metric tonne of bigeye caught, stratified by set type and 1° square, was calculated for each year/quarter of the recovery period (from 2006 to 2011). For each quarter of the recovery period, all available tag recoveries were aggregated once the tagged fish had been at liberty for a specified mixing period. Maps are presented for a two-quarter mixing period for the FAD recoveries (Figures A1 & A2) and 4 quarter mixing period for the free school fishery (Figures A3 & A4).

The diagnostics for the tag recoveries indicate a higher degree of mixing with the fished population. There is no strong evidence of persistent heterogeneity in the distribution of the tagged population, although some anomalies have been identified.

This indicates that the period of about 12 months required for most tagged fish to reach a size that is vulnerable to free-school fishery (> 90 cm) is probably adequate for the tagged fish to disperse throughout the (free-school) population.

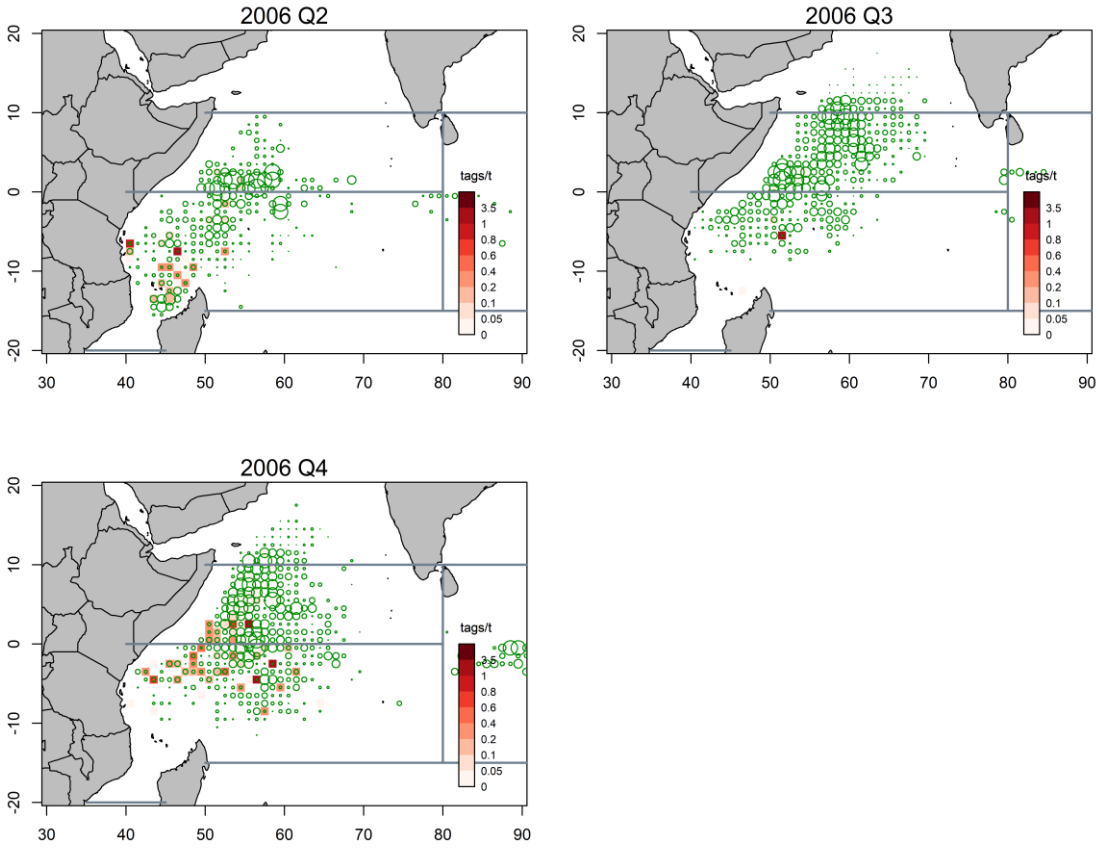

Figure A1: Recoveries of tags of bigeye by the FAD fishery in the 2nd, 3rd, and 4th Quarter in 2006 for tags at liberty for at least two quarters (2Q mixing period). The green circles on the map represent the relative distribution of the big purse-seine FAD catch. The coloured squares represent the tag mark rate of the catch (number of tags per t).

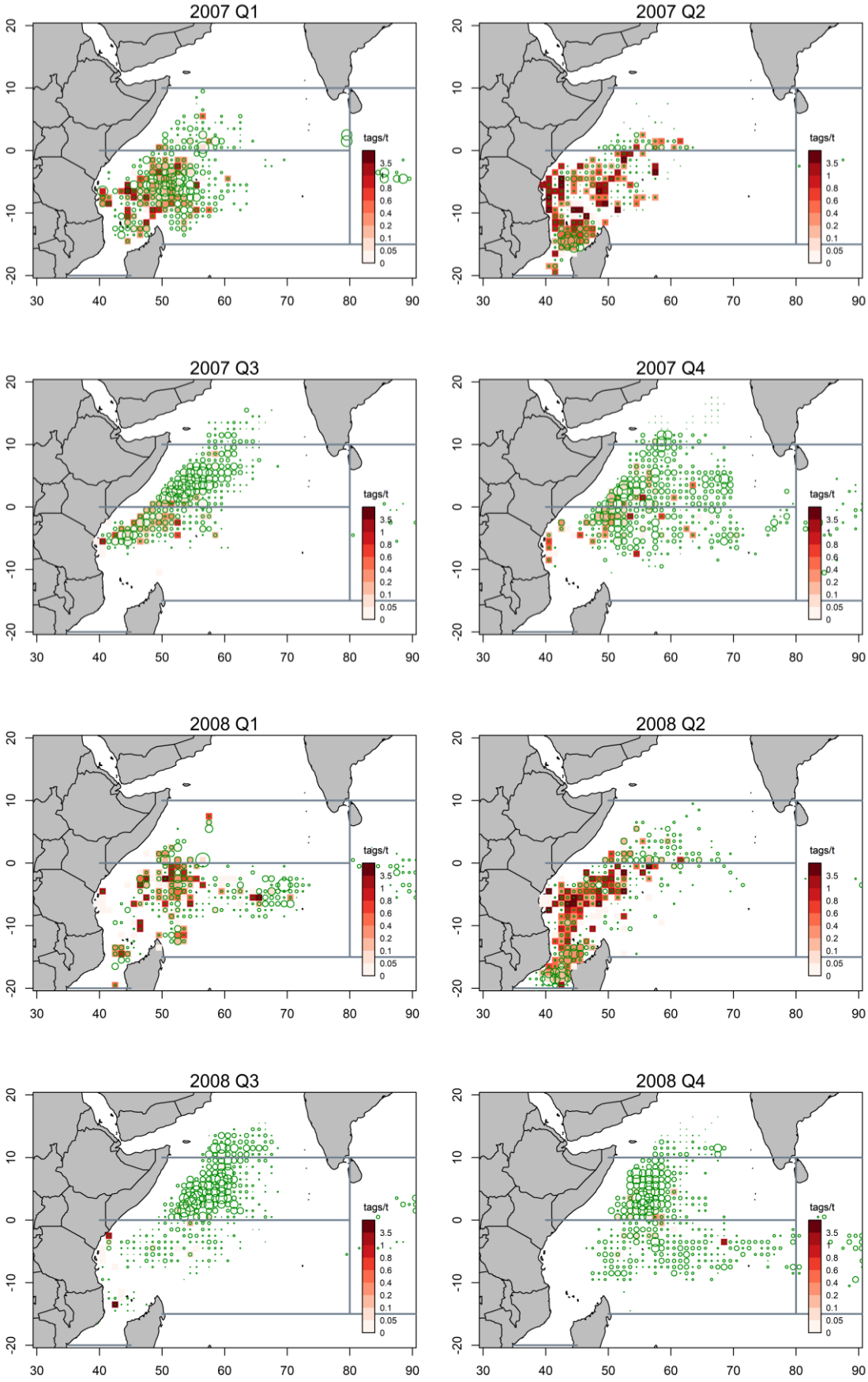

Figure A1 – continued: Recoveries of tags of bigeye by the FAD fishery in the 1st – 4th Quarter in 2007 and 2008 for tags at liberty for at least two quarters (2Q mixing period).

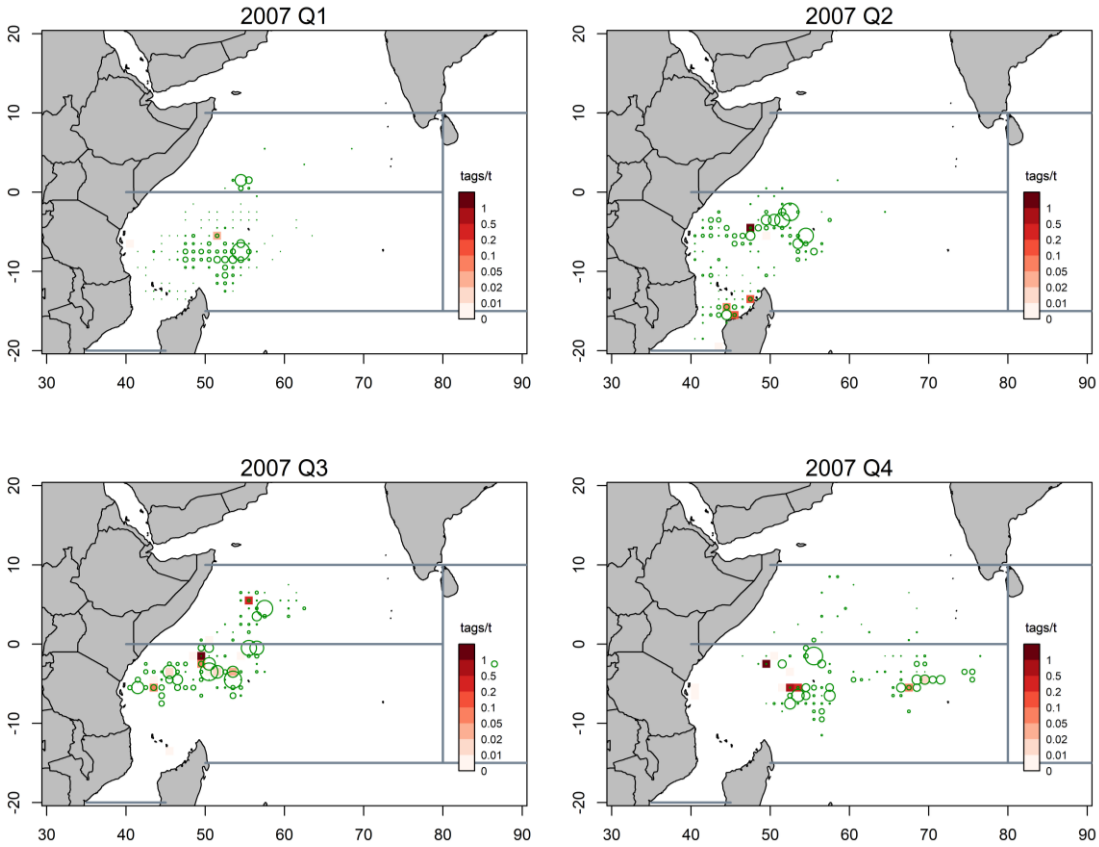

Figure A2: Recoveries of tags of bigeye by the purse seine free school fishery in the 1st – 4th Quarter in 2007 for tags at liberty for at least four quarters (4Q mixing period). The green circles represent the relative distribution of the big purse-seine FAD catch. The coloured squares represent the number of tags per t).

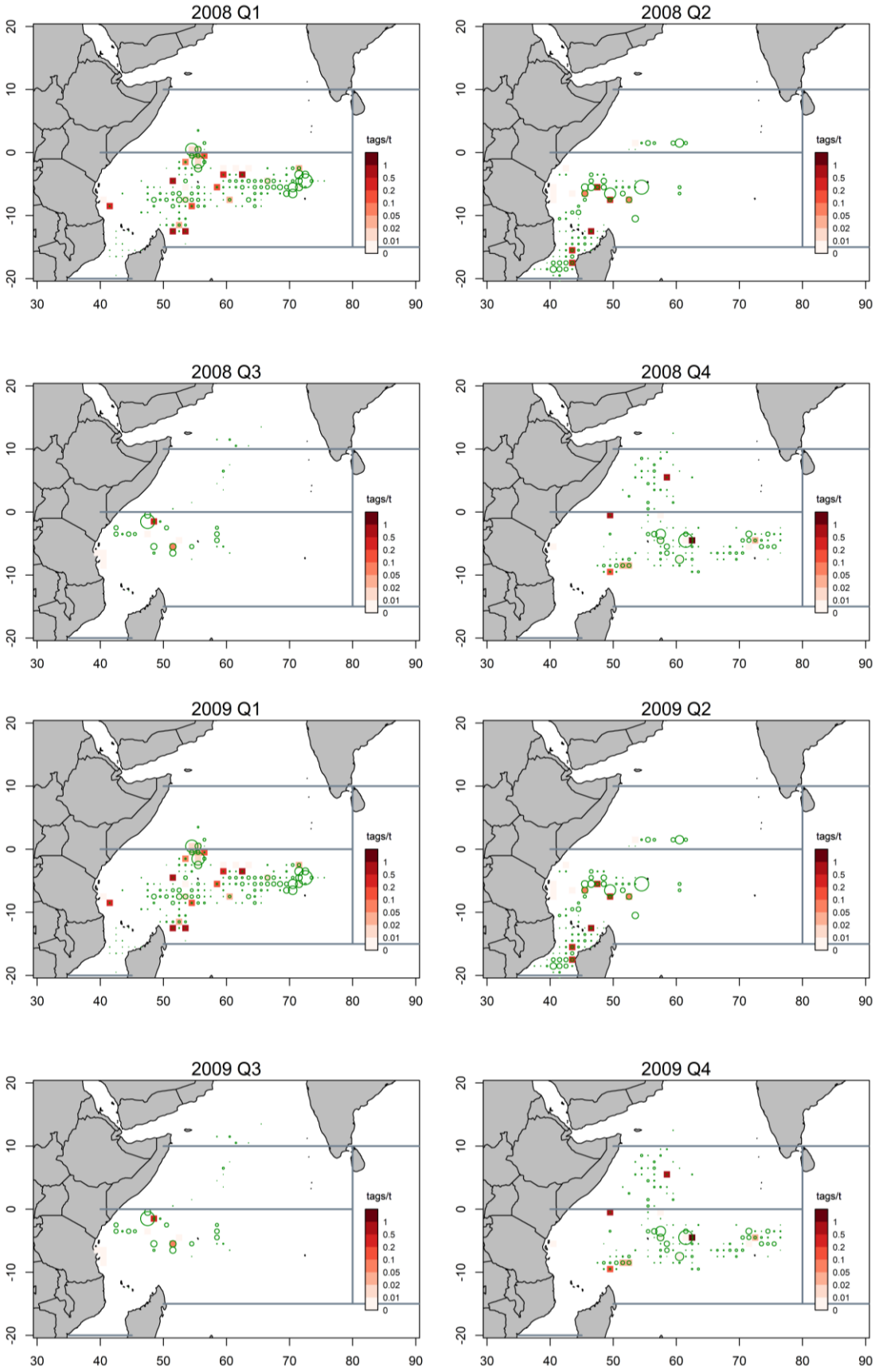

Figure A1 – continued: Recoveries of tags of bigeye by the FAD fishery in the 1st – 4th Quarter in 2008 and 2009 for tags at liberty for at least four quarters (4Q mixing period).

APPENDIX B: RESULTS FROM THE EXPLORATORY MODELLING

Table B1. Maximum Posterior Density (MPD) estimates of the main stock status indicators from the exploratory model options.

	SB_0	SB_{MSY}	SB_{MSY}/SB_0	SB_{2018}	SB_{2018}/SB_0	SB_{2018}/SB_{MSY}	F_{2018}/F_{MSY}	MSY
eRevised	1,936,380	536,362	0.28	504,545	0.26	0.94	1.09	86,952
eRecruitVar	2,121,010	462,210	0.22	654,452	0.31	1.42	0.71	89,660
eQhyper	2,177,520	540,833	0.25	821,791	0.38	1.52	0.63	109,543
eSelLLRegion	1,897,250	348,461	0.18	489,620	0.26	1.41	0.88	90,730
eDwPSLSLF	1,921,840	475,139	0.25	504,870	0.26	1.06	1.06	86,575
eDwLLLF	2,231,720	498,701	0.22	602,224	0.27	1.21	0.86	107,849
eTagNewProc	2,002,220	478,780	0.24	520,749	0.26	1.09	0.98	92,059
eGrowthVB	1,835,810	418,755	0.23	493,638	0.27	1.18	0.80	100,918
eMconst	2,224,640	473,768	0.21	614,288	0.28	1.30	0.88	86,652
eMhigh	1,149,030	273,874	0.24	280,822	0.24	1.03	0.76	111,853
eRegion1-lambda1	1,325,470	412,769	0.31	309,568	0.23	0.75	1.53	80,600
eRegion3	2,032,890	449,724	0.22	588,829	0.29	1.31	0.82	91,197
eRegion3MoveHigh	2,033,430	420,250	0.21	613,241	0.30	1.46	0.74	118,210

Table B2: Details of objective function components for the exploratory model options.

	TOTAL	CPUE	Length_comp	Tag_comp	Tag_negbin	Recruitment	Parm_priors	Parm_devs	Catch	Parm_softbounds
eRevised	1348.7	-420.4	1349.0	223.0	194.6	-16.9	18.2	0.0	0.91	0.01
eRecruitVar	1260.9	-496.7	1327.1	222.0	203.8	-30.7	20.3	14.8	0.04	0.02
eQhyper	1299.3	-470.5	1349.5	223.2	196.5	-21.9	21.6	0.0	0.45	0.01
eSelLLRegion	1296.6	-455.1	1322.0	226.5	193.1	-16.3	24.0	0.0	2.17	0.02
eDwPSLSLF	1073.1	-461.4	1090.1	231.4	203.0	-15.4	22.4	0.0	2.75	0.01
eDwLLLF	678.0	-440.5	725.8	218.7	196.8	-47.7	22.9	0.0	1.48	0.01
eTagNewProc	1303.4	-437.1	1334.1	229.3	168.7	-18.1	22.3	0.0	3.85	0.01
eGrowthVB	1368.8	-456.3	1452.6	232.3	139.3	-33.0	28.9	0.0	4.81	0.02
eMhigh	1343.2	-446.5	1355.1	226.7	202.2	-19.5	19.9	0.0	5.20	0.01
eMconst	1357.9	-435.8	1357.8	234.7	203.5	-25.0	19.8	0.0	2.46	0.02
eRegion1-lambda1	5254.8	-305.5	1439.3	2245.8	1778.5	21.9	74.6	0.0	0.00	0.01
eRegion3	1365.2	-412.9	1345.4	240.8	198.2	-18.7	12.0	0.0	0.00	0.01
eRegion3MoveHigh	1511.9	-303.4	1407.3	201.0	210.7	-25.4	21.2	0.0	0.02	0.03

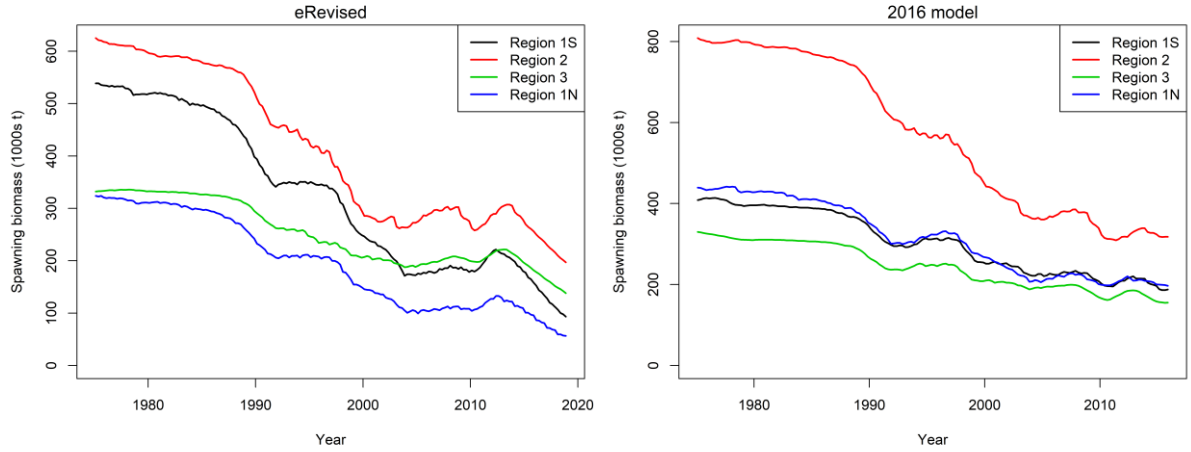

Figure B1: A comparison of estimated spawning biomass by region from model eRevised and the 2016 reference model.

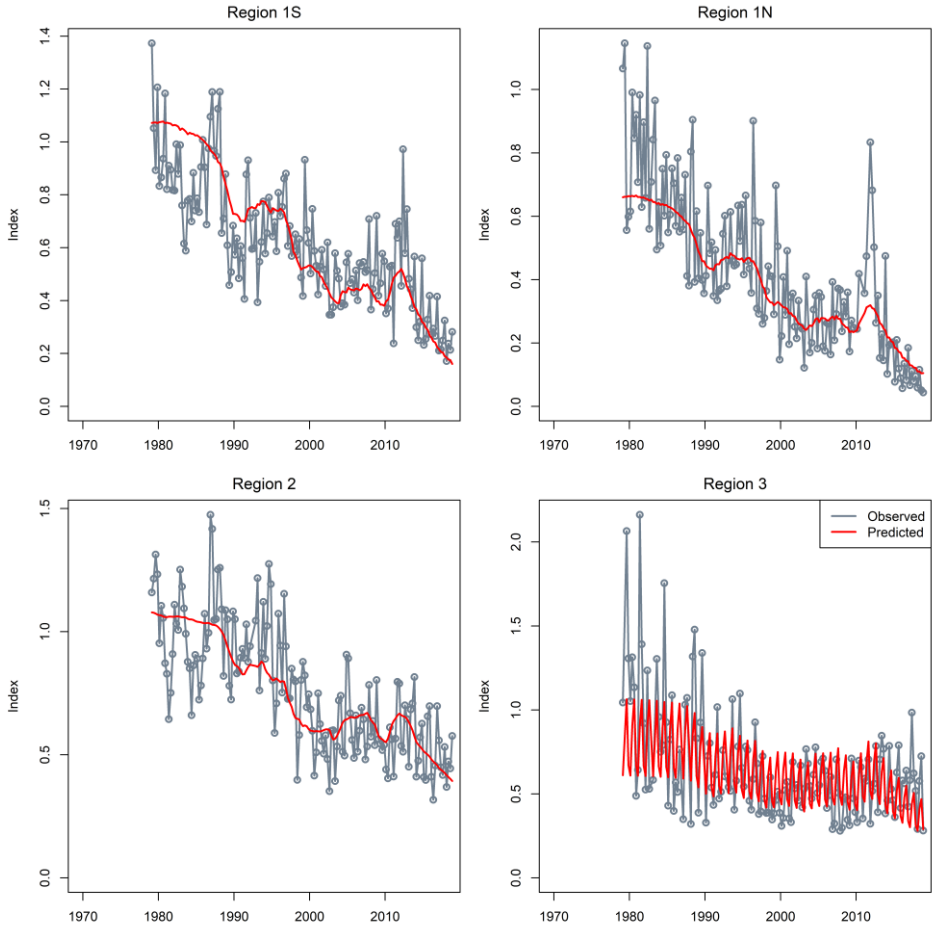

Figure B2: Fit to the regional longline CPUE indices from the model eRevised, 1979–2018. In region 3, Individual catchability (q) was estimated for each season.

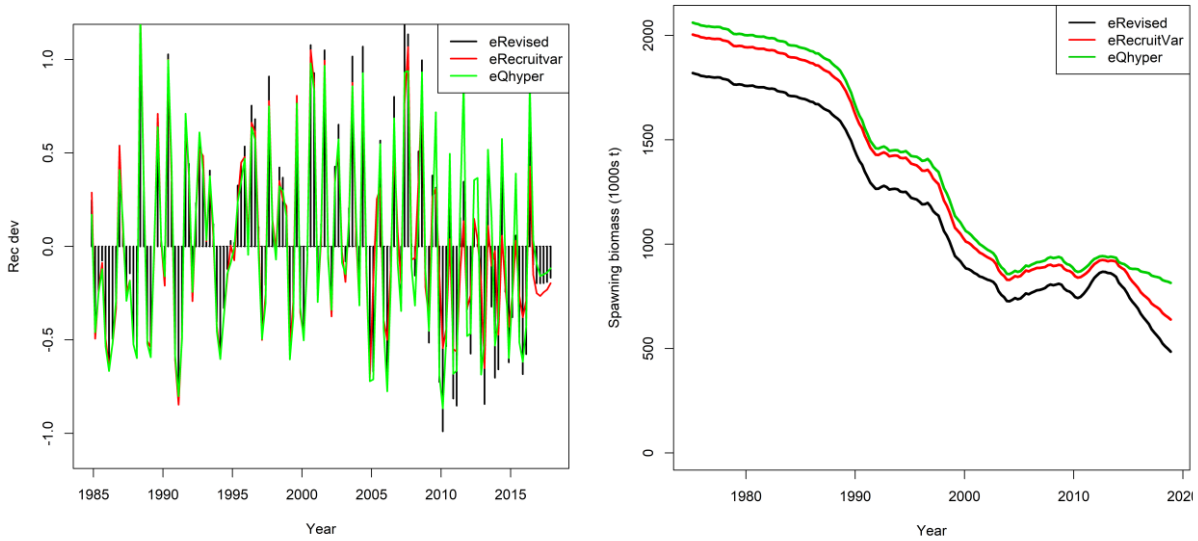

Figure B3: A comparison of estimated recruitment deviations (left) and spawning biomass (right) from exploratory models eRevised, eRecruitVar, eQhyper.

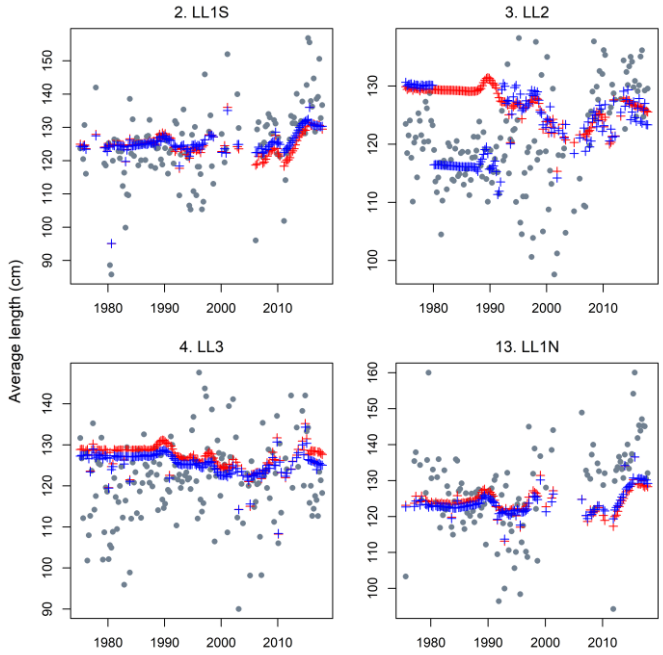

Figure B4: A comparison of fits to average fish length (FL, cm) of bigeye tuna by the main LL fisheries from exploratory model eRevised (red) and eSelLLRegion (blue).

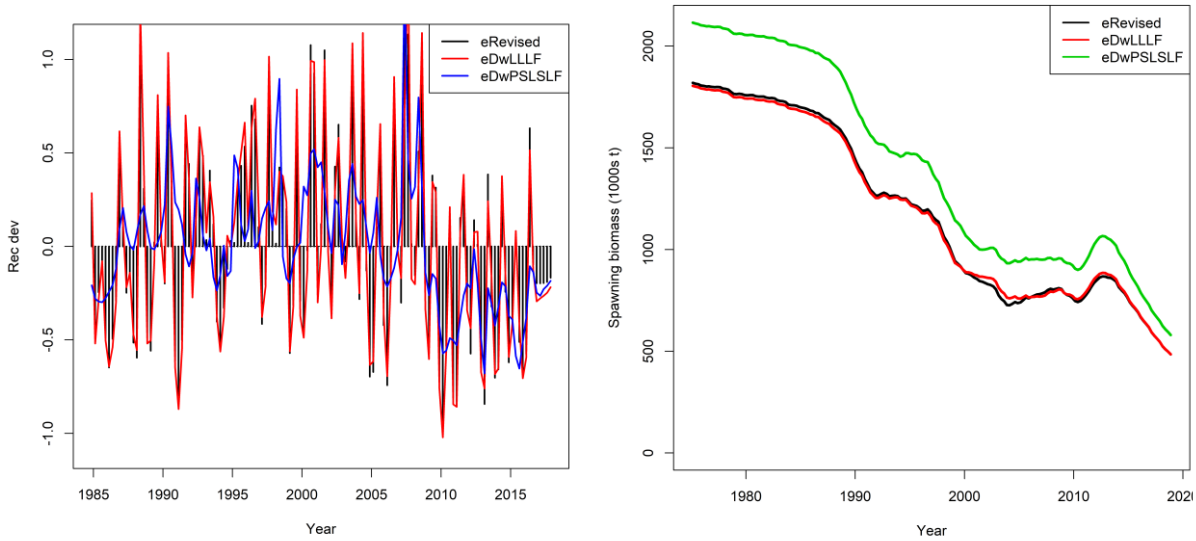

Figure B5: A comparison of estimated recruitment deviations (left) and spawning biomass (right) from exploratory models with different LF weighting options: eRevised, eDwLLLF, eDwPSLSLF.

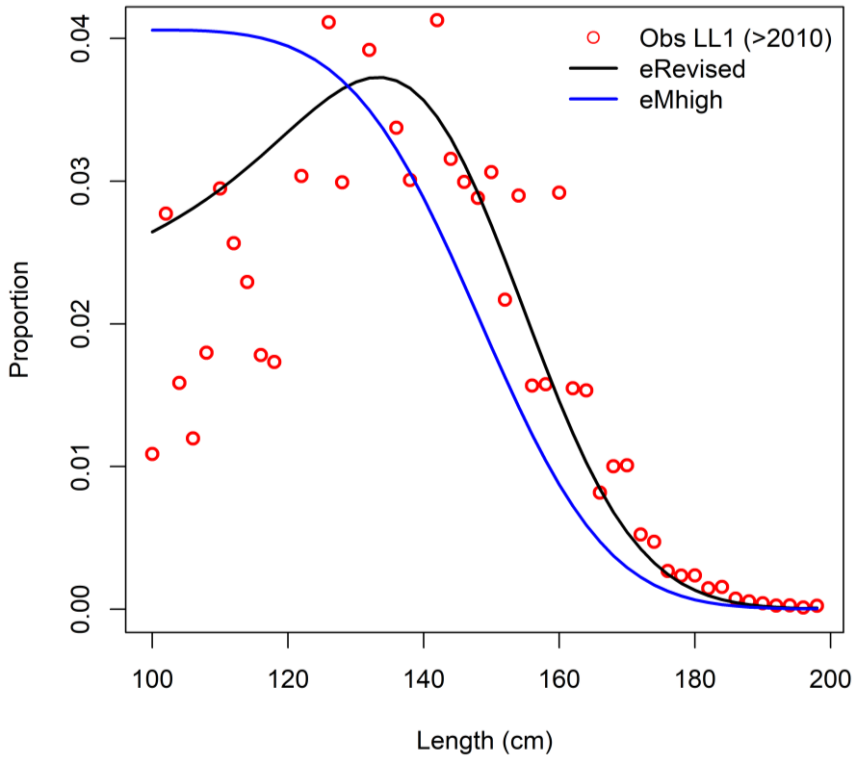

Figure B6: A comparison of predicted population size structure (only fish greater than 100 cm is shown) from exploratory models with low (eRevised) and high natural mortality options (eMhigh), overlaid with observed longline size frequency data in region 1S (aggregated for 2011-2015).

(a) eMhigh ***(b) eMconst***

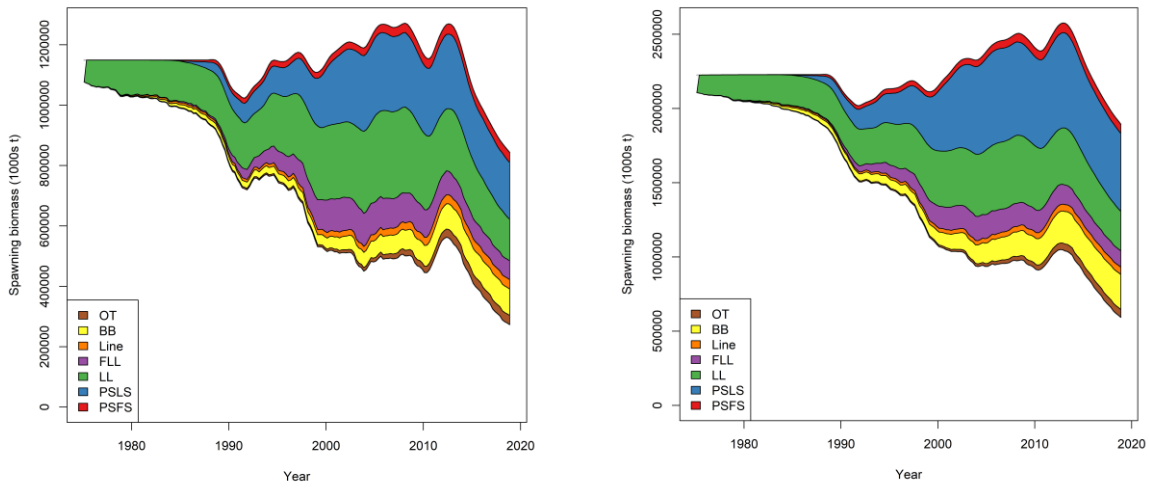

Figure B7: A comparison of estimated fishing impact (reduction in spawning biomass due to fishing over attributed to various fishery groups) for exploratory models with high (eMhigh, left) and low natural mortality options (eMconst, right).

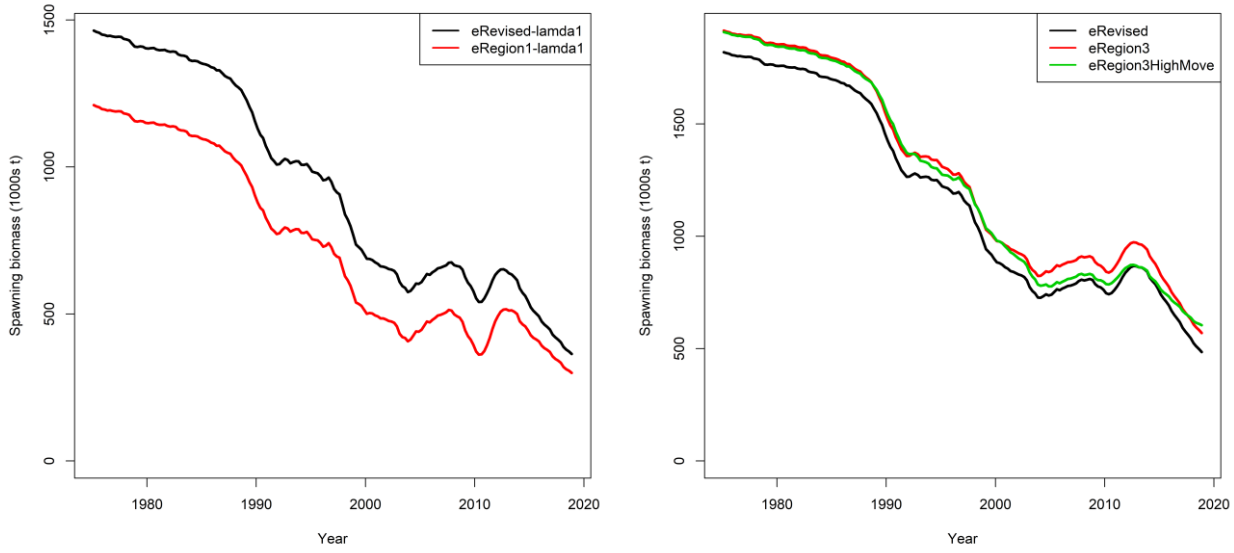

Figure B8: A comparison of estimated spawning biomass from exploratory models with alternative regional structure: between eRevised-lambda1 and eRegion1-lambda1 (left), and between models eRegion3 and eRegin3HighMove (right).

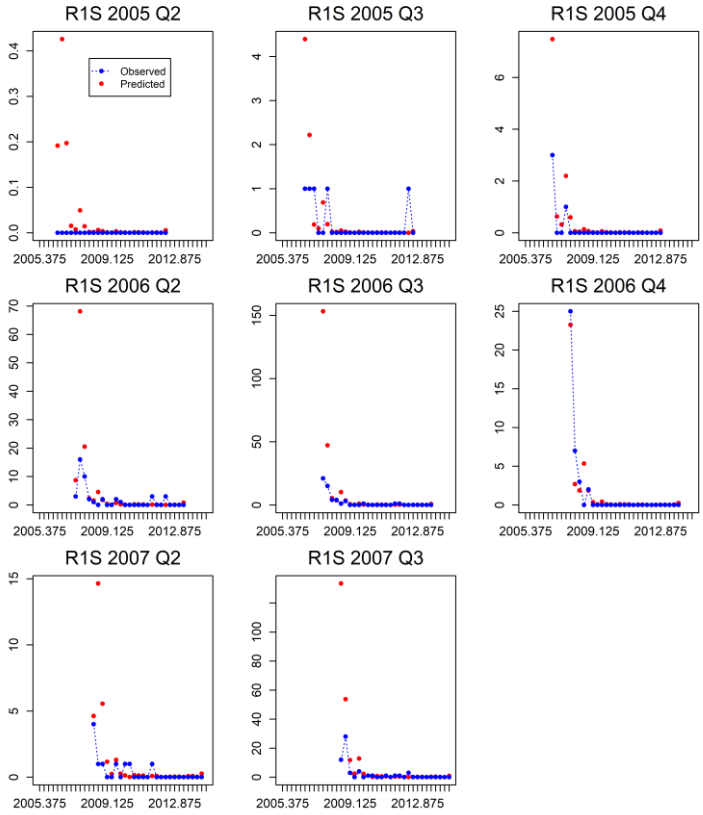

Figure B9: Observed and predicted the number of tag recoveries by the PSLS1N fishery by quarter following the mixing period from model eRegion3. Tag release groups (1-8) represent the total releases in each quarter (aggregating the age groups that define individual SS release groups).

(a) eRegion3 **(b) *eRegion3HighMove***

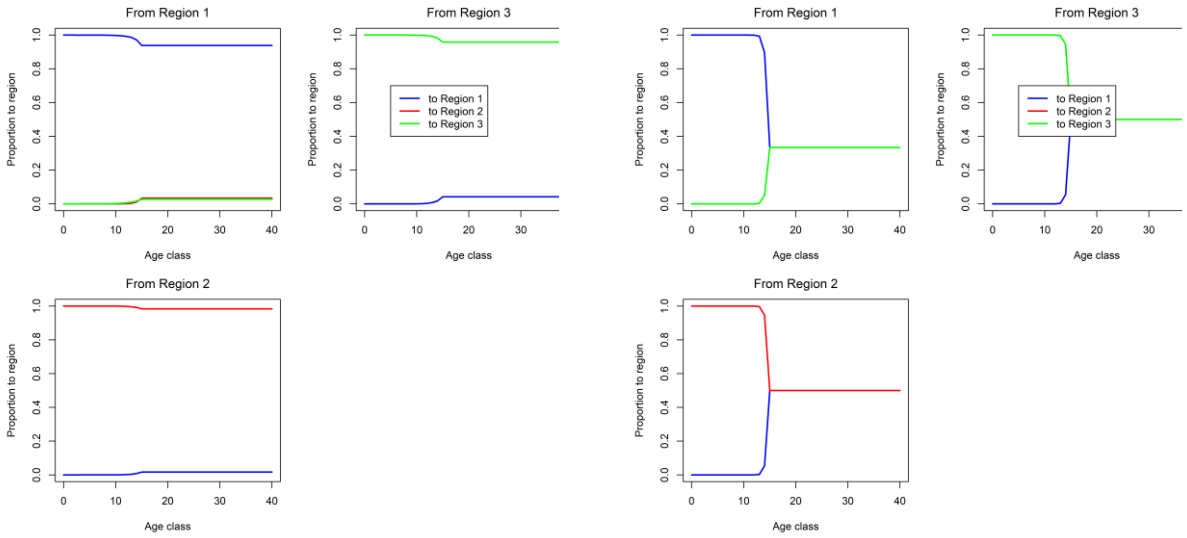

Figure B10: Estimated movement rates among regions from exploratory model eRegion3 (left), and the assumed (fixed) movement rates for model eRegion3HighMove (right).

APPENDIX C: FITS TO TAG RECOVERIES FOR MAIN FLEETS FROM THE REFERENCE MODEL

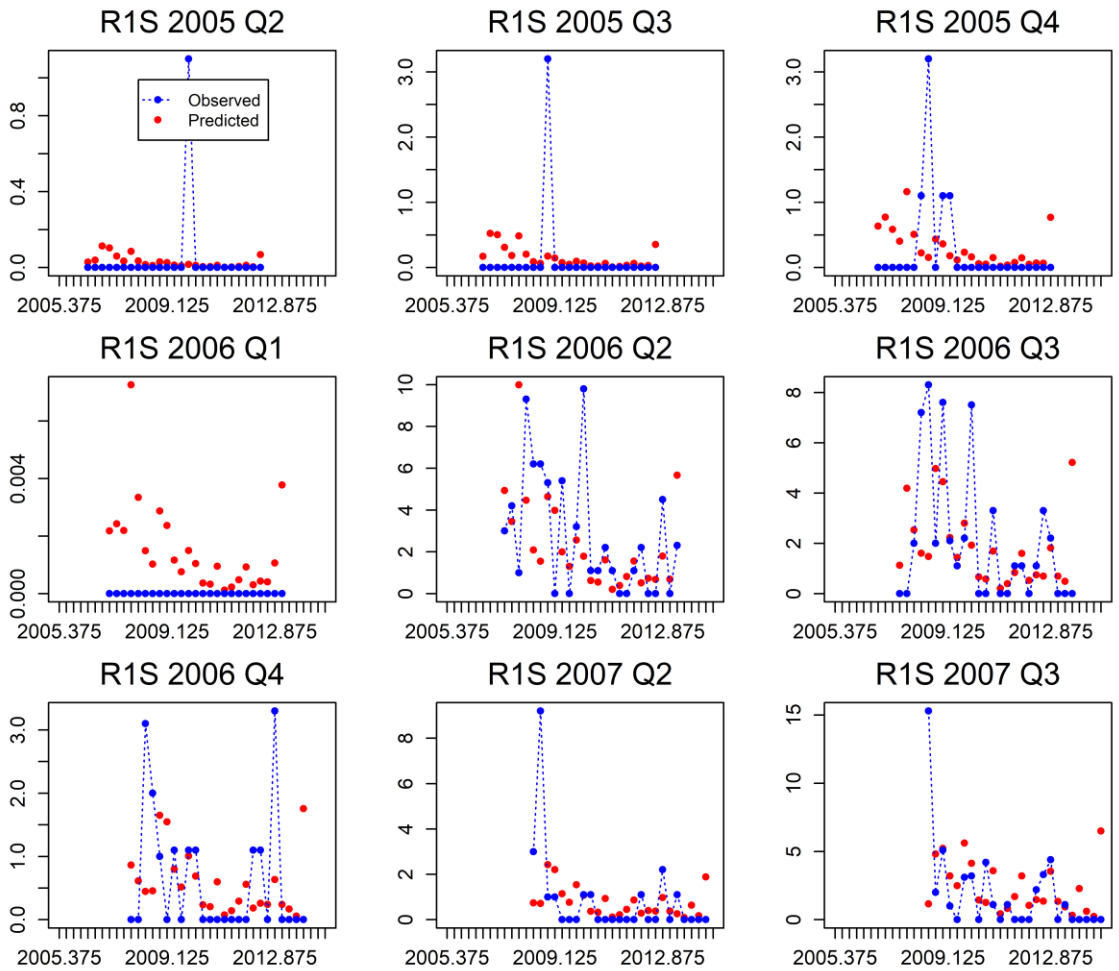

Figure C1: Observed and predicted the number of tag recoveries by the LL1S fishery by quarter following the mixing period from the reference model. Tag release groups (1-9) represent the total releases in each quarter (aggregating the age groups that define individual SS release groups).

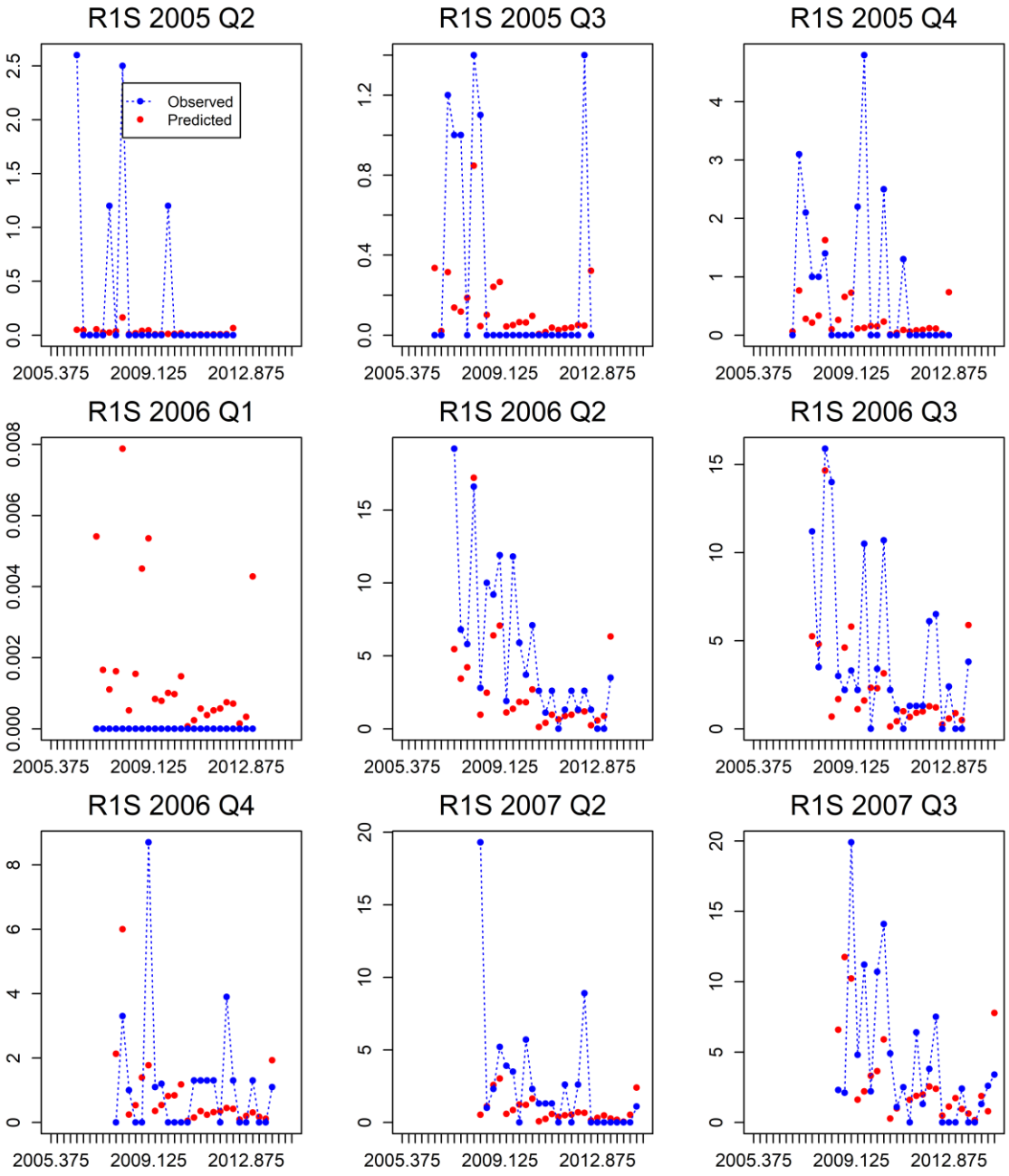

Figure C2: Observed and predicted the number of tag recoveries by the PSFS1S fishery by quarter following the mixing period from the reference model. Tag release groups (1-9) represent the total releases in each quarter (aggregating the age groups that define individual SS release groups).

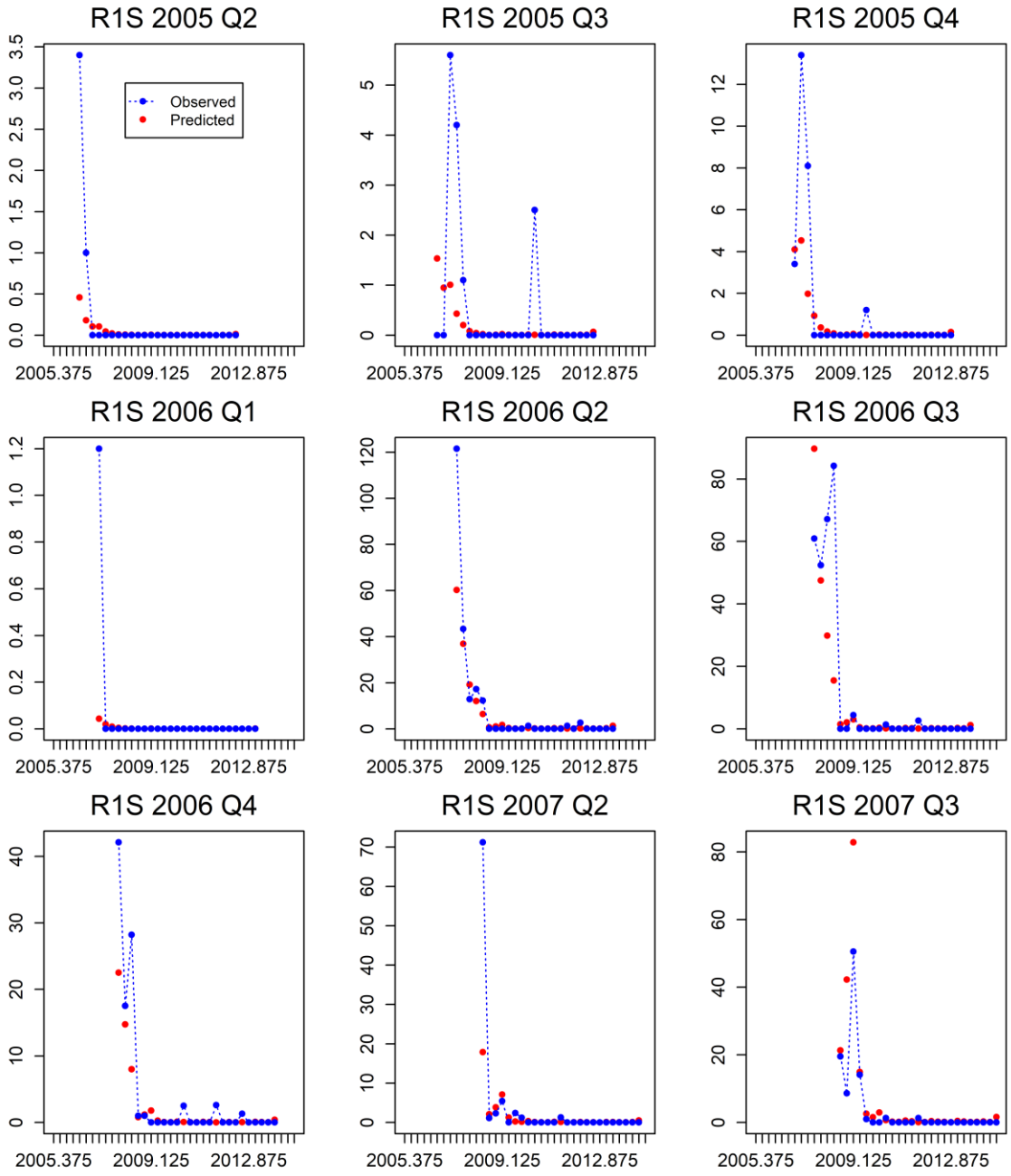

Figure C3: Observed and predicted the number of tag recoveries by the PSLS1S fishery by quarter following the mixing period from the reference model. Tag release groups (1-9) represent the total releases in each quarter (aggregating the age groups that define individual SS release groups).

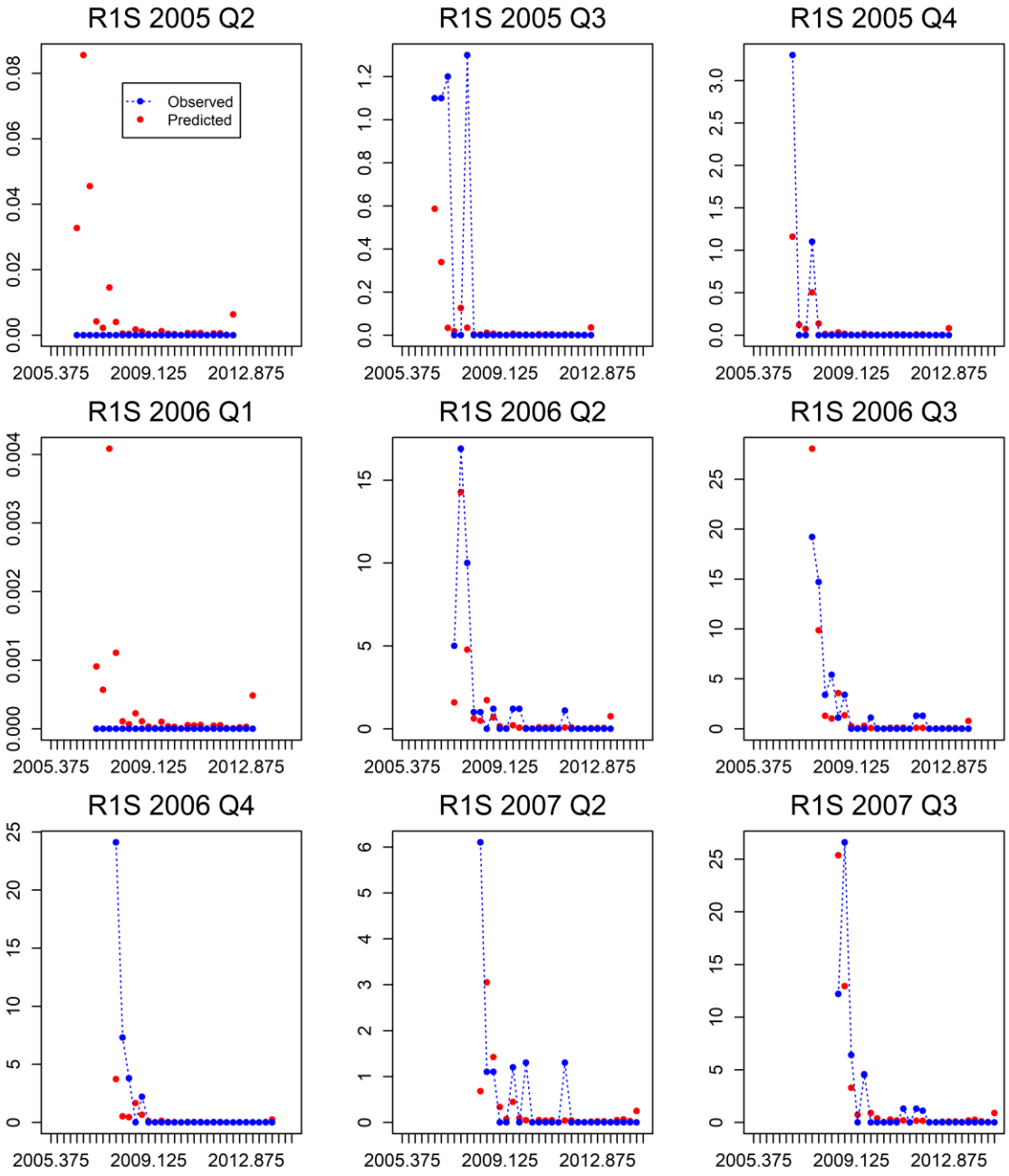

Figure C4: Observed and predicted the number of tag recoveries by the PSLS1N fishery by quarter following the mixing period from the reference model. Tag release groups (1-9) represent the total releases in each quarter (aggregating the age groups that define individual SS release groups).

APPENDIX D: RUN TEST RESULTS FROM MODEL 'rQhyper'

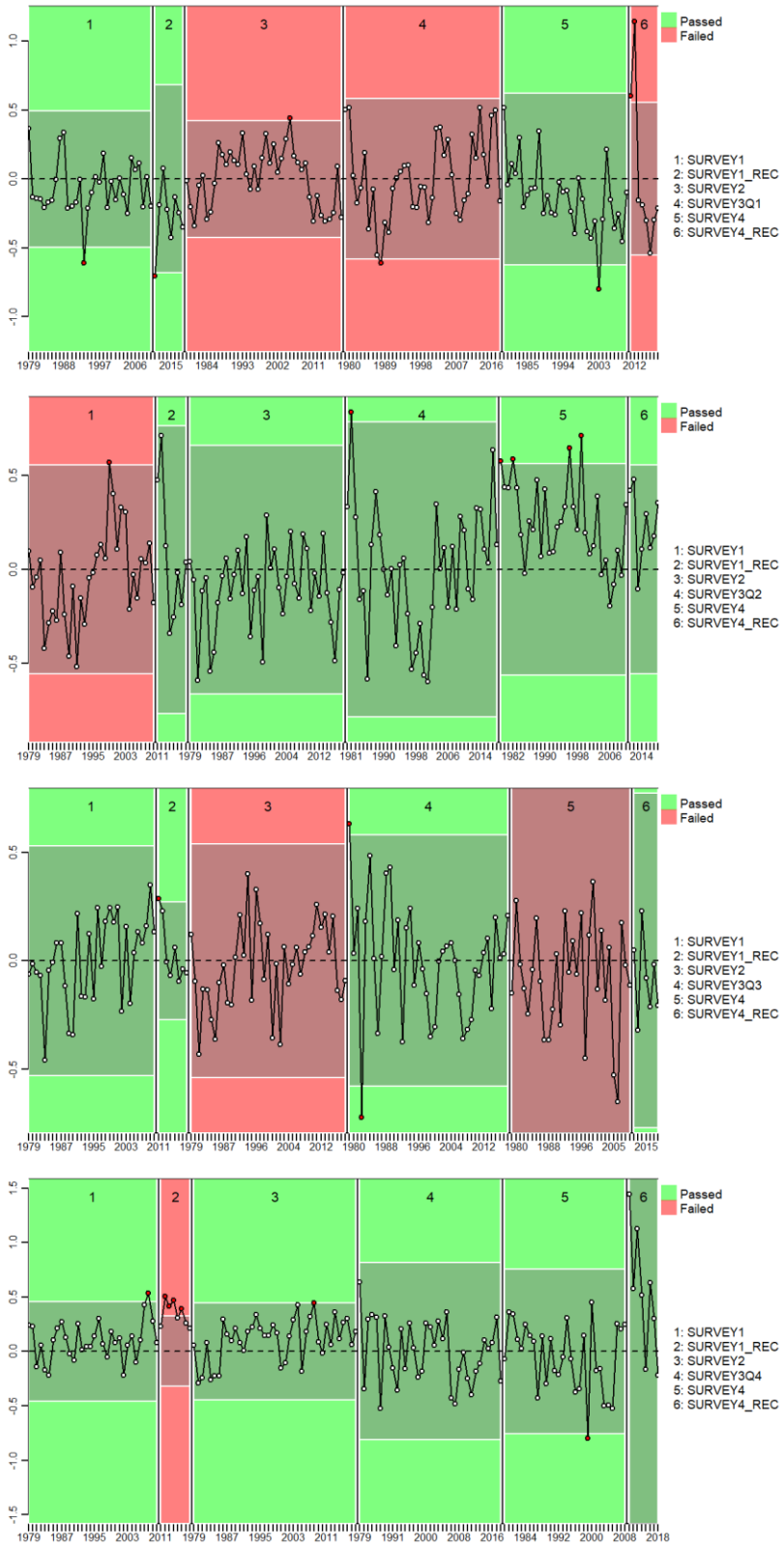

Figure D1: Runs tests performed to the time series of residuals from fits to CPUE indices by quarter (Q1 – Q4 from top to bottom). 1, LL1S 1975 – 2010; 2, LL1S 2011 – 2018; 3, LL2; 4, LL3; 5, LL1N 1975 – 2010; 6, LL1N 2011 – 2018.

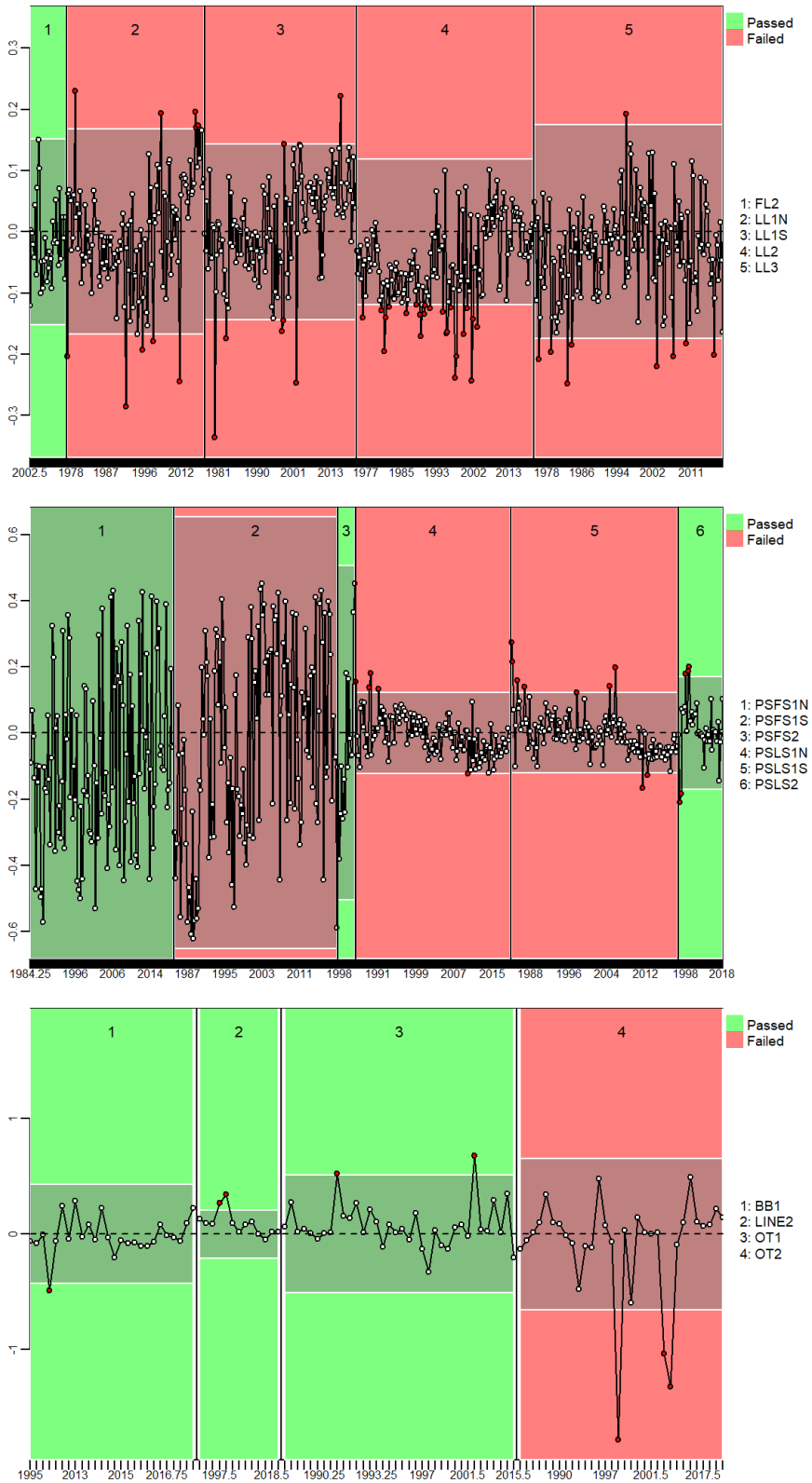

Figure D2: Runs tests performed to the timer series of residuals from fits to length composition data (by fishery).

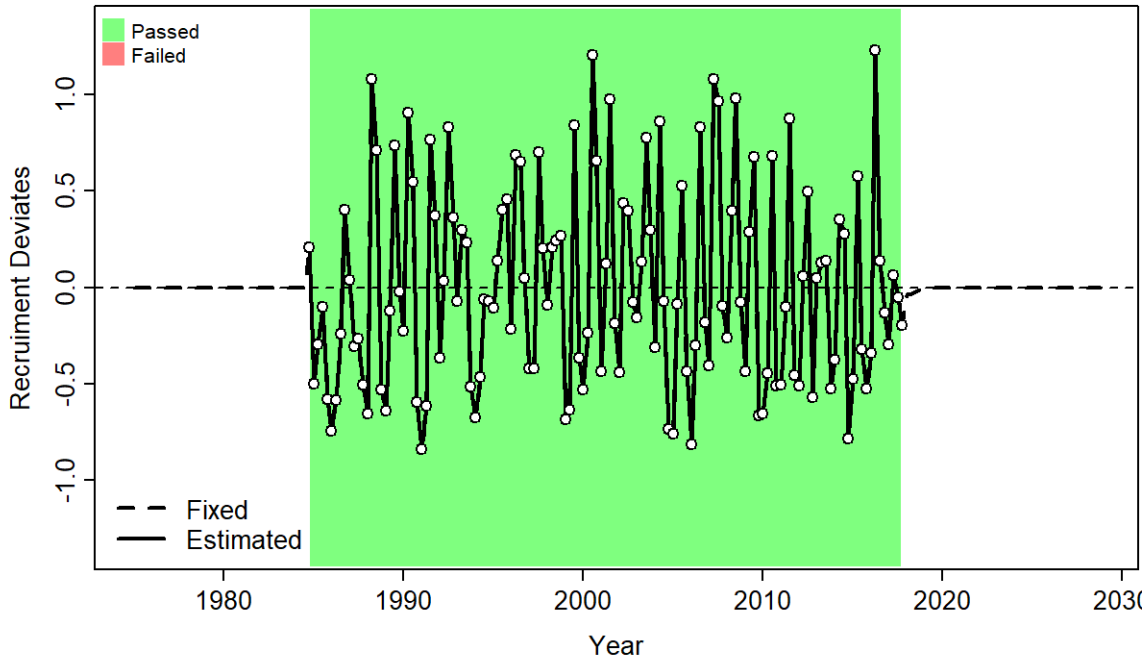

Figure D3: Runs tests performed to the timer series of recruitment deviations from fits to length composition data (by fishery).